Doctoral Dissertation

Responses of plants to environmental stresses: Understanding basic mechanisms and practical applications

Division of Thermo-Biosystem Relations

Specialty of Cryobiosystems Science

United Graduate School of Agricultural Sciences

Iwate University

KAMAL MD MOSTAFA

2021.3

Table of Contents

Summary

Abiotic stresses, such as cold, heat, flood, drought, and salinity, are major limiting factors of global crop and plant production. In the era of unpredictable climate fluctuations due to ongoing global climate change, the abiotic stress extremes are getting more frequent over the years. Sessile plants cannot avoid any extreme environmental factors, and over 90% of field crops experience abiotic stress. Moreover, abiotic stress always occurs in combination in the field, and one abiotic stress can lead to several secondary abiotic stresses. Even though the global climate is treading towards warmer periods, it is not diminishing cold stress threats. For example, reports show that a warmer climate causes extreme and unpredictable out of season cold stress, cold shock, localized frost, and freezing events. Furthermore, reduced length of cold autumns or warm and short winters affect the cold acclimation, vernalization, bud dormancy period in crop and tree plants. Therefore, understanding abiotic stress response and developing sustainable stress tolerance methods are the critical steps towards assuring global food security.

Elucidating how plants sense and respond to cold is essential for identifying genetic and chemical methods that may improve plant performance under low-temperature conditions. However, most studies that focus on cold stress are either under prolonged cold stress or cold acclimation conditions. The molecular mechanisms involved in early cold perception and response are not clearly understood yet. Plant proteins go through cascades of post-translational modifications and form complex signaling pathways that regulate essential biological processes, including the external environmental response. Protein phosphorylation is one of the most common and crucial post-translational modifications, and nearly one-third of proteins are modified through phosphorylation. Identification of differentially phosphorylated proteins in response to environmental factors has led to the discovery of important components of signaling pathways. Mass spectrometry-based methods to quantify phosphoproteome changes are a well-established system for identifying key phosphorylation events involved in stress response. The plasma membrane and its adjacent extracellular and cytoplasmic sites are the first checkpoints for sensing temperature changes and subsequent events such as signal generation and solute transport. Here, I report a large-scale, comprehensive study on *Arabidopsis* membrane phosphoproteomics during early cold response events. In this study, I focused on the temporal change in microsomal membrane protein phosphorylation in response to a brief 5 to 60 min cold exposure. Subsequently, using hydroxy acid-modified metal oxide chromatography (HAMMMOC) phosphopeptide enrichment method coupled with a powerful state of the art mass spectrometer, I detected around 1900 peptides. Gene ontology (GO) analysis of these phosphorylated proteins revealed that cold exposures led to rapid phosphorylation of proteins involved in cellular ion homeostasis, solute and protein transport, cytoskeleton organization, vesical trafficking, protein modification, and signal transduction processes. Even under such a brief cold exposure, phosphorylation of ion channel or

transporter proteins such as Ca^{2+} (hyperosmolality-gated Ca2+ permeable channels/OSCAs, Ca^{2+}-ATPases/ACAs), K^+ (potassium transporters/POTs), Na^+/H^+ (Na^+/H^+ exchanger/NHX), which are involved in maintaining ionic homeostasis inside the cell, indicated that plant cell tries to maintain its ionic balance in steady state under cold. Accumulation of cryoprotectants such as soluble sugar is a crucial defense mechanism to survive under cold extremes. Activation of sugar and monosaccharide transporters, sugar will eventually be exported transporter12 (SWEET12), early responsive to dehydration6/6 like (ERD6/6like) and transmembrane transporter 1/3 (TMT1/3), at such an early stage indicate that plant starts to deploy its defense mechanism as soon as they sense the cold. With phosphorylation motif analysis using the Motif-X algorithm, I identified 16 characteristic target motifs of essential kinases such as receptor-like kinases (RLKs), mitogen-activated protein kinases (MAPKs), Calcium/Calmodulin dependent protein kinases (CDPK/CaMK), casein kinases (CK), and GSK3/shaggy-related protein kinase (GSK). Further, the kinase-substrate network revealed that the kinases and substrates form a complex network of phosphorylation events even during a brief cold exposure. Ca^{2+}, phosphoinositide, abscisic acid (ABA), auxin, and brassinosteroid (BR) and reactive oxygen species (ROS) mediated signaling pathways were also found to be involved in the early cold response, which gives a further complex response from the plants during cold sensing. Phosphorylation of microtubule-cytoskeleton related proteins (myosin-binding protein7(MyoB7), myosin motor XI-K/C, and 65-kDa microtubule-associated protein1 (MAP65-1) involved in cytoplasmic streaming and cytoskeleton organization) and vesicle trafficking-related proteins (ARF guanine-nucleotide exchange factor GNOM, Sorting nexin/SNX, vacuolar protein sorting-associated protein41/VPS41, Syntaxin/SYP121/132, and dynamin-related protein/DRP2A/B) gives a clear idea that these proteins and their respective functions are an essential part of the early cold response mechanism.

Subsequently, besides understanding the molecular mechanisms of early cold response in *Arabidopsis*, I focused on developing a cost-effective, time-, and labor-saving method to improve plant performance against a range of abiotic stresses, including cold. Here I developed a seed treatment method using an optimized level •OH generated from Fenton/Haber-Weiss reaction. I showed the effects of a single/one-time application of this •OH to seeds on germination and growth in germinating seedlings under optimum and sub-optimum conditions such as chilling, high temperature, heat, and salinity. A one-time treatment of *Arabidopsis* seeds with •OH improved germination and early growth in young seedlings. The treatment effect was also not limited to the germination and early growth stage, and plants from the treated seeds showed an increased daily root growth and increased number of lateral roots. More interestingly, the treatment effect became prominent under suboptimum conditions. I observed a clear advancement in germination speed after the •OH treatment compared to water treated and H_2O_2 treated seeds. Almost in all the abiotic stress conditions, the •OH seeds took significantly less time to reach 50% germination. Moreover, the germinating seedlings showed faster radical and hypocotyl elongation and cotyledon expansion and greening after the •OH treatment. Under different

2

abiotic stress conditions, such as cold, early germination and seedling survival are essential criteria for assuring a better production.

The outcomes of this •OH treatment were surprising, and the superior effects of •OH treatment than its precursor H_2O_2 led to the question of what molecular mechanisms are behind this better performance. Even though H_2O_2 is frequently used as a seed priming or treating agent that showed promising effects in improving different abiotic stress tolerance, no study ever considered the possible conversion of H_2O_2 into •OH by endogenous Fenton/Haber-Weiss reaction. Therefore, to understand the molecular mechanisms behind increased stress tolerance by •OH treated seeds and seedlings, I employed a mass spectrometry-based proteomics method to study the change in seed proteins under chilling stress. Surprisingly, GO analysis showed that proteins that were exclusively accumulated in •OH treated group were mostly antioxidation-related (such as glutathione reductase1/GR1, dehydroascorbate reductase/DHAR, and ascorbate peroxidase/APX), chaperones (such as heat-shock protein60/HSP60, chaperonin 60 subunit beta1/CPN60B1/LEN1, and Calreticulin/CRT), late embryogenesis related (LEA) proteins, and proteins involved stress response, toxin catabolism, embryo development. These results indicate that the •OH enhanced the antioxidant properties of the treated seeds, which may be contributed to maintain a basal ROS level in the embryo and germinating seeds. The treatment also contributed to the maintenance of protein homeostasis, which is essential for cells to perform better under abiotic stress. Overall findings from this study showed the positive sides of •OH in plant performance.

To conclude, I revealed the early cold response events in plants with a first-ever large-scale membrane phosphoproteomic study. The findings from this study will be a valuable resource for scientists to narrow down target genes associated with the proteins for better functional genomic studies in the future. Furthermore, the time and cost-efficient seed treatment with just a one-time application of •OH can potentially solve emerging extreme abiotic stresses. This study also provides a first-ever view of the positive sites of the deleterious reactive oxygen species, •OH. I expect both of my studies will contribute to developing methods to improve stress-tolerant/resistant crop varieties.

Chapter 1

General introduction

Plants under abiotic stress

When living organisms migrated from the water to land, plants changed the course of evolution and evolved as a sessile organism, spending whole life within the defined area marked by anchored roots. Thus, being incapable of moving, plants are always exposed to the surrounding biotic and abiotic stresses. Both biotic and abiotic stresses are the major factors limiting plant growth, development, and crop production (Mittler, 2006; Suzuki et al., 2014). For example, in between 1980-2012 abiotic stress caused over 500 billion US dollar damage in crop production (Mittler, 2006; Suzuki et al., 2014). Moreover, abiotic stress never occurs as single stress at a time. One abiotic stress always causes the initiation of additional abiotic stresses in the cell. For example, chilling stress can alter the osmotic homeostasis in cells and cause dehydration stress (Farooq et al., 2009a); freezing can cause mechanical stress and dehydration stress (Yamazaki et al., 2009). Moreover, in nature, the plant itself is simultaneously exposed to multiple abiotic stresses (Mittler, 2006; Suzuki et al., 2014). For example, high-temperature and drought can co-occur in arid regions and be devastating for crop production and quality (Prasad et al., 2011; Vile et al., 2012).

Almost all the major abiotic stresses such as cold, heat, salinity, drought, and so on lead to secondary oxidative stress, which affects the cellular system by reactive oxygen species (ROS) (You and Chan, 2015). Thus, the effect of intracellular and extracellular multiple abiotic stresses at the same time is much more devastating for a plant than individual stress. Additionally, climate variation accounts for over 32%–39% of yield variability, and extreme climate events, which are also affecting arable land availability, are exacerbating the loss of global crop yield (Xiao and Ximing, 2011; Ray et al., 2015). Therefore, to face the ongoing and upcoming challenges to crop and plant production due to global climate change, it is vital to understand how plants sense these surrounding abiotic stresses and, with the results obtained, develop new methods to improve plant performance against emerging abiotic stresses.

Plants under low temperature

Despite the ongoing global warming and alarming predictions on future high-temperature extremes, climate models show that the global cold extreme will persist throughout the 21st century, and even it may become more intense and unpredictable than the 20th century (Kodra et al., 2011). Unpredictable, out of the pattern, and localized extreme cold events are more damaging than a regular seasonal cold during the winter. These unpredictable events are likely to be more frequent and intense in the upcoming decades (Marengo et al., 1997; Kodra et al., 2011). Approximately 57% of the global

land area and 26% of the rural land area are affected by cold and cold-related stresses (Cramer et al., 2011).

Among all the abiotic stresses, cold stress, which results from both chilling (0-10/15ºC) and freezing (< 0ºC) conditions, is one of the major abiotic stresses that happens all over the world and affects every process in the plant life cycle, including growth, development, survival, and productivity (Levitt, 1980). Cold stress response and its effect vary with plant species and geographical distribution; for example, agronomically important plants, such as rice (*Oryza sativa)*, corn (*Zea mays)*, banana (*Musa* spp.), tomato (*Lycopersicon esculentum*) originated in the tropical and subtropical area, are sensitive to chilling stress and result in injury (Thomashow, 1999; Chinnusamy et al., 2007; Zhu et al., 2007; Miura and Furumoto, 2013). On the other hand, plants native to the temperate climatic zones can take advantage of the chilling autumn temperature and prepare themselves for the upcoming freezing conditions by an adaptive strategy called cold acclimation (CA) (Gilmour et al., 1988; Thomashow, 1999; Miura and Furumoto, 2013).

The effect of cold or cold stress on plants depends on the duration of cold exposure, the rate of temperature drops towards the chilling/freezing limit, and the sensitivity of the plant species to cold. Depending on the duration of the cold, it can be chilling stress, which can affect the plants within a few hours to days, whereas a sudden drop can cause cold shock within few minutes (Phadtare et al., 1999; Nievola et al., 2017). After cold perception, even before the degree of cold becomes injurious to lethal plants, depending on their nature (tropical, subtropical, or temperate), plants act accordingly to prepare for extreme temperatures. Therefore, understanding how plants percept and generate signals to deploy molecular and physiological countermeasures holds an essential key to improving cold tolerance in plants.

Cold stress and membranes

The plasma membrane (PM) and the adjacent extracellular space are the primary checkpoints for external stimuli perception, signal generation, and solute transport (Chen and Weckwerth, 2020). As mentioned earlier, responses to cold by plants varies depending on the plant type and geographical distribution. Temperate plants can acclimate to survive freezing conditions after sensing and responding to chilling autumn conditions and decreasing day length (Levitt, 1980). Studies showed that during the CA process, plants increased the accumulation of soluble sugars, proteins, amino acids, and proline as cryoprotectants to prevent membrane damage and maintain osmotic potential during cold stress (Levitt, 1980; Xin and Browse, 2001; Furtauer et al., 2019). PM lipid composition changes during the CA period, and PM becomes less fluid and more rigid (Steponkus, 1984; Uemura and Yoshida, 1984; Uemura and Steponkus, 1994). Studies showed that PM proteins also undergo compositional changes during the CA process (Yoshida and Uemura, 1984). Large-scale mass spectrometry-based proteomics studies gave insight into specific proteins and their abundance that changes during CA (Kawamura and Uemura,

5

2003; Li et al., 2012a; Takahashi et al., 2013a; Takahashi et al., 2013b; Takahashi et al., 2016a; Takahashi et al., 2016b; Miki et al., 2019).

Rigidified membrane alters activities of channels, transporters, kinases, and receptors, and increases cellular phosphatidic acid (PA), calcium, and ROS. For example, cold-induced change in membrane fluidity led to excessive ROS production, such as H_2O_2 in the apoplast by membrane-bound NADPH oxidase RBOHD and by phospholipase D (PLD) activated PA in the cytosol (Ruelland et al., 2002; Nievola et al., 2017). Over-production and -accumulation of ROS can induce oxidative stress in plants, causing damage to plant cells, and the ultimate fate can be cell death (Demidchik, 2015). A balanced and optimum state of ROS, on the other hand, can work as a signaling component for stress response, growth, and development (Mittler, 2017). Apoplastic NADPH oxidase generated H_2O_2 is reported to play a crucial role in increasing chilling tolerance in tomato (Zhou et al., 2012).

Most of these studies were done under the CA process, which involves long cold exposure to the plants. However, to start the CA process, plants need to percept the earliest change in a temperature drop and send signals to the nucleus for the subsequent alternation of gene expression and other adaptive responses. Emerging studies are showing the role of membrane proteins in cold perception and signal transduction. A study in *Arabidopsis* found that cold activated PM localized cold-responsive protein kinase 1 (CRPK1). Activated CRPK1 could phosphorylate and translocate 14-3-3 proteins from the cytosol to the nucleus for fine-tuning the c-repeat binding factor (CBF) mediated signaling pathway (Liu et al., 2017). Another study on rice showed that PM and endoplasmic reticulum (ER) localized G-protein regulator COLD1 could activate the Ca^{2+} channel and confer chilling tolerance (Ma et al., 2015). Cold-induced PM rigidification could increase the Ca^{2+} influx, and phosphorylate PM localized calcium/calmodulin-regulated receptor-like kinase 1 (CRLK1), which in turn activated the canonical cold-responsive mitogen-activated protein kinase (MAPK) pathway via a cascade of protein phosphorylation (Furuya et al., 2013; Furuya et al., 2014). However, how plants sense the early cold exposure, what cold-responsive signaling events occur and lead to the CA process in temperate plants, and chilling stress response in tropical sub-tropical plants are still poorly understood. Therefore, studying early cold-responsive events in PM will increase understanding of cold perception and response by plants. Proper understanding of cold perception will ultimately help to develop cold-tolerant or resistant plant varieties.

Mass spectrometry-based proteomics for studying abiotic stress response mechanisms

Proteins play a crucial role in stress response because they are directly involved in regulating stress-responsive phenotypes by adjusting the physiological traits under suboptimal conditions. Abiotic stress significantly affects plant proteome by changing relative abundance, post-translational modifications, subcellular localization, protein-protein/protein-DNA interaction, and, ultimately, the biological function (Kosova et al., 2018). Moreover, protein characteristics analysis is one of the most

direct approaches to identifying associated genes via functional genomics studies (Komatsu et al., 2003). Furthermore, large-scale cellular and subcellular proteomics studies led to the discovery of many novel proteins involved in stress response (Hashiguchi et al., 2010). Still, most studies for characterizing cold and other abiotic stress signaling components were focused on genetic and transcriptomic levels (Saijo et al., 2000; Lee et al., 2005). However, most early responses to abiotic stresses occur through post-translational modifications (PTMs), and phosphorylation is the most frequent PTM in plants for signal transduction (Willems et al., 2019). Plant proteins go through cascades of protein phosphorylation and form complex signaling pathways that regulate essential biological processes, including external environmental response (Mishra et al., 2006; Li et al., 2015; Chen and Weckwerth, 2020). Untangling these complex signaling networks is one of the major challenges to study signaling pathways. Fortunately, advancements in modern mass spectrometry-based proteomics and phosphoproteomics enhanced the ability to understand and point out major components of signaling networks. Studying differential phosphorylation in response to environmental stresses led to the discovery of critical components of signaling pathways (Umezawa et al., 2013; Haruta et al., 2014).

Not only the phosphoproteomics of early stress response, proteomic studies of seed germination and germinating seedling may also provide essential information on how early stages of development shaped by protein abundance (Gallardo et al., 2001; Gallardo et al., 2002). Even though proteomics of seed has always been challenging due to the abundance of storage proteins that reduce the detection of regulatory proteins via liquid chromatography-tandem mass spectrometry (LC-MS), a few strategies have been developed to deplete the abundant storage proteins (Krishnan et al., 2009). However, there is no proteomic study on germinating seeds under any abiotic stress conditions. The advancement in proteomic technologies became a reliable method for studying protein abundance and PTM under environmental stress conditions (Kosova et al., 2018). Therefore, studying protein abundance change and PTM under stress conditions using both proteomics and phosphoproteomics together will help us better understand the stress response and design functional genomic experiments to improve stress-resistant crop varieties.

Practical approaches to improve stress tolerance or resistance

In the last couple of decades, several strategies have been developed to fight against biotic and abiotic stresses, including strategies using conventional breeding, genetic engineering, and selection of resistant varieties, some of which are tightly associated with mitigating the impact of stresses arising from global climate changes. However, some of these methods are time-consuming, expensive, and controversial in different countries. For example, genetically modified organisms can increase tolerance against stresses, but their use is unpopular among growers, consumers, and government in Europe. Additionally, the gaps in knowledge on the application between the labs and field, and from model plant

to crop plant transitions require extensive studies (Zhang et al., 2004; Savvides et al., 2016; Ahanger et al., 2017).

Alongside the methods mentioned above, a growing number of alternative approaches are emerging to deal with multiple abiotic stresses. For example, priming treatments, in which plants are pre-treated under stressed conditions or with endogenous, natural, or synthetic chemicals to prepare them against upcoming stresses, have gained popularity (Chen and Arora, 2011; Chen et al., 2012; Savvides et al., 2016). Among the different kinds of priming treatments, the most promising and commonly used chemicals are polyamines, hormones such as salicylic acid, reactive sulfur species such as NaHS, reactive nitrogen species such as nitric oxide, and reactive oxygen species (ROS) such as hydrogen peroxide (H_2O_2) (Tanou et al., 2009; Gill and Tuteja, 2010a; Parra-Lobato and Gomez-Jimenez, 2011; Hossain et al., 2015). Exogenous application of these chemicals has been found to be effective against different abiotic stresses (Tanou et al., 2009; Li et al., 2012b). However, most of these treatments are focused on single abiotic stress at a single stage of growth and development. Therefore, developing non-laborious, environment-friendly crop improvement methods against a wide range of abiotic stresses is still an ongoing demand.

Aims and objectives of the thesis

Although emerging studies show how plants perceive early abiotic and biotic stresses, how plants perceive the early cold and what role membrane proteins play in the earliest exposure to temperature drop are still unknown. Despite numerous attempts to improve crop and plant performance to against multiple abiotic stresses, there is a substantial demand for sustainable and straightforward practical methods.

As the background described above on the plant's response and changes under cold and other abiotic stresses, one of the objectives of my thesis was to understand how plants percept the exposure to a brief cold. To understand the early cold signaling events, I used modern mass spectrometry-based phosphoproteomics methods to study membrane phosphoproteomics in *Arabidopsis thaliana* (chapter 2).

Subsequently, alongside the basic understanding of early stress perception (Chapter 2), I also focused on a practical approach to develop a cost-effective, environment-friendly, single seed treatment method to improve abiotic stress tolerance in model plant rice and *Arabidopsis* (Chapter 3). In this method, I, for the first time, used Fenton-Haber Weiss reaction-based hydroxyl radical (•OH) to treat seeds for a single time and studied against a wide range of abiotic stresses, including cold. Furthermore, I used large-scale mass spectrometry-based proteomics to study early changes in seeds and germinating seedlings after the •OH treatment under cold stress (chapter 4).

Chapter 2

Large-scale phosphoproteomic study of *Arabidopsis* membrane proteins reveals early signaling events in response to cold

Summary

Cold stress is one of the major factors limiting global crop production. For survival at low temperatures, plants need to sense temperature changes in the surrounding environment. How plants sense and respond to the earliest drop in temperature is still not clearly understood. The plasma membrane and its adjacent extracellular and cytoplasmic sites are the first checkpoints for sensing temperature changes and the subsequent events, such as signal generation and solute transport. To understand how plants respond to early cold exposure, I used a mass spectrometry-based phosphoproteomic method to study the temporal changes in protein phosphorylation events in *Arabidopsis* membranes during 5 to 60 min of cold exposure. The results revealed that brief cold exposures led to rapid phosphorylation changes in the proteins involved in cellular ion homeostasis, solute and protein transport, cytoskeleton organization, vesical trafficking, protein modification, and signal transduction processes. The phosphorylation motif and kinase–substrate network analysis also revealed that multiple protein kinases, including RLKs, MAPKs, CDPKs, and their substrates, could be involved in early cold signaling. Taken together, my results provide a first look at the cold-responsive phosphoproteome changes of *Arabidopsis* membrane proteins that can be a significant resource to understand how plants respond to an early temperature drop.

Introduction

Throughout the Earth's history, plants have evolved adaptive mechanisms against multiple abiotic and biotic stresses. Cold stress, which results from both chilling (0-10/15 ºC) and freezing (<0 ºC) conditions, is one of the major abiotic stresses that happens all over the world and affects every process in the plant life cycle, including growth, development, survival, and productivity (Levitt, 1980). Cold stress responses vary with plant species. Agronomically important plants such as rice (*Oryza sativa*), corn (*Zea mays*), banana (*Musa* spp.), and tomato (*Lycopersicon esculentum*) originated from tropical and subtropical regions and are sensitive to cold stress. (Thomashow, 1999; Chinnusamy et al., 2007; Zhu et al., 2007; Miura and Furumoto, 2013). On the other hand, plants native to temperate climatic zones can take advantage of the colder autumn temperature and prepare themselves for the upcoming freezing conditions using an adaptive strategy called cold acclimation (Gilmour et al., 1988; Thomashow, 1999; Miura and Furumoto, 2013). Therefore, perception of and response to a drop in temperature is essential for plants that originate in tropic and sub-tropic regions to deploy survival mechanisms and for those in temperate climatic zones to start the acclimation processes and prepare for upcoming freezing stress. Responses to cold under acclimating and freezing conditions are studied extensively on both genomic and proteomic levels (Medina et al., 2011; Li et al., 2012a; Takahashi et al., 2013a; Takahashi et al., 2013b; Takahashi et al., 2016a; Takahashi et al., 2016b; Miki et al., 2019). However, there is little or no information available on how plants sense temperature drops over a short time (i.e., seconds and minutes) and how they respond and form adaptive signals to the cold. Sensing early changes is an essential step for the plant to initiate the adaptive process and survive under cold temperatures. Furthermore, how plants respond to early temperature drops is necessary to develop cold-resistant/-tolerant plant varieties and secure crop supply in the global climate change era.

The cell wall (CW), the extracellular/apoplastic region, and the plasma membrane (PM) are the outermost layers of a plant cell. Therefore, upon exposure to external environmental stimuli (biotic and abiotic), these layers are the most likely to receive, generate, and transmit signals further downstream and ultimately to the nuclei to form an appropriate response (Kim et al., 2009; Marshall et al., 2012; Osakabe et al., 2013; Mattei et al., 2016). PM is the outermost living part of the cell and has received the most attention for cold response studies in plants (Yoshida and Uemura, 1984; Takahashi et al., 2013a; Takahashi et al., 2013b; Takahashi et al., 2016a; Takahashi et al., 2016b; Miki et al., 2019; Takahashi et al., 2019). Few studies have also emerged on CW modifications during prolonged cold acclimation and in freezing response (Novaković et al., 2018; Willick et al., 2018; Takahashi et al., 2019). These studies indicate that the outer layers work in concert, as the first checkpoint to sense and generate signals from cold and other environmental factors, by changing their physicochemical conformation and composition and utilizing the power of posttranslational modifications (PTMs) such as phosphorylation of receptor-like kinases (RLKs) and other membrane-localized kinases (Yoshida and Uemura, 1984; Schulze, 2010; Furuya et al., 2013; Furuya et al., 2014; Zhu, 2016). Within 30 min

to cold exposure at 4 °C, PM rigidifies and increases Ca^{2+} influx into the cell, which in turn activates Ca^{2+}/calmodulin (CaM)-regulated receptor-like kinase1 (CRLK1), leading to mitogen-activated protein kinase (MAPK) pathway activation via a chain of phosphorylation events (Yang et al., 2010a; Furuya et al., 2014). The MAPK pathway is one of the canonical signaling pathways that enhance freezing tolerance in *Arabidopsis* (Teige et al., 2004; Furuya et al., 2013). A phosphoproteomic study of cold-tolerant and cold-sensitive bananas (*Musa* spp.) showed that Thr31 phosphorylation of MAPK kinase 2 (MKK2) is an essential component of the cold tolerance mechanism (Gao et al., 2017). CRLK1, MEKK1 (MAPK kinase kinase 1), and MKK2 are all reported to be localized in the PM (Benschop et al., 2007; Yang et al., 2010b). Similarly, another membrane-localized kinase, named cold-responsive protein kinase 1 (CPPK1), was activated upon prolonged cold exposure and directly sent a signal to the nucleus to fine-tune the C-repeated binding factor (CBF) signaling pathway by phosphorylating its 14-3-3 protein substrate (Liu et al., 2017). Another membrane-bound receptor-like kinase, receptor-like protein kinase 1 (RPK1), also increased cold tolerance along with tolerance to other abiotic stresses (Osakabe et al., 2010). CW, apoplast, PM-bound and localized RLKs, and transmembrane kinases (TMKs) and their signaling events are better documented in biotic stresses than abiotic stresses (Tenhaken, 2014; Novaković et al., 2018). Therefore, further studies are needed to discover cold stress-responsive RLKs and other protein kinases that are localized in the membranes and membrane-adjacent extracellular spaces.

Furthermore, these examples strongly indicate that protein phosphorylation of membrane-bound kinases and their targets (e.g., transporters, ion channels, and transcription factors) plays a crucial role in cold and other abiotic stress-triggered molecular events. Along with stress signal transduction, protein phosphorylation/dephosphorylation is also involved in regulating diverse biological and molecular functions such as cell division, differentiation, gene expression, hormone perception, homeostasis, and metabolism. Therefore, protein phosphorylation is one of the most important PTMs in plants (Kersten et al., 2006; Tichy et al., 2011; Chen and Hoehenwarter, 2015; Chen and Weckwerth, 2020). Signals for all the processes mentioned above originate at the PM and its adjacent regions either by a change in its physicochemical properties or by phosphorylation of the kinases associated with these regions. Therefore, studying and profiling the membrane-localized phosphoproteome and kinome on a large scale at earlier stages of cold exposure will help us to understand the plant's response to cold and other signaling events related to cold response.

Mass spectrometry (MS)-based shotgun phosphoproteomics has emerged as a powerful analytical tool to study protein phosphorylation on a large scale. MS-based phosphoproteomics has become a standard method to study global changes in phosphorylation dynamics (Nuhse et al., 2003; Niittyla et al., 2007; Engelsberger and Schulze, 2012; Xue et al., 2013; Stecker et al., 2014; Mattei et al., 2016). Although significant technical improvements have been made to study global or total phosphoproteins, characterization of membrane phosphoproteins is still challenging. Low abundance, short-lived

11

dynamic signaling events under specific conditions, contamination from other non-membrane proteins, and the overabundance of non-phosphopeptides are a few of the major roadblocks in studying membrane phosphoproteins (Nakagami et al., 2010; Savas et al., 2011; Chen and Weckwerth, 2020). Here, to improve the detection of low-abundance membrane phosphopeptides, I used a well-established membrane protein extraction method (Wu et al., 2017) with minor modifications and enriched phosphopeptides with TiO_2. I further analyzed TiO_2-enriched membrane phosphopeptides using a high-resolution mass spectrometer coupled with a long monolithic column to improve separation capacity. I prepared the microsomal membrane fractions (MMFs) from two-week-old *Arabidopsis* aerial parts after exposure to 2 °C for short periods (i.e., 5, 15, 30, or 60 min). Using these samples, I successfully identified phosphorylated proteins from different membrane-localized kinases and their substrates and analyzed their dynamics upon short cold exposure.

Materials and methods

Plant growth conditions and cold exposure

Twenty-five surface-sterilized seeds of *Arabidopsis thaliana* ecotype Colombia-0 (Lehle Seeds, Round Rock, USA) were sown in 9 cm square petri dishes containing modified Hoagland solution (Uemura et al., 1995) with 0.8% agar (Wako, Tokyo, Japan). The seeds were then cold stratified for 48 h at 4 °C. The seeds were germinated and grown for two weeks at 23 °C and 16/8 h photoperiod at 80-100 $\mu mol\,m^{-2}\,s^{-1}$ light intensity in a growth chamber (CLE-303, Tomy Digital Biology, Tokyo, Japan). For cold exposure analysis, agar plates containing two-week-old *Arabidopsis* seedlings were exposed to 2 °C for 0 min (control: no cold exposure), 5 min, 15 min, 30 min, and 60 min without the lid of the petri dish. Plates were flash-frozen in liquid nitrogen at the end of each cold exposure duration. The frozen plants were used for protein extraction or stored at -80 °C for later use. For each time point three independent biological replicates were used.

Microsomal membrane fraction (MMF) extraction

MMF was extracted according to the method of Wu et al. (Wu et al., 2017) with modifications. Around 75 two-week-old prefrozen seedlings (~1-1.5 g) were broken into small pieces and homogenized in 10 ml of homogenization buffer consisting of 500 mM sorbitol, 50 mM 3-(n-morpholino) propanesulfonic acid-KOH (MOPS-KOH) (pH 7.6), 5 mM ethylenediaminetetraacetic acid (EDTA), 5 mM dithiothreitol (DTT), 1 mM phenylmethylsulfonyl fluoride (PMSF), 2 mM salicylhydroxamic acid (SHAM), 25 mM sodium fluoride (NaF), 0.5 x protease inhibitor cocktail (p9599, Sigma-Aldrich, St. Louis, MO, United States), and 1 x phosphatase inhibitor cocktail 2 and 3 (P5726 and P0044, Sigma-Aldrich) using a 30 ml motorized glass homogenizer (81-0487, Sansyo Co., Ltd, Tokyo, Japan) on ice. For proper homogenization, the rotary pastel was moved up and down slowly for at least 3 min. The homogenate was filtered through six layers of cheesecloth and centrifuged

at 7500 x g for 15 min at 4 °C. The supernatant was collected and ultracentrifuged at 100000 x g for 50 min at 4 °C. The pellet was washed twice with homogenization buffer by centrifugation at 100000 x g for 20 min at 4 °C. The final washed pellet was collected as MMF and resuspended in a minimum volume of Tris-UTU buffer (100 mM tris aminomethane, 6 M urea, 2 M thiourea, pH 8.5). Protein concentration was measured using Bradford (Bio-Rad, Hercules, CA, United States) assay (Bradford, 1976). The MMF samples were used for peptide processing immediately or stored at -80 °C for later use.

Phosphoproteomic analysis

In-solution trypsin digestion

Phosphoproteomic analysis was carried out according to methods previously reported (Sugiyama et al., 2007; Nakagami et al., 2010; Umezawa et al., 2013; Choudhary et al., 2015; Ishikawa et al., 2019a; Ishikawa et al., 2019b) with minor modifications. For trypsin digestion, aliquots of MMF (1 mg protein) were used. The digested MMF was diluted four times with sterile distilled water, reduced with 10 mM DTT for 60 min, and then alkylated in the dark with 55 mM iodoacetamide for 30 min at room temperature. After alkylation, proteins were digested overnight at room temperature with trypsin gold (1:100, w/w; Promega, Madison, WI, United States). After digestion, the sample tubes were centrifuged for 5 min at 21000 x g at room temperature. The supernatant was transferred to a fresh tube and used for phosphopeptide enrichment.

Phosphopeptide enrichment and desalting

Phosphopeptides were enriched at room temperature using hydroxy acid-modified metal oxide chromatography (HAMMOC) with minor modifications (Sugiyama et al., 2007). Titansphere® Phos-TiO columns (syringe barrel type SPE cartridge, cat. No. 5010-21291, GL Sciences Inc., Tokyo, Japan) were used according to the manufacturer's instructions. Enriched phosphopeptides were desalted using two-step washing with a combination of GL-Tip SDB and GC columns (GL Sciences Inc., Tokyo, Japan) according to the manufacturer's instructions. Desalted phosphopeptides were dried in a vacuum evaporator (Tomy, Tokyo, Japan), resuspended in 10 μl of 0.1% (v/v) TFA, and stored at -80 °C for later LC-MS/MS analysis.

LC-ESI-MS/MS analysis

Desalted phosphopeptides were analyzed in the TripleTOF5600 system (AB SCIEX, Framingham, MA, USA) equipped with Autosampler-2 1D plus (Eksigent, Framingham, MA, USA) and NanoLC Ultra (Eksigent) using a MonoCap C18 High-Resolution 2000 column (GL science) and PicoTip emitter SilicaTip (New Objective Inc., Woburn, MA, USA). Peptides were eluted at a flow rate of 500 nl/min^{-1} with a four-step gradient, 0.5% (v/v) acetic acid: 0.5% (v/v) and 80% (v/v) acetic acid = 98:2 (0 min),

60:40 (300 min), 10:90 (20 min) and 98:2 (40 min). The eluate was sprayed into the mass spectrometer by electrospray ionization (ESI). The mass spectrometry (MS) scan range was 400–1,250 m/z, and the MS/MS scan range was 100–1,600 m/z.

Phosphopeptide identification and quantification

The spectrum files (.wiff and .wiff.scan) generated from the mass spectrometer were converted to peak lists in mascot generic format (.mgf) using Protein Pilot software (v5.0.0.4769; AB-SCIEX). The .mgf files were searched against the *Arabidopsis* protein database Araport11 (11 July 2019) (Cheng et al., 2017) obtained from the *Arabidopsis* information resource (TAIR) (https://www.*Arabidopsis*.org/) (Huala et al., 2001) in the Mascot ion search platform (v2.6, Matrix Science, London, UK). The search parameters were applied as follows: a precursor mass tolerance of 3 ppm, a fragment ion mass tolerance of 0.8 Da, and a cut-off value of 0.95, allowing for up to two missed cleavage from trypsin digestion. Fixed modification of carbamidomethylation of cysteine and variable modifications of oxidation of methionine and phosphorylation of serine, threonine, and tyrosine were used (Olsen et al., 2004; Nakagami et al., 2010; Umezawa et al., 2013; Choudhary et al., 2015; Ishikawa et al., 2019a). The false discovery rate (FDR) was calculated using the Benjamini–Hochberg method and set to 5%. Phosphorylation site localization confidence was assessed by site localization probability scores calculated from the mascot delta score, and the threshold level was set to > 0.75 to identify class-I phosphorylation sites (Savitski et al., 2011; Ishikawa et al., 2019a).

Skyline-Daily software (v20.1.1.83; https://skyline.ms/project/home/software/Skyline/daily) (MacLean et al., 2010) was used to quantify the peak areas/intensities. Search parameters in the Skyline-Daily were the same as those in the Mascot search parameters. A minimum of two peptides identified per protein was considered as a confident identification of that protein. The peak intensities, from both phosphorylated and proteotypic non-phosphorylated peptides generated from Skyline-Daily, were normalized using the EigenMS normalization method (Karpievitch et al., 2009; Karpievitch et al., 2012; Stetson et al., 2020) in the ProteoMM R-Bioconductor package (Karpievitch et al., 2020). All raw data files were deposited in the Japan Proteome Standard Repository/Database (jPOST; JPST000993, Kyoto, Japan).

Bioinformatic analysis

Identified phosphopeptides and proteotypic non-phosphopeptides from all biological replicates from each time point (0, 5, 15, 30, and 60 min) were compared using unsupervised Principal component analysis (PCA). Phosphopeptides identified in all five conditions were selected for further analysis. The changes in phosphorylation dynamics were studied by K-means clustering of the log-transformed normalized phosphopeptide intensities in MeV, MultiExperiment Viewer using Euclidean distance (Howe et al., 2010). Comparative analysis between untreated (0 min) and treated (cold exposed) was

performed in each characteristic K-means clusters; increased phosphorylation was assigned if the $\log_2$ fold change (Log_2FC) ratio of treated/untreated was ≥ 1 in at least two of the three biological replicates for each time point, and decreased phosphorylation was when the Log_2FC was ≤ 0.5 in at least two of three replicates. Individual phosphopeptides were compared using pairwise t-tests between average intensities at 0 min and each cold exposure time point. The relative time profile for significant phosphopeptide changes in each cluster was also created based on the Log_2FCs between 0 min and all other cold exposure time points. All time-profile clusters were visualized using a heatmap in the online platform ClustVis (https://biit.cs.ut.ee/clustvis/) (Metsalu and Vilo, 2015).

Gene ontology analysis

Gene Ontology (GO) annotation (GO-Slim, last update: 1 May 2020) for all *Arabidopsis* proteins was obtained from the latest TAIR (Huala et al., 2001). The GO annotation database was created by excluding genes with gene ontology-consortium evidence code IEA (Inferred from Electronic Annotation) and ND (No biological Data available) for further analysis. Over-representative GO term analysis was carried out in AgriGO (v2.0: http://systemsbiology.cau.edu.cn/agriGOv2/) (Du et al., 2010; Tian et al., 2017), uploading the GO annotation database as background. The Singular Enrichment Analysis (SEA) tool was used in the AgriGO platform combined with Fisher's exact test and Yekutieli's test (FDR under dependency) for a multi-test *P*-value (0.05) adjustment method; the minimum number of mapping entries was five, and plant GO-Slim was the Gene Ontology type. To decrease the chance of false discovery, GO cross-validation was also carried out in DAVID: BP_Direct (v6.8: https://david.ncifcrf.gov/) (Huang da et al., 2009; Huang et al., 2009) and CluterProfiler: groupGO function (Yu et al., 2012) using the same updated GO annotation database used in AgriGO as background, in g:Profiler g:GOSt using *Arabidopsis* as background and g:SCS threshold 0.05 (Raudvere et al., 2019), and finally matched with SUBA4 localization (Hooper et al., 2017). Significantly (adjusted *P*-value ≤ 0.05) enriched GO cellular component (GO_CC) terms related to MMF, such as plasma membrane (PM), endoplasmic reticulum (ER), Golgi (G), vacuole (V), cell wall (W), apoplast (A), cytoskeleton (CS), plasmodesma (PD), and other membrane-related proteins, were selected as the protein group of interest for further analysis. Proteins that belong to the cytosol (C), plastid (P), mitochondria (M), and nucleus (N) were excluded from further analysis.

For the over-representation analysis of GO biological processes (GOBP) and molecular function (GOMF), only the protein group of interest was used in process similar to that for GOCC. Significantly over-represented GO terms (BH adjusted $P < 0.05$ of Fisher' Exact test) were grouped to similar categories using REViGO (http://revigo.irb.hr/) (Supek et al., 2011). Settings used in REViGO were as follows: medium (0.7) similarity, UniProt *Arabidopsis* database (https://www.uniprot.org), and SimRel semantic measure. The negative log10-transformed, adjusted *P*-value < 0.05 for each GO term in the

REVIGO groups was scaled with vector scaling and visualized in a heatmap in the online platform ClustVis (https://biit.cs.ut.ee/clustvis/) (Metsalu and Vilo, 2015).

Phosphorylation motif dynamics analysis

Phosphorylation motifs were predicted using the motif-x (Chou and Schwartz, 2011) algorithm in rmotifx (https://github.com/omarwagih/rmotifx) (Wagih et al., 2016) R package. All confident phosphopeptides were used for motif prediction. Phosphopeptide sequences were centered around the phosphorylation sites (STY), and 13 amino acids ($\pm$6) around phosphorylated residues were extracted and submitted to the rmotifx. In cases where the phosphorylation sites were near the N/C terminal, the motif sequences were filled in using 13 amino acids with the required number of "X", which denotes any amino acid (Lin et al., 2015). The settings for rmotifx were as follows: the minimum number of central amino acid residues was set to 30 for Ser (S) and 20 for Thr (T) and Tyr (Y), the significance threshold was set to $P < 10^{-6}$, and background database was extracted from Araport11 (Cheng et al., 2017). Any enriched motif was attributed to a kinase or kinase group if the identical motif was reported in the literature or matched in the PhosPhAt database (Heazlewood et al., 2008; Durek et al., 2010; Zulawski et al., 2013). Similar motifs were grouped according to van Wijk et al. (van Wijk et al., 2014).

To predict kinase activity and kinase regulation dynamics, each enriched motif was assessed at each time point. The activity of upstream kinases affects the phosphorylation intensity of the downstream target motifs. To reveal the effect of kinases on targets, I computed the total average intensities from the phosphopeptides that belong to each enriched motif or motif groups at each time point and calculated the fold change between 0 min and any other cold exposure time point (Umezawa et al., 2013). Motif dynamics were assessed using Fisher's exact test using a 2 x 2 contingency table, as described by Lin et al. (Lin et al., 2015).

Kinase–substrate network construction

An updated kinase–substrate network was built by collecting experimental data from the literature (Wang et al., 2020) and the PhosPhAt database (Heazlewood et al., 2008; Durek et al., 2010; Zulawski et al., 2013). The constructed network was used as a benchmark for mapping and visualizing identified kinases and putative substrates in this study by Cytoscape (Shannon et al., 2003).

Results

Description of phosphoproteomic data of early cold treatment in *Arabidopsis*

The purpose of this study is to elucidate the signaling events in response to cold stress in the model plant *Arabidopsis* by a time-course (0, 5, 15, 30, and 60 min) based phosphoproteomic study (Figure 2.1A). I identified a total of 2795 unique phosphopeptides, which were phosphorylated in at least two biological replicates at all five time points, and these phosphopeptides constitute a total of 1360 proteins

(Table S2.1A, B). I performed a principal component analysis (PCA) to evaluate the quality of the biological replicates at each time point. PCA analysis showed all biological replicates at each time point cluster together, and simultaneously, were separated from each other (Figure 2.1B). Furthermore, about 90% of these phosphopeptides were singly phosphorylated (Figure 2.1C). From the identified phosphopeptides, a total of 2930 phosphosites were enriched, where the most frequent phosphorylation was observed in serine (S, 85%), followed by in threonine (T, 12%), and tyrosine (Y, 3%) (Figure 2.1D). The frequency distribution of phosphorylation sites was similar to those previously reported in plant phosphoproteomic studies (Nakagami et al., 2010; Umezawa et al., 2013; Wu et al., 2017; Hsu et al., 2018; Haj Ahmad et al., 2019; Ishikawa et al., 2019a; Ishikawa et al., 2019b).

The MMF used in the present study is a mixture of various cellular membranes and compartments and enriched in lighter membranes such as the PM, endoplasmic reticulum, Golgi body, and vacuole, but it also contains fractions from the extracellular space, cell wall, apoplast, cytoskeleton, plasmodesmata, cytosol, mitochondria, plastid, nucleus, and other cellular compartments. Because the objective of my study was to observe the phosphorylation level changes in proteins potentially involved in the early cold response in the MMF, I performed an over-representation analysis on the cellular localization of the proteins and divided them into two groups based on significant enrichment (Fisher test $P < 0.05$): (A) the protein group of interest, which includes proteins from the PM, endoplasmic reticulum, Golgi body, vacuole, extracellular space, cell wall, apoplast, cytoskeleton, and plasmodesmata; (B) the sub-portion of proteins from the cytosol, mitochondria, plastid, nucleus, and macromolecular complexes. Out of 1360 phosphoproteins, 858 were from group A. My detailed study in the following sections only included group A proteins, and the proteins from group (B) were not included in further analyses (Figure 2.1E). Group A contains 1821 phosphopeptides and 1894 phosphosites. Next, I analyzed the relative changes in the phosphopeptides after cold exposure compared to the control (0 min cold exposure) in a time-course manner (Table S2.1B).

Temporal profile of the phosphopeptides in response to cold

Previous phosphoproteomic studies of osmotic stress and systemin treatment reported that total protein abundance does not change within a time frame of minutes; instead, the peptide abundance comes from the changes in phosphorylation dynamics (Stecker et al., 2014; Wu et al., 2014; Haj Ahmad et al., 2019). To determine whether this was the case under my experimental conditions, I performed a proteomic study on plants exposed to cold for up to 60 min. I did not see any significant changes in protein abundance (Table S2.2). Therefore, the changes in peptide abundance I observed in this study were due to changes in phosphorylation itself rather than de novo protein synthesis. I next studied the phosphorylation dynamics upon cold exposure using K-means clustering of the log-transformed normalized phosphopeptides from the group A proteins. The temporal dynamics of phosphopeptides created eight characteristic K-means clusters (Figure 2.2). Upon cold exposure, a large number (481)

of peptides were dephosphorylated (Figure 2.2, clusters F and G). Among the dephosphorylated peptides, 140 peptides stayed in the dephosphorylated state relative to the control throughout the cold exposure period (Figure 2.2, cluster F). Cluster G, which contains 341 peptides, showed a fluctuation in its dephosphorylation pattern, but none of these peptides showed increased phosphorylation relative to the control. Next, four characteristic clusters were found where peptide phosphorylation transiently peaked at each of the four cold exposure time points (Figure 2.2, Clusters A, B, C, D, and E). Cluster A peaked very early at 5 min with 243 phosphopeptides, and cluster B with a peak at 15 min contained 177 phosphopeptides. I then grouped these two clusters as "early response" to cold exposure. The two clusters C (285 phosphopeptides) and D (209 phosphopeptides) peaked at later time points, 30 and 60 min, respectively. In cluster E, peptides were immediately phosphorylated upon cold exposure and maintained phosphorylation states throughout the cold exposure period. Even though peptides in this group (cluster E) showed continuous phosphorylation, their peak intensities fluctuated at different time points. In further steps, I redistributed 177 phosphopeptides from cluster E to clusters A and B (early response) and clusters C and D (late response) based on their highest peak intensities at each time point during cold exposure. Cluster H, containing 230 phosphopeptides, did not show any changes upon cold treatment compared to the control; it was classified as "unresponsive" and was excluded from further analysis. For quantitative analysis, I compared significant (Student's t-test, P-value < 0.05) fold changes (cold exposed/non-exposed: $0.5 \leq \log_2 FC \geq 1$) for individual phosphorylated/dephosphorylated peptides in each cluster and visualized them in a heatmap (Figure 2.3). All significantly (P-value < 0.05) phosphorylated peptides (1009) in early and late response groups were subjected to gene ontology over-representation analysis (ORA) of molecular function (GOMF) and biological processes (GOBP), and motif analysis.

Cold signal responsive molecular functions in *Arabidopsis*: GOMF

To gain insight into the biological relevance of phosphorylation, I performed an over-representation analysis (Fisher exact test) in early response and late response group proteins. The overrepresented GO terms revealed characteristic shifts in the molecular function (GOMF) of these phosphoproteins in response to cold exposure. Proteins involved in binding, catalytic activity, signaling, and transport were phosphorylated upon cold exposure (Figure 2.4). Binding proteins in the early response group were mostly phospholipid, calmodulin, clathrin, calcium, and other ion-binding phosphoproteins. Interestingly, ATP, chloride ions, the cytoskeleton, and microtubule-binding phosphoproteins were highly abundant in the late response clusters, and nucleic acid binding phosphoproteins were over-represented in both clusters (Figure 2.4A). Phosphoproteins with catalytic/hydrolase activity were significantly over-represented in the late response clusters, except for phosphoproteins related to serine/threonine phosphatase activity (Figure 2.4B). Proteins related to blue light photoreceptor activity were in the phosphorylated state throughout the cold exposure period.

Signal-transducing phosphoproteins were enriched only within 15 min of cold exposure, and soluble N-ethylmaleimide-sensitive factor (NSF) adaptor protein (SNAP) receptors were only phosphorylated in the late response group (Figure 2.4C). Signal transduction related proteins (kinase/transferase/transducers) were also significantly overrepresented after 30 min of cold stress; however, serine/threonine/tyrosine kinase, palmitoyltransferase, and galactosyltransferase activity-related phosphoproteins were only found in the early response group (Figure 2.4D). Transport and transmembrane transport-related phosphoproteins were enriched in early and late response clusters, where transmembrane transporters involved in auxin influx and ion/cation/carbohydrate transportation were only phosphorylated within 15 min of cold exposure (Figure 2.4D). Transporters and transmembrane transporters involved in auxin efflux, auxin proton symporter, anion channel activity, and ATPase-mediated transportation were highly enriched in the late cold response clusters (Figure 2.4E). In brief, these results show a large number of proteins involved in important molecular functions are temporally phosphorylated under cold exposure.

Cold signal responsive biological processes in *Arabidopsis*: GOBP

Changes in the molecular function of a gene product, such as protein or a group of proteins, in response to external or internal stimuli, initiate a collection of molecular events in different locations (cellular components) relative to the cell. These changes ultimately lead to a collective response from the cells, tissues, organs, and even the organism itself, contributing to a broader biological response/process (Balakrishnan et al., 2013; Thomas, 2017). To understand how the protein functionally changes due to phosphorylation upon cold exposure, I performed an over-representation analysis of biological processes (GOBP) in early and late response clusters (Figures 2.10, 2.11). Proteins involved in phosphorylation and signal transduction were over-represented in both early and late response to cold exposure; however, these processes were highly abundant in the late response group compared to the early response group (Figure 2.5A). A large group of proteins involved in trafficking and transport-related events (ion transport, vesicle-mediated transport, protein/peptide, and carbohydrate transport) was differentially overrepresented in response to cold (Figure 2.5B), such as ion transport-related proteins phosphorylated in an early responsive manner, except for chloride ion transport. Vesicle-mediated transport-related proteins were over-represented throughout cold exposure. However, proteins involved in Golgi-to-PM transport, exocyst assembly, exocytosis in vesicle docking, and receptor-mediated endocytosis were only enriched in early response clusters. Interestingly, exocytosis, vesicle docking, and transport proteins targeting the PM were exclusively found in late response clusters. Protein and glucose transport-related protein phosphorylation events took place early in cold exposure, but transmembrane transport, intracellular protein transport, peptide transport, and secretory protein transport-related processes were enriched in late cold exposure. Auxin-related processes were most abundant in late response clusters, including polar transport, basipetal transport, efflux, and auxin

homeostasis. Proteins that play a role in maintaining homeostasis, such as carbohydrate homeostasis and pH regulation, responded to cold early (Figure 2.5C). Biological processes related to phytohormones such as indole butyric acid, cytokinin, and gibberellic acid were exclusive in the late response clusters, whereas ethylene inhibitor cobalt ion responsive phosphoproteins were only found in the early response clusters. Interestingly, abscisic acid (ABA)-responsive proteins showed an increase in phosphorylation with cold exposure duration (Figure 2.5D). Proteins involved in responding to external stimuli such as biotic stress and abiotic stress, including blue light, cold stress, and osmotic stress response, were significantly over-represented in the early response group. With few exceptions, such as red light-responsive proteins, proteins involved in cold acclimation, and cellular response to heat, phototropism, and gravitropism were found in late response clusters (Figures 2.5E, 2.6). Defense response-related protein phosphorylation was also abundant in early response clusters, and interestingly cell death, negative response to cell death, and negative regulation of defense response-related proteins were highly enriched in the early response group. However, proteins responsible for CW callose deposition in response to stress were only found in late response clusters (Figure 2.5E). Another interesting group of proteins phosphorylated under cold exposure belonged to the cytoskeleton/actin filament/ microtubule-based process-related proteins. Most of the proteins from this cellular process were highly abundant in the late response clusters, except for the proteins involved actin-filament severing process (Figure 2.5E). Proteins involved in other cellular/metabolic processes were mostly phosphorylated in late response to cold (Figure 2.6). In summary, brief temporal exposure to cold results in dynamic changes in a wide range of biological processes in *Arabidopsis*. These biological processes may be involved in early cold perception.

Cold-responsive phosphorylation kinase-motifs

I performed a motif analysis using all the differentially phosphorylated phosphosites ($0.5 \leq \log_2 FC \geq 1$; $P < 0.5$) to gain insight into which kinases are involved in the early cold response. The Motif-x algorithm extracted 16 characteristic kinase motifs, where 15 were serine centered, and 1 was threonine centered, but no tyrosine-centered motifs were enriched (Figure 2.7A). These motifs were further grouped into eight major motif types, according to van Wijk et al. (Figure 2.7A) (van Wijk et al., 2014). The SP or [pS/pTP]-type motif group in this study consisted of [pSP], [pTP], [GpSP], [pSPXR], and [pSPK] motifs. The RXXS or [R/KXXpS/pT] motif group contained [RXXpS], [KXXpS], and [RRXXpS] motifs. The [pS/pTXD/E] or [pS/pTXXD/E] motif group contained [pSXD], [pSXE], and [pSXXE] motifs. The other individually enriched motifs were [SXpS], [LXR/KXXpS/pT], [pS/pTF], [pS/pTG], and [pSXP]. Most of these motif sequences are well annotated to their up-stream kinases in the literature and databases (Zhang et al., 1997; Ku et al., 1998; Schwartz and Gygi, 2005; Heazlewood et al., 2008; Durek et al., 2010; Khan et al., 2013; Zulawski et al., 2013; Lv et al., 2014; van Wijk et al., 2014; Wang et al., 2020). Proline-directed motifs [pS/pTP] are a potential substrate for MAPK, cyclin-

dependent protein kinase (CDK), CDK-like, and glycogen synthase kinase-3/shaggy- like kinase (GSK3/SLK). [R/KXXpS/pT] is a target motif for SNF1-related kinase II (SnRK2), calcium-dependent protein kinase (CDPK), Ca^{2+}/calmodulin dependent protein kinase (CaMKII), and CBL- interacting protein kinase (CIPK); it was also reported to be a binding motif for 14-3-3 proteins (Zhang et al., 1997; Ku et al., 1998; Schwartz and Gygi, 2005). Another basic motif [LXR/KXXpS/pT] was also found to be targeted by CDPK, SnRK2s, and SnRK3s (Wang et al., 2020). It was reported that SnRK2.6 targeted [GpS] motifs (Wang et al., 2020). Interestingly, I also found the [GpSP] motif, which is similar to [GpS]. Even though I classified [GpSP] under the general [pS/pT] motif group, it might also be a potential recognition site for SnRK2.6. [SXpS/pT] has been reported to be recognized by MAPK, CDK, RLKs, and receptor-like cytoplasmic protein kinases (RLCKs) (van Wijk et al., 2014). *Arabidopsis* AGC serine/threonine-protein kinase OXI1 (oxidative signal-inducible 1) and CIPK24/SnRK3.11 kinase SOS2 (salt overly sensitive 2) can recognize [pS/pTF], which is also known as a target for minimal MAPK (Wang et al., 2020). The motif group [pS/pTXXD/E] or [pS/pTXD/E] is a target for casein kinase II (CKII), and [pSXE] is also a potential recognition site for plant ERK1 and ERK2 (Umezawa et al., 2013; Pi et al., 2018). [pS/pTG] is a glycine-rich motif that mostly belongs to the secreted protein group and can be targeted by CDPK and protein phosphatase 2C (PP2C) (van Wijk et al., 2014). Even though the [pSXP] motif has yet to be assigned to a specific kinase, it has been reported as a potential target site for 14-3-3 binding proteins (van Wijk et al., 2014). Enrichment of these diverse groups of kinases indicates that brief exposure to cold significantly perturbed the kinome, and these potential kinases are involved in early cold-sensing and signaling networks.

Next, I targeted each motif/motif group and assigned them to their corresponding source phosphopeptides to study the time-course based dynamics using a Fisher's exact test (Figure 2.7B). The motifs showed a characteristic response pattern to cold exposure. Even though few motifs were significantly enriched at all time points, their activity indicates the upstream kinase actions during cold exposure, which may affect the change in intensities in the corresponding target motifs (Figure 2.7C) (Umezawa et al., 2013; Lin et al., 2015). In my data, I found that phosphopeptides containing [pS/pTP], [R/KXXpS/pT], [pS/pTF], and [pS/pTXXD/E]/[pS/pTXD/E] motifs were significantly enriched at all time points (Figure 2.7B). The phosphorylation tendency increased with cold exposure time, which was also visible from the increasing abundance of the phosphorylated peptides, indicating a higher level of kinase activity might belong to these motifs (Figure 2.7C). [SXpS] showed significantly increased enrichment at 30 and 60 min; however, the maximum abundance in the corresponding phosphopeptides was at 5 to 30 min with a decreasing trend at 60 min (Figure 2.7B and C). [LXR/KXXpS/pT] and [pS/pTG] showed increasing enrichment from 15 min, and phosphopeptide abundance peaked in the late response clusters with an increase in the cold exposure period (Figure 2.7B and C). Even though the [pSXP] motif was not significantly enriched under cold exposure, its corresponding peptide abundance peaked at 30 and 60 min (Figure 2.7B and C).

Kinase–substrate interaction network

I constructed an updated kinase–target network containing 3461 interactions (Figure 2.8, Table S3A) based on databases and a literature search (Heazlewood et al., 2008; Durek et al., 2010; Zulawski et al., 2013; Lin et al., 2015; Wu et al., 2017; Wang et al., 2020). Differentially and significantly ($P <$ 0.05) phosphorylated proteins in my study were then mapped into the kinase–substrate network to extract a subnetwork (Figure 2.9, Table S2.3B). The interaction network revealed that early cold signaling involved 695 highly complex kinase–substrate interaction events among MAPKs, SnRKs, CDPK/CaMKs, LRR-RLKs, SLKs, GSKs, CKs AGCs, and other kinases, and I also found their corresponding substrates in the motif-x analysis. Out of 695 interactions, MAP kinases, including MAPK, MAP2K, and MAP3Ks, formed nearly 350 interactions. ABA signaling related kinases SnRKs, including SnRK1, SnRK2, and SnRK3, were involved in 95 interactions, followed by 59 interactions by LRR-RLKs, 45 interactions by CDPK and CaMK, 40 interactions by AGC and STKs, 38 interactions by SLK and GSKs, and 36 interactions by CKs and CKLs (Table S2.3C). The complex interactions between different kinase–kinase and kinase–substrate counterparts indicate that the early cold response involves different signaling pathways to adjust to a low-temperature environment.

Discussion

This report provides dynamic evidence that signaling and molecular events in the model plant *Arabidopsis* switch by reversible protein phosphorylation after short exposure to cold. In this study, I found early cold response in plants at the posttranslational level associated with a complex network of cold signaling composed of various kinases and their targets. So far, to my knowledge, this is the first large-scale time-course phosphoproteomic study on *Arabidopsis* membranes and membrane-related proteins under brief cold exposure. This study will provide new insight into cold perception from a reversible phosphorylation point of view.

Cold-responsive kinases and signaling proteins might play a crucial role in early cold perception and signal transduction

Changes in phosphorylation to a large number of proteins in response to brief cold exposure indicate a significant perturbation in activity associated with kinases and phosphatases. A large number of enriched kinase target motifs from different major kinase families and direct identification of 152 kinases also imply a strong response from the kinases to cold exposure.

Ca^{2+} is one of the essential signaling components in plants, and cytosolic Ca^{2+} changes have been reported as one of the first sensors of cold stress as well as other stresses (Knight et al., 1996a; Knight and Knight, 2000; Marti et al., 2013; Yuan et al., 2018; Hiraki et al., 2019). Ca^{2+}/calmodulin (CaM) binding, CaM/CaM-like proteins, and calcineurin B like (CBL) and CBL-interacting proteins (CIPKs) play significant roles in sensing and interpreting Ca^{2+} signals (Luan, 2009; Mao et al., 2016) as well as

recruiting and activating other signaling components such as RLKs, CDPK/CaMKs, MAPKs, and ROS in response to cold stress (Zeng et al., 2015). PM-localized Ca^{2+}/CaM-regulated receptor-like kinase 1 (CRLK1), a serine/threonine kinase, in *Arabidopsis* is reported to be involved in cold stress response and activated by Ca^{2+}/CaM (Yang et al., 2010a). Further studies showed that this CRKL1 could interact and phosphorylate MEKK1, a core component of the cold-regulated MAP kinase signaling pathway (Yang et al., 2010b; Furuya et al., 2013). A phosphoproteomic study of cold stress in rice showed OsCDPK13 is an essential part of the cold response system (Khan et al., 2005). CDPK phosphorylation, in response to chilling stress, was also reported in plants, including Broussonetia papyrifera and Jatropha curcas (Pi et al., 2017; Liu et al., 2019). Similar to these studies, I also found several members of CDPK and CaM-domain protein kinase (CPK) (Tables 2.1, S2.1A) that were not reported to be regulated at the phosphorylation level in response to a brief cold response. In my study, a large number of CDPK/CaMK and CIPK target motifs ([LXR/KXXpS/pT], [R/KXXpS/pT], and [pS/pTG]) were enriched at the phosphorylation sites (Figure 2.7A) and in the kinase–target interaction network (Figure 2.9; Table S2.3), indicating the role of Ca^{2+}-mediated signaling pathways regulated at the phosphorylation level in the early cold response.

Receptor kinases (RKs) or RLKs have been extensively studied at the phosphorylation level in response to pathogens and hormones. However, out of 600 RLKs, only about 60 have been functionally characterized so far (Wu et al., 2016). Furthermore, only very few RLKs, for example, CRLK1 and RPK1, are functionally connected to cold response when exposed for more than several hours (Lee et al., 2005; Yang et al., 2010b; Furuya et al., 2013). Thus, questions remain about whether any other RLKs respond to cold and how they respond at the PTM level. In this study, I found a large number of RLKs were phosphorylated in response to cold exposure (Tables 2.1, S2.1A). For instance, multifunctional somatic embryogenesis receptor kinase 4 (SERK4) is involved in brassinosteroid (BR) signaling and regulation of BR-dependent growth, and it also negatively regulates cell-death growth and phytohormone signaling (He et al., 2007; Albrecht et al., 2008; Oh et al., 2009; Kong et al., 2016). Another peptide hormone-like receptor, RGF1 insensitive 3 (RGI3), is involved in meristem growth (Ou et al., 2016; Song et al., 2016). Transmembrane kinase 1 and 3 (TMK1 and TMK3) were reported to be involved in auxin-mediated cell growth and development and ROP GTPase signaling (Xu et al., 2014; Cao et al., 2019). These RLKs might be involved in growth and development under cold stress. Botrytis-induced kinase 1 (BIK1) is one of the vastly studied RLKs that is central to the plant immune response and is also involved in Ca^{2+}-dependent reactive oxygen (ROS) signaling, ethylene, and BR response (Lin et al., 2013; Liu et al., 2013; Li et al., 2014), but it has never been reported to be phosphorylated in response to cold (Lin et al., 2013; Liu et al., 2013; Li et al., 2014). Receptor cytoplasmic kinase PBS1-like protein 27 (PBL27) activates the MAPK signaling cascade in response to chitin (Yamada et al., 2016). These findings imply that early RLK-mediated cold signaling might share, at least in part, some common pathways with other biotic, abiotic, ROS, and hormone signaling

23

processes. Furthermore, the close phylogenetic relationship (Figure 2.10) between these cold-responsive RLKs could indicate a coordinated response from related gene family members at the PTM level under cold and could potentially be involved in cold perception and signaling in *Arabidopsis*.

The most studied cold response pathway in *Arabidopsis* is the MAP kinase pathway, which is linked to freezing tolerance in cold-acclimated plants (Teige et al., 2004; Furuya et al., 2014). I have found four phosphoproteins from poorly characterized MAP4K members of MAP kinases. Interestingly, three of these MAP4Ks were found to be closely positioned in the phylogenetic tree (Figure 2.11A). Moreover, MAP4K5 and MAP4K6 were phosphorylated at the SXS motif in the central region of the protein but not inside any kinase domain. It could be possible that upstream RLKs or CDPKs phosphorylate these two proteins in the target SXS motif and regulate the function. It has been reported that some members of MAP4Ks can phosphorylate MAP3Ks or Raf kinases or directly phosphorylate MAP2Ks; others can function as adapters (Sun et al., 2000; Champion et al., 2004). Similar to MAP4Ks, phylogenetic analysis of MAP3Ks and MAP3K-Raf (Figure 2.11B, C) showed most phosphorylated proteins are closely related to their gene family members, with a few exceptions such as raf22, raf36, and raf47. For example, raf18 in this study, raf20, and raf24 (Miki, 2015), which are closely positioned in the phylogenetic tree, were phosphorylated within 5 to 30 min of cold exposure in the RXXS motif (Figure 2.11B). Even though there are no known functions ascribed to most Raf kinases, their response at the phosphorylation level to different stresses, including early cold (in this study) and early osmotic stress (Stecker et al., 2014), indicates a potential involvement of Raf kinases in early cold stress signaling. Other members of MAP3Ks phosphorylated in response to cold are also closely related in their phylogenies, such as M3KE1 and MAP3KE2, YDA/YODA, and MAP3Kγ (Figure 2.11C). These four MAP3Ks are reported to be involved in plant growth, development (Bergmann et al., 2004; Chaiwongsar et al., 2006; Chaiwongsar et al., 2012), and the MAPK signaling pathway (Meng et al., 2012; Yamada et al., 2016). Similar cold response phosphorylation patterns within identical phosphosites in closely related subfamily members of a large gene family could indicate coordinated phosphorylation and may be important for cold perception/signaling. Furthermore, phosphorylation of more downstream kinases such as MKK2, MAPK6, MAPK8, and MAPK16 suggests that MAP kinases are involved in the early cold response and signal transduction. In summary, reversible phosphorylation of these MAP kinases, the highest enrichment in MAP kinase target motifs, and the highest number of kinase-substrate interactions indicate that the MAP kinase families play an essential role in early cold signaling.

Enrichment of SnRK2 target motifs [R/KXXpS/pT] and [LXR/KXXpS/pT] as well as a large number of SnRK targets from the kinase-substrate network also indicate that the ABA signaling pathway is triggered in response to brief cold exposure. GOBP analysis showed that ABA-responsive proteins were phosphorylated throughout the cold exposure (Figure 2.5D). Although I could not detect any SnRKs in my data, I found several SnRK substrates reported to be involved in different biological

processes in response to different abiotic stresses, such as respiratory burst oxidase homolog protein D (RBOHD), ATP-binding cassette (ABC) protein G36 (ABCG36), plasma membrane intrinsic protein 2-7 (PIP2-7), phototropin 2 (PHOT2), syntaxins of plants 121 (SYP121), and myosin motor XI-K (Tables 2.1, S2.1A, S2.3A, B).

A few other important kinases and their substrates were also phosphorylated in response to cold exposure (Tables 2.1, S2.1A) such as GSK3/shaggy-like kinase (ASK) brassinosteroid (BR) insensitive 2 (BIN2/ASK7), a positive regulator of BR signaling (Li et al., 2001), and GSK3/SHAGGY-like protein kinase 1 (ASK9) and BSK4, negative regulators of BR signaling (Sreeramulu et al., 2013). Phosphorylation of the BR signaling pathway regulators might indicate an involvement of BRs in early cold response in *Arabidopsis*. Casein kinase-like 2 (CKL2) was also phosphorylated immediately upon cold exposure. In addition, I found several reported and putative substrates of CK2 in the kinase-substrate network. A recent phosphoproteomic study in tomatoes also showed that CKL2 homologs were phosphorylated in response to prolonged cold stress, where SnRK2E could directly phosphorylate CKL2 (Hsu et al., 2018).

Early cold response mediated protein phosphorylation can activate phospholipid / phosphoinositide signaling events

Phospholipids are the main building blocks of PM and responsible for maintaining the membrane structure and function. Phosphoinositides (PIs), one of the lipid family members present in small amounts in the membrane, are involved in various crucial functions in plant growth and development, including environmental adaptation. From the gene ontology analysis (Figure 2.5A), I found that phospholipid, phosphatidylinositol binding, and signaling-related proteins were phosphorylated within 15 min of cold exposure, indicating that phospholipids respond to the temperature drop at a very early stage. I found a total of 44 phosphopeptides from different lipid-related proteins, and 16 were involved in the phosphatidylinositol metabolism pathway (Tables 2.1, S2.1A). The phosphatidylinositol metabolism pathway members found in this study are involved in the generation and degradation of PIs. It has been reported that PIs are continuously generated and degrade rapidly and dynamically in response to different abiotic stresses such as wounding (Mosblech et al., 2008), heat stress (Mishkind et al., 2009), and salt stress or osmotic stress (DeWald et al., 2001). Phosphatidylinositol 4-kinase (PI4Ks) can phosphorylate PIs and generate PI monophosphates PI3P and PI4P. PI monophosphates can further be phosphorylated by forms aploid and binucleate1 (FAB1) and phosphatidylinositol 4-phosphate 5-kinase (PIP5K) into phosphatidylinositol 3,5-bisphosphate (PI(3,5)P$_2$) and phosphatidylinositol 4,5-bisphosphate (PI(4,5)P$_2$), respectively (Heilmann, 2016). Vacuolar localization of PI(3,5)P$_2$ under osmotic stress is essential for maintaining the proper structure and function of vacuoles in yeast (Dove et al., 1997; Bonangelino et al., 2002; Ho et al., 2012). PI(3,5)P$_2$ also accumulates in the early osmotic stress response in *Arabidopsis* (Stecker et al., 2014). FAB1 and/or

its product PI(3,5)P$_2$ are essential for ABA-mediated stomatal closure, pollen tube growth, development, viability, endosome maturation, and interaction with microtubules (Hirano et al., 2015). In moss, PI(3,5)P$_2$ are required for polarized cell growth and actin-cytoskeleton arrangement (van Gisbergen et al., 2012). Endomembrane-localized FAB1 kinase knockout or knockdown results in enlarged vacuole formation in yeast because of impaired membrane trafficking (Cooke et al., 1998; Gary et al., 1998; Hirano et al., 2011). The PI4P-5K product PI(4,5)P$_2$ is also well known for its role in exocytosis, actin cytoskeleton organization, vesicle-mediated trafficking, and regulation of ion channels (Suh and Hille, 2005; Yao and Xue, 2011).

Furthermore, suppressor of actin 1 (SAC1) and phospholipase C/D (PLC/D) can degrade different PI species and generate downstream second messengers (Heilmann, 2016). For example, PLC2 is one of the critical enzymes that can catalyze the hydrolysis of PI(4,5)P$_2$ into diacylglycerol (DAG) and inositol 1,4,5-trisphosphate (IP3), which in turn increases Ca^{2+} influx into the cytoplasm (Kim et al., 2001; Hunt et al., 2004). Diacylglycerol kinases (DGKs) can convert DAG into phosphatidic acid (PA) (Munnik, 2001), and PA is well known as a signaling molecule under different kinds of abiotic stresses, including cold. Interestingly, in my study, Sec14p-like phosphatidylinositol transfer family protein PATL3, responsible for transferring PIs to the PM (Di Paolo and De Camilli, 2006), was found to be phosphorylated throughout the cold exposure duration (Tables 2.1, S2.1A). Phosphorylation of these PI kinases, phosphatases, and trafficking-related proteins clearly indicates that PI is involved in early cold perception, signaling, and cytoskeleton organization and might be regulated by posttranslational modifications.

Early cold response events can be associated with cytoskeletal and vesicle trafficking systems

The cytoskeleton in plants mainly consists of microtubules and actin filaments. It is essential for maintaining cell shape, and it facilitates organellar and vesicular trafficking inside the cell (Wang et al., 2011). Several cytoskeleton-related proteins were phosphorylated in response to early cold exposure, including myosin and myosin-binding (MyoB) proteins myosin 1 (VIII-1), myosin-5 (XI-1), myosin-9 (XI-C), myosin-17 (XI-K), and MyoB7 (Tables 2.1, S2.1A). MyoB7 phosphorylation peaked at 5 min, and other myosin and myosin family proteins mostly peaked after 30 min of cold exposure. The myosin-binding protein MyoB1 showed increased phosphorylation within 2 min of osmotic stress (Stecker et al., 2014). In addition, myosin-like protein abundance was also found to be increased under cold stress in rice and perennial grasses (Yan et al., 2006; Xuan et al., 2013). Myosin and myosin-binding proteins facilitate cytoplasmic streaming (Peremyslov et al., 2013). Even though myosin and myosin-binding proteins respond to cold and osmotic treatments, their exact function has yet to be determined. Perhaps, phosphorylation in the myosin-binding and myosin motor proteins could act as an early adaptive response to cold to maintain proper growth via cytoplasmic streaming and maintain cytoskeletal integrity of the cell under prolonged cold.

Microtubule-related proteins, 65 kDa microtubule-associated protein 1 (MAP65-1), microtubule-associated protein 70-2 and 70-3 (MAP70-2 and MAP70-3), tubulin alpha-3 (Tuba-3), and microtubule-associated protein TORTIFOLIA1 (TOR1) were also phosphorylated and categorized in the late response clusters (30 min and 60 min, Tables 2.1, S2.1A). These proteins are responsible for the bundling and stabilization/destabilization of microtubules, the formation of tubulin dimers, and cell division (Mattei et al., 2016). Microtubules also act as sensors that perceive mechanical membrane stress derived from cold (Nick, 2013). Furthermore, the sensory function of microtubules is determined by dynamic instability and subsequent formation of stable microtubules during stress adaptation (Nick, 2013). The MAP65-1 protein is phosphorylated in the microtubule-interacting region (pS532), and phosphorylation in this region disrupts the interaction properties (Smertenko et al., 2006). Moreover, in the gene ontology analysis, I also observed that actin filament and microtubule-based processes were enriched in the late response group (Figure 2.5F). It might be possible that with the increasing duration and intensity of cold exposure, plant cells sense the cold via phosphorylation mediated microtubule disruption, which acts as a cue for further cold adaptation-related processes.

Endosomal trafficking plays a crucial role in plant growth and development and maintains organellar homeostasis under different stressful conditions. Several studies showed endosomal transcript or protein abundance changes in response to longer durations (several hours to days) of cold stress (Minami et al., 2009; Ashraf and Rahman, 2019; Miki et al., 2019; Li et al., 2020). However, before this study, it was unclear whether endosomes also respond to early cold exposure at the protein phosphorylation level. In my study, I observed changes in several previously described members of vesicle-mediated transport cargoes in plants at the phosphorylation level (Tables 2.1, S2.1A). For example, dynamin-like protein 2A and 2B (DRP2A, DRP 2B), sec7 domain-containing protein GN (GNOM), SYP121 and SYP132, soluble n-ethylmaleimide-sensitive factor adaptor protein 33 (SNAP33), sorting nexin 1 and 2A (SNX1, SNX2A), vacuolar protein sorting 41 (VPS41), and other proteins (Tables 2.1, S2.1A) showed cold-responsive phosphorylation within 60 min of cold exposure, suggesting that their PTM level changes might prepare plants for a longer cold exposure or stress.

Transporters respond to early cold stress to maintain homeostasis

Under any environmental stress situations, for proper growth, development, and survival, plants consistently need to maintain ionic and cellular homeostasis through different transporter and channel proteins located in the membranes by balancing the influx and efflux of different ions, toxic byproducts, and carbohydrates (Conde et al., 2011). Phosphorylation changes in transporter proteins are also one of the rapid adaptive responses in plants under environmental stresses (Chen and Hoehenwarter, 2015). Many proteins related to solute and ion transport were also phosphorylated upon cold exposure (Tables 2.1, S2.1A). I found that two Ca^{2+} channel/transporters hyperosmolality-gated Ca^{2+} permeable channel 1.1 and 1.2 (AtOSCA1.1 and 1.2) were phosphorylated in the conserved C-terminal cytoplasmic domain

at a close distance to each other at pT750 (at 15 min only) and pS757 (5 min and peaked at 30 and 60 min) (Tables 2.1, S2.1A). Both of these channels are known to permeate Ca^{2+} in response to osmotic stress, and AtOSCA1.1 is an essential component of osmosignaling (Hou et al., 2014; Yuan et al., 2014). However, these two phosphorylation sites were never functionally characterized in any stress response. Moreover, AtOSCA1.1 is also the first genetically identified Ca^{2+} channel. It is possible these two phosphosites, similar to osmosensing, play an essential role in sensing cold. Interestingly, I also found two autoinhibited Ca^{2+} ATPase (ACA), ACA1 and ACA4, were phosphorylated within 5 min and decreased gradually with the cold exposure duration (Tables 2.1, S2.1A). These ACAs are responsible for Ca^{2+} efflux out of the cell and maintaining Ca^{2+} balance in the cell (Bose et al., 2011). Elevation of Ca^{2+} concentration inside the cell under cold is a significant signaling event that initiates further downstream canonical signaling pathways (Knight et al., 1996a; Carpaneto et al., 2007; Yuan et al., 2018; Hiraki et al., 2019). In this study, phosphorylation in both Ca^{2+} influx and efflux channels is possibly involved in modulating a balanced Ca^{2+} level for fine-tuning Ca^{2+}-mediated signaling events under cold.

During the cold acclimation process, plants accumulate various cryoprotectants. Soluble sugars are one of the major cryoprotectants and can protect plants from freezing damage and maintain cellular integrity and functions (Guy et al., 1992). In my study, I found several sugar and carbohydrate transmembrane transporters respond to early cold exposure, such as bidirectional sugar transporter SWEET12, polyol/monosaccharide transporter 5 (PLT5), tonoplast monosaccharide transporter 1 and 2 (TMT1, TMT2), sugar transporter ERD6, and ERD6-like 6 (ERDL6) (Tables 2.1, S2.1A). Reports showed disruption of SWEET12 resulted in thinner stems and reduced freezing tolerance in *Arabidopsis* (Le Hir et al., 2015), and its transcript levels increased under drought stress (Durand et al., 2016). However, before this study, there was no report on phosphoproteome level changes in SWEET12 in response to cold. Vacuolar monosaccharide transporters TMT1 and TMT 2 were reported to be phosphorylated at S385 and S376 under 5 days cold acclimation at 4 °C (Schulze et al., 2012). In my study, I found TMT1 was phosphorylated at pS277 throughout the cold exposure, and phosphorylation at pS446 immediately decreased at 5 min, then increased four-fold at 15 min and decreased at 30 and 60 min. TMT2 showed increased phosphorylation at pS448 peaked at 5 min and was maintained throughout the cold exposure, where pS287 peaked at 60 min only (Tables 2.1, S2.1A). All phosphorylation took place between transmembrane domains 5 and 6, and 6 and 7, which generally agrees with in silico prediction studies of phosphorylation sites in TMTs (Wingenter et al., 2011). Similar to the reports showing that phosphorylation regulates sugar transport under prolonged cold stress and other abiotic stresses (Schulze et al., 2012), my study indicates that in *Arabidopsis*, the early cold response also initiates sugar transport-related events in PM and vacuoles and might be regulated by phosphorylation.

I observed strong phosphorylation in two PM proton pump members: H^+ATApase1 (AHA1) and H^+ATPase4 (AHA4) (Tables 2.1, S2.1A). AHA1 was phosphorylated at multiple sites, including the canonical 14-3-3 protein binding YTV domains such as T881, T948, and the inhibitory S899 site. AHA4 showed constant phosphorylation at pT959 inside the 14-3-3 protein binding YTV domain throughout the cold exposure after peaking at 5 min. The binding of 14-3-3 protein at pT948 and pT959 in the YTV domain activates the proton pump (Olsson et al., 1998; Axelsen et al., 1999). On the other hand, phosphorylation at pS899 inhibits pump activity by an unknown mechanism (Haruta et al., 2014). The observed phosphorylation at both 14-3-3 protein binding sites and the pS899 inhibitory site in this study seem to be contradictory to the cold response. Even though AHA1 is phosphorylated at the inhibitory pS899 site, the pumps might be hyperactivated by the phosphorylated interactor isoform 1 (PPI1). It has been reported that PPI1 can hyperactivate AHAs (Viotti et al., 2005). I observed immediate phosphorylation of PPI1 at 5 min, and increased phosphorylation was maintained at 30 min and 60 min (Tables 2.1, S2.1A).

One of the most potent transporter groups in plants is the ATP-binding cassette (ABC) transporters. ABC transporters are reported to be involved in sequestration of toxic byproducts and in exchanging compounds like phytohormones (auxin), secondary metabolites, and defense molecules(Kang et al., 2011; Hwang et al., 2016). ABC transporters have mostly been studied at genomic and transcriptomic levels; for example, plants with overexpressed ABCG36 show improved resistance to salt and drought stress (Kim et al., 2010). ABCC1 acts as a pump for glutathione S-conjugates (Lu et al., 1997), and ABCB1, ABCB14, ABCB19, ABCG36, and ABCG37 were reported to be involved in auxin transport mediated plant growth and development (Lewis et al., 2009; Ruzicka et al., 2010; Cecchetti et al., 2015). In addition, a few studies showed their regulation and function at the phosphorylation level; for example, ABCB19 is a direct phosphorylation target of kinase PHOT1, which can transiently deactivate ABCB19 and result in the accumulation of auxin (Christie et al., 2011), and ABCG36 is phosphorylated in response to pathogen attack. I also found several ABC transporters to be phosphorylated under early cold exposure, and 75% of these were immediately phosphorylated within 5 min of cold exposure (Tables 2.1, S2.1A). The most notable transporters found in my study were ABCG36/37, ABCB1, and ABCC1, which were involved in detoxification, auxin transport, biotic and abiotic stress responses, and resistance (Hwang et al., 2016). PTM or phosphorylation-level regulation of these ABC transporters found in this study might play a crucial role in maintaining homeostasis and detoxification as an adaptive early cold response in *Arabidopsis*.

Auxin is a key phytohormone involved in different regulatory processes in plants. Spatiotemporal distribution of auxin is critical for auxin-mediated growth and development under normal and stressful conditions, including cold (Shibasaki et al., 2009; Grunewald and Friml, 2010; Bielach et al., 2017). Studies reporting the involvement of auxin transport or homeostasis are mostly carried out under prolonged exposure (several hours to days), but not short (within minutes) exposure to stress as I

employed in my study. Furthermore, most studies have focused on functional regulation at the genomic or transcriptomic level than the PTM level. Reversible phosphorylation at conserved serine and threonine residues could control the spatiotemporal distribution of auxin efflux carrier family protein 1 (PIN1) and its transport activity (Huang et al., 2010). In my study, I found auxin transporter proteins such as AUX1/LAX (influx) and PIN3, 4, and 7 (efflux) were phosphorylated in response to early cold stress (Tables 2.1, S2.1A). AUX1 was phosphorylated immediately and maintained its phosphorylation throughout the cold exposure time at two different phosphosites, pS14 and pS27, and inside the target SXXD/E motifs for casein kinase (CKII). On the other hand, PIN3 was phosphorylated at conserved pS366 with a 1.8-fold increase at 5 min and peaked at 60 min. PIN4 was also phosphorylated at conserved pS395 within the SXXD/E motif and maintained its phosphorylation throughout the cold exposure/treatment time and peaked at 60 min. I also found a phosphosite of PIN7 at pS431 in the SXXD/E motif, which maintained a continuous phosphorylation state. CKII was also reported to play an essential role in auxin transport and auxin-mediated growth and development in *Arabidopsis* (Moreno-Romero et al., 2008; Mulekar et al., 2012). Interestingly, PIN7 was also phosphorylated at T242 in the conserved TPRXSN motif. The TPRXSN motif is involved in phosphorylation-dependent control of PIN1 localization (Huang et al., 2010). Cold-responsive phosphorylation of PIN and AUX1 at different conserved sites indicates an essential role of protein phosphorylation under a short period of cold exposure, which might be involved in auxin transport and homeostasis for maintaining growth and development for upcoming longer and extreme cold conditions.

My data also showed that PM intrinsic proteins (PIPs) respond actively and temporally to brief cold exposure (Tables 2.1, S2.1A). I observed continuous phosphorylation of PIP2-5 (pS279) throughout cold treatment. A doubly phosphorylated peptide of PIP2-6 (pS279 and pS282) was phosphorylated over two-fold at 60 min, and PIP2-7 (pS276) showed decreasing phosphorylation after peaking at 5 min of cold exposure (Tables 2.1, S2.1A). PIPs are transmembrane transporters for water and small molecules and operate in a gated, controlled way. Gating properties vary under different abiotic stresses and are controlled by pH in flooding/anoxic conditions (Tournaire-Roux et al., 2003; Fischer and Kaldenhoff, 2008), phosphorylation/dephosphorylation under drought stress and low temperature (Shelden et al., 2010; Lee et al., 2012), and calcium under salt stress (Prak et al., 2008). It was also reported that chilling-induced H_2O_2 could be diffused by PIPs in a phosphorylation-dependent manner in maize (Aroca et al., 2005). Previously it was shown that phosphorylation at pS280 and pS283 of PIP2-1 was associated with gating or hydraulic conductivity (Prado et al., 2013). Multiple sequence alignment analysis showed that pS279 of PIP2-5 and PIP2-6, and pS276 of PIP2-7 are conserved with pS280 of PIP2-1, and the pS282 of PIP2-5 is also conserved with pS283 of PIP2-1 (data not shown). Phosphorylation of PIP2s in all these phosphosites suggests that the activity of the PIPs is controlled in a phosphorylation-dependent manner under cold and maintains cellular water and H_2O_2 in a balanced state. Previous studies also showed that PIP1-4 and PIP2-5 could regulate cold acclimation and freezing

tolerance in *Arabidopsis* (Rahman et al., 2020). Thus, continuous phosphorylation of PIP2-2 at its regulatory S279 position throughout cold exposure, along with other PIP2s, might play a crucial role in cold response and prepare plants for long-term cold acclimation.

ROS signaling under cold response

ROS generating respiratory burst oxidase homolog D (RBOHD) was also phosphorylated, as shown in this study, which has been never reported in response to brief cold exposure (Tables 2.1, S2.1A). In this study, RBOHD was phosphorylated in pS8, pS148, pS163, and pS347 within 15 min of cold exposure (Tables 2.1, S2.1A). RBOHD can generate ROS via Ca^{2+}-dependent and -independent phosphorylation by CDPKs/CIPKs and BIK1 kinase, respectively (Kadota et al., 2014; Li et al., 2014). Ca^{2+}-dependent protein kinase 5 (CPK5) and BIK can phosphorylate and regulate RBOHD at the same amino acid positions (pS148, pS163, and pS347) (Boudsocq et al., 2010; Kadota et al., 2014; Kadota et al., 2015), which are the same positions I observed as cold-responsive phosphorylated sites in this study. Interestingly, in my data, I detected both CPK5 and BIK were phosphorylated in response to brief cold (Tables 2.1, S2.1A). Furthermore, the phosphosites showed increased phosphorylation containing characteristic RXXS/LXRXXS motifs, a potential target motif of CDPKs (Tables 2.1, S2.1A). This rapid phosphorylation of ROBHD and its kinases indicates ROS signaling involvement in early cold response.
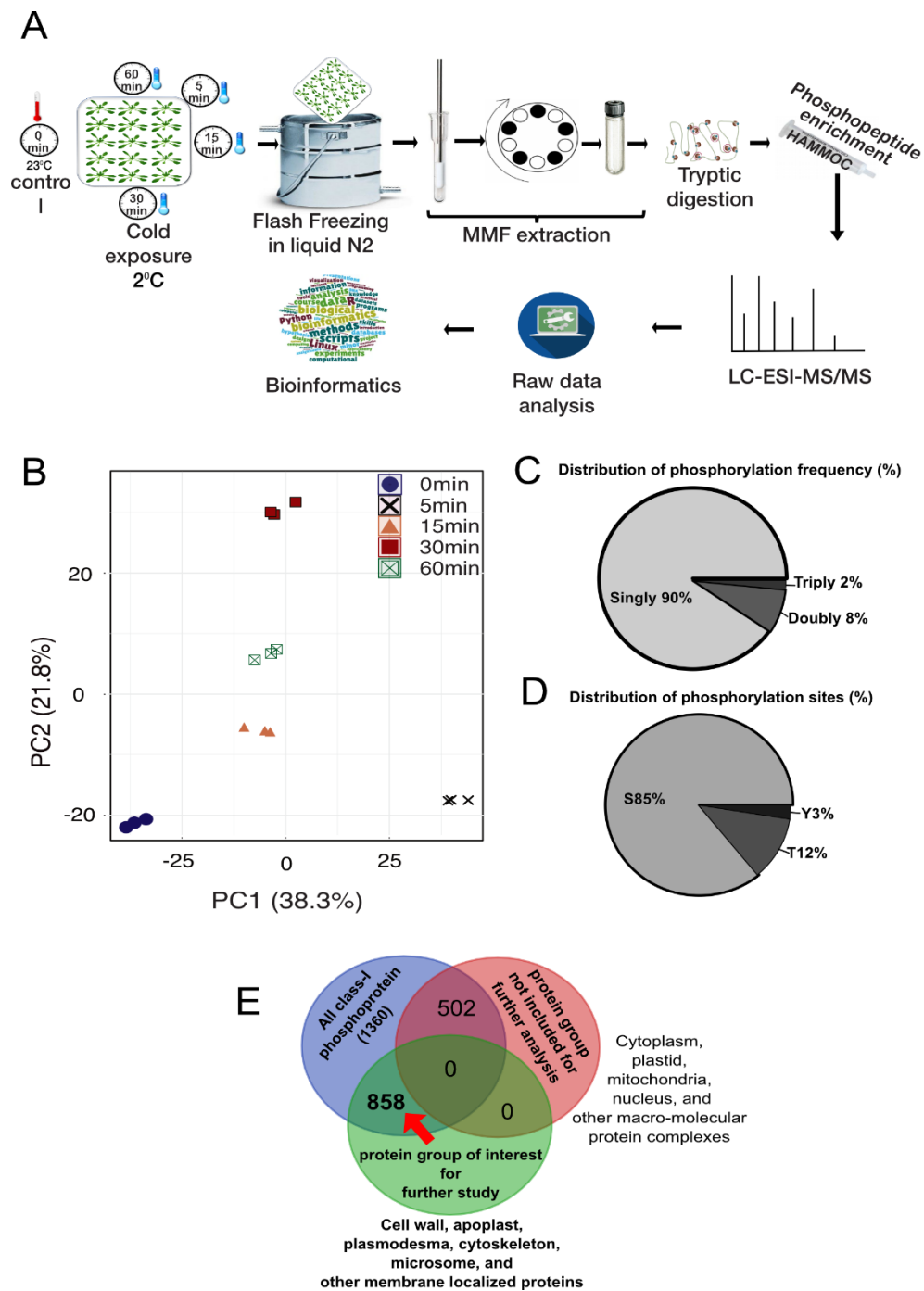
Figures: Chapter 2

A

B

C Distribution of phosphorylation frequency (%)

Singly 90%   Triply 2%   Doubly 8%

D Distribution of phosphorylation sites (%)

S85%   Y3%   T12%

E

Figure 2.1. Analysis of the cold-responsive phosphoproteins in *Arabidopsis thaliana*. (**A**) Experimental design and analytical workflow. (**B**–**E**) Quantitative analysis of the phosphopeptides: (**B**) Principal component analysis (PCA) of all the identified peptides (including phosphorylated and non-phosphorylated peptides). The times indicate the cold exposure duration: 5 to 60 min. (**C**) Frequency distribution of all the identified phosphopeptides based on the number of phosphorylation sites and phosphorylated amino acids. (**D**) Frequency of phosphosites per peptide: S, serine; T, threonine; Y, tyrosine. (**E**) Gene-ontology enrichment of cellular localization and the distribution of the proteins of interest. Class-I phosphoprotein: phosphopeptides with a mascot variable modification confidence score ≥ 0.75. The red arrow indicates the number of proteins that come from the MMFs.
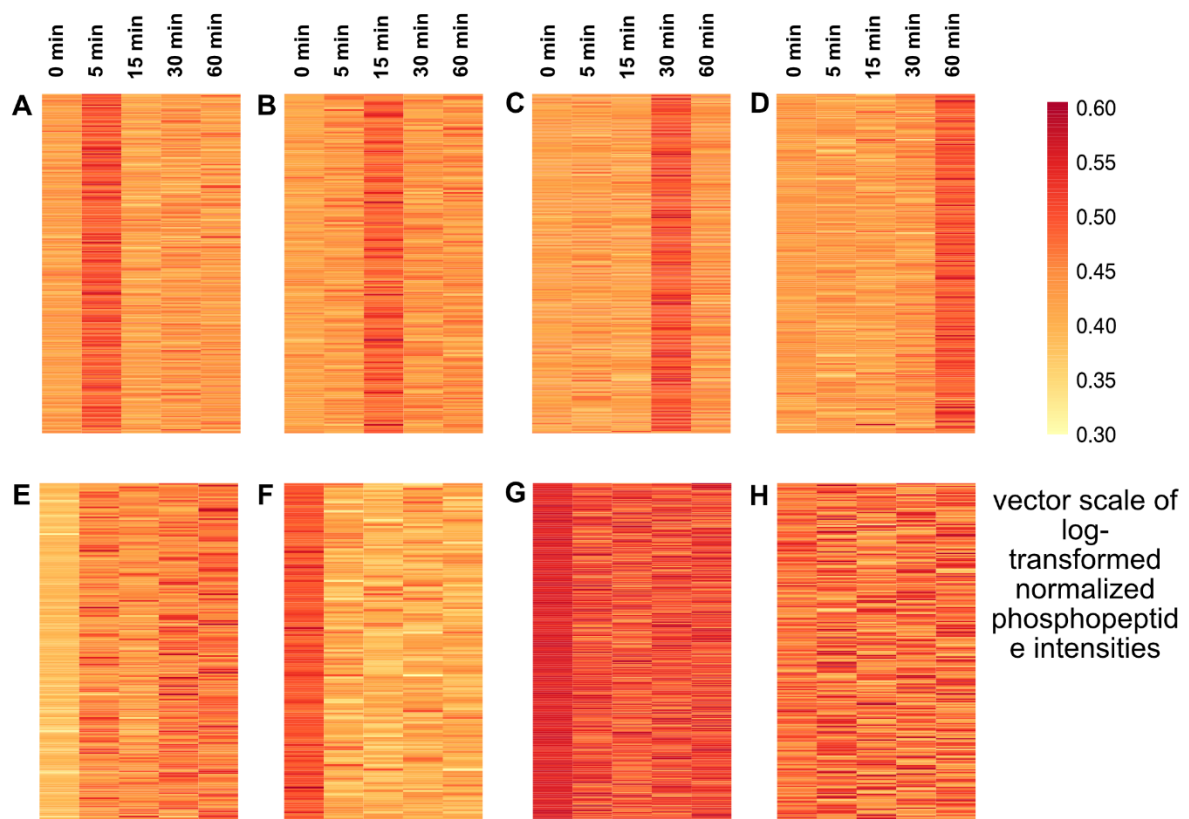
Figure 2.2. K-means clusters in the time-course analysis of phosphopeptide intensities in response to cold. Clusters are positioned based on their similar time-based characteristics. (**A**) Phosphorylation peaked at 5 min. (**B**) Phosphorylation peaked at 15 min. (**C**) Phosphorylation peaked at 30 min. (**D**) Phosphorylation peaked at 60 min. (**E**) Continuous phosphorylation under cold exposure. (**F**) Continuous dephosphorylation in response to cold. (**G**) Phosphopeptides dephosphorylate under cold exposure, but not continuously. (**H**) Unresponsive to cold exposure. The scale represents the vector transformation of the log2-transformed normalized phosphopeptide intensities.
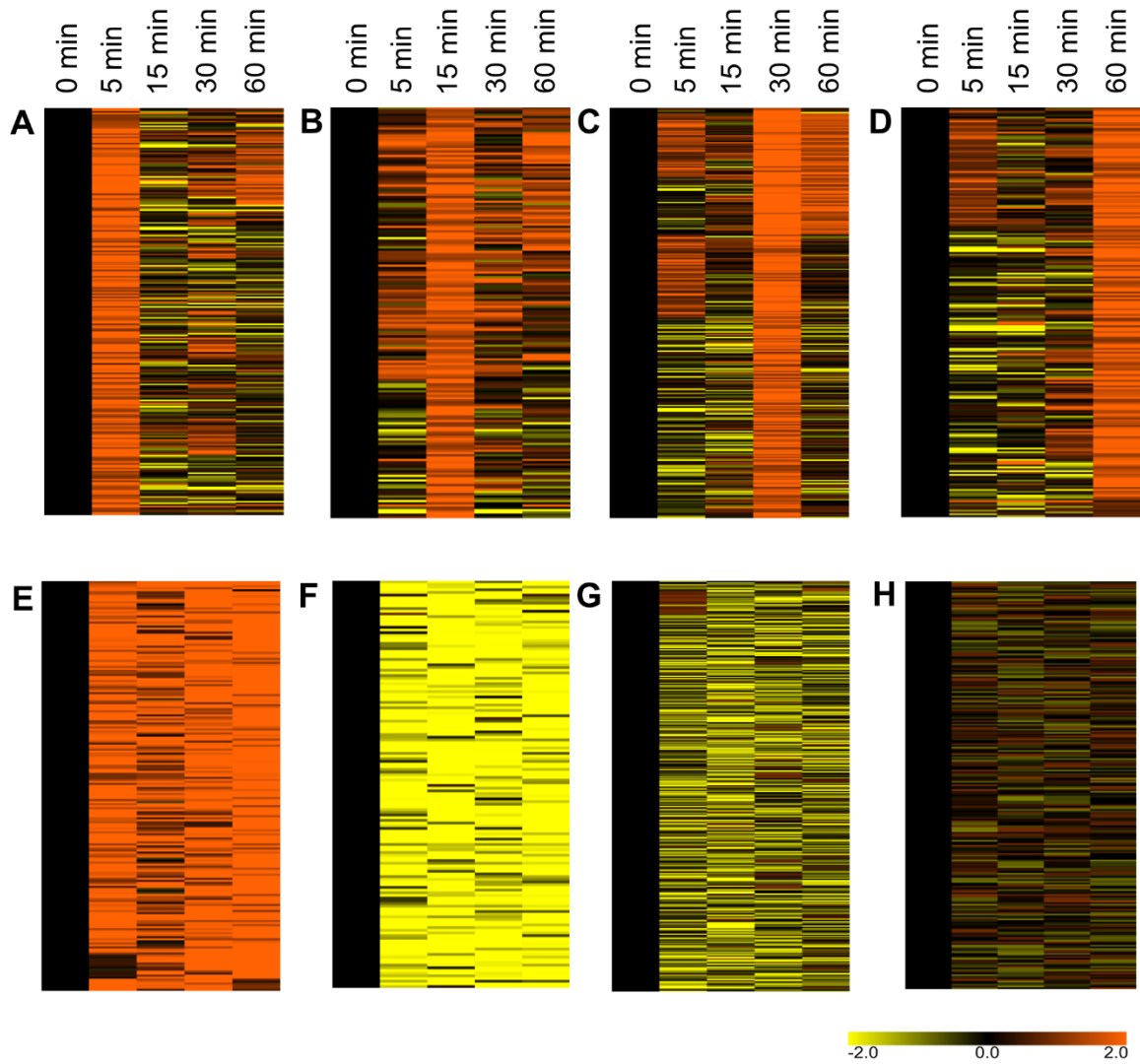
Figure 2.3. K-means clusters of differentially expressed phosphopeptides (DEPS) in response to cold at different time points. Times at the top indicate the duration of cold exposures. The scale indicates the log2 fold change in the cold exposed groups mentioned in Figure 2.2. (A) Fold change increased at 5 min. (B) Fold change increased at 15 min. (C) Fold change increased at 30 min. (D) Fold change increased at 60 min (E) Continuous increase in fold change under cold exposure; (F) Continuous decrease in fold change under cold exposure. (G) Fold change decreased under cold exposure, but not continuously. (H) Unresponsive to cold exposure.
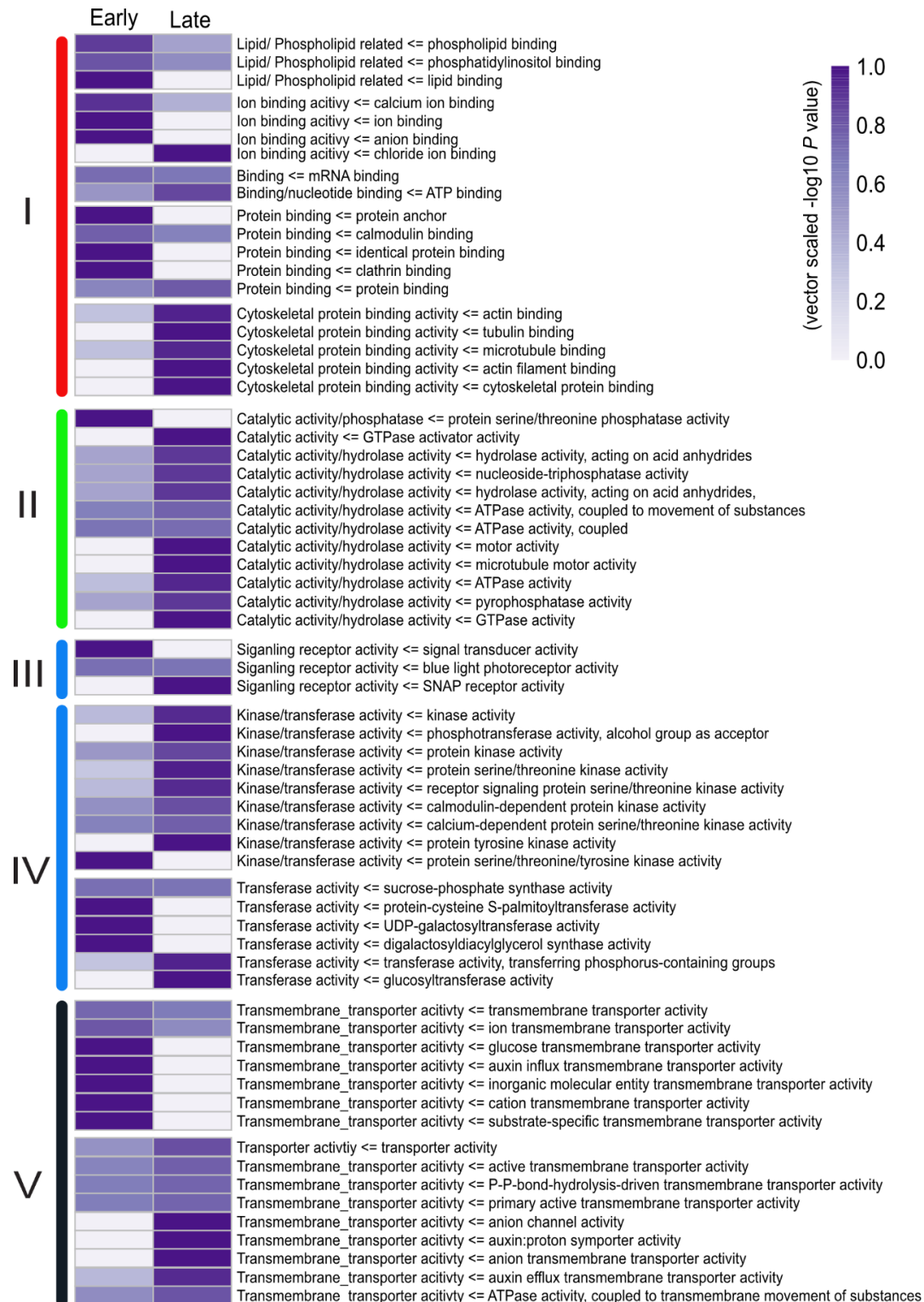
Figure 2.4. Gene ontology overrepresentation of molecular function (GOMF) for the phosphorylated proteins under cold exposure. Negative log 10 p-values of the GO terms enriched in the K-means clusters mentioned in Figure 2.2 were vector-scaled and visualized. Sub-clusters (A–E) are based on the similarity of GO terms extracted from ReViGO. Early, GO terms enriched within 5 to 15 min of cold exposure; Late, GO terms enriched within 30 to 60 min of cold exposure.
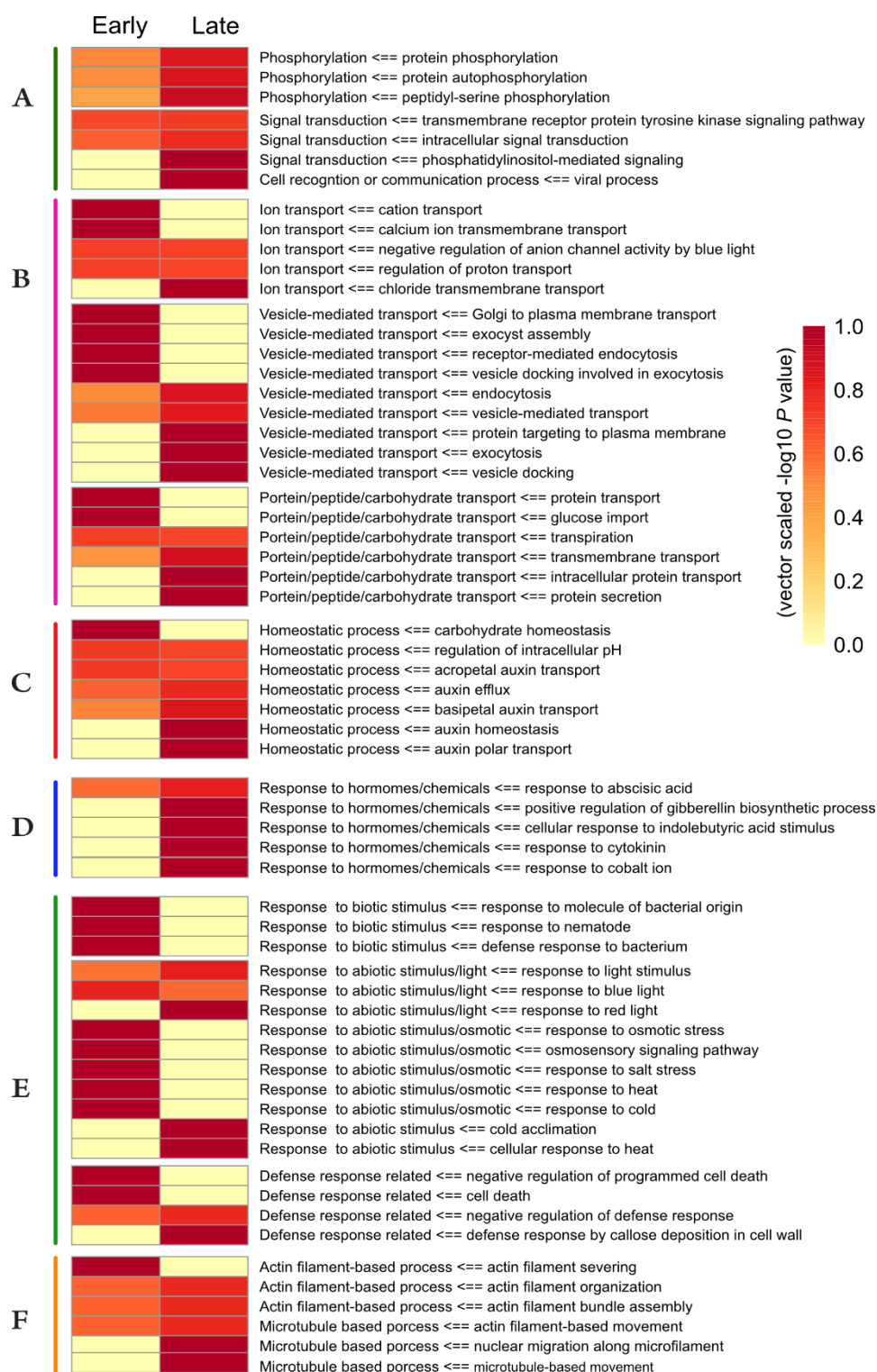
Figure 2.5. Gene ontology overrepresentation of biological processes (GOBP) for the phosphorylated proteins under cold exposure. Negative log 10 p-values of the GO terms enriched in the K-means clusters mentioned in Figure 2.2 were vector scaled and visualized. Sub-clusters (A–F) are based on the similarity of the GO terms extracted from ReViGO. Early, GO terms enriched within 5 to 15 min of cold exposure; Late, GO terms enriched within 30 to 60 min of cold exposure.

Figure 2.6. Gene ontology over-representation analysis of biological processes (GOBP). Continuation of Figure 2.5. Negative log 10 of *P* -values of GO terms enriched in the K-means clusters mentioned in Figure 2.5 were vector scaled and visualized. GO terms enriched within 5 to 15 min of cold exposure; Late, GO terms enriched within 30 to 60 min of cold exposure.

A

| #	motifs	alternative names	major motif groups	Corresponding/putative kinases	Enriched # in DEPS
1	.L.R..S......	LXRXXS	[LXK/RXXpS/pT]	CDPK, SnRKs	110
2	......SF.....	SF	[pS/pTF]	AGC, CIPK24, MAPK	104
3	......SG.....	SG	[pS/pTG]	CDPK	54
4	......SP.....	SP	[pS/pTP]	MAPK, CDK, GSK3	290
5	......SP.R...	SPXR	[pS/pTP]	MAPK, CDK, GSK3, GHK	63
6	......TP.....	TP	[pS/pTP]	MAPK, CDK	61
7	......SPK....	SPK	[pS/pTP]	MAPK, CDK, GSK3	40
8	.....GSP.....	GSP	[pS/pTP] or [GpS/pTP]	MAPK, CDK, GSK3, SnRK2.6	64
9	......S.D....	SXD	[pS/pTXXD/E] or [pS/pTXD/E]	CKII	54
10	......S.E....	SXE	[pS/pTXXD/E] or [pS/pTXD/E]	CKII, MAPK/ERK1, MAPK/ERK2	51
11	......S..E...	SXXE	[pS/pTXXD/E] or [pS/pTXD/E]	CKII	42
12	......S.P...	SXP	[pSXP]	putative 14-3-3 recognition site	21
13	...R..S......	RXXS	[R/KXXpS/pT]	SnRK2, CDPK, CaMK, CIPK	209
14	..RR..S......	RRXXS	[R/KXXpS/pT]	SnRK2, CDPK, CaMK, CIPK	58
15	...K..S......	KXXS	[R/KXXpS/pT]	SnRK2, CDPK, CaMK, CIPK	52
16	....S.S......	SXS	[SXpS/pT]	MAPK, CDK, CDPK, RLK, RLCK	87

B
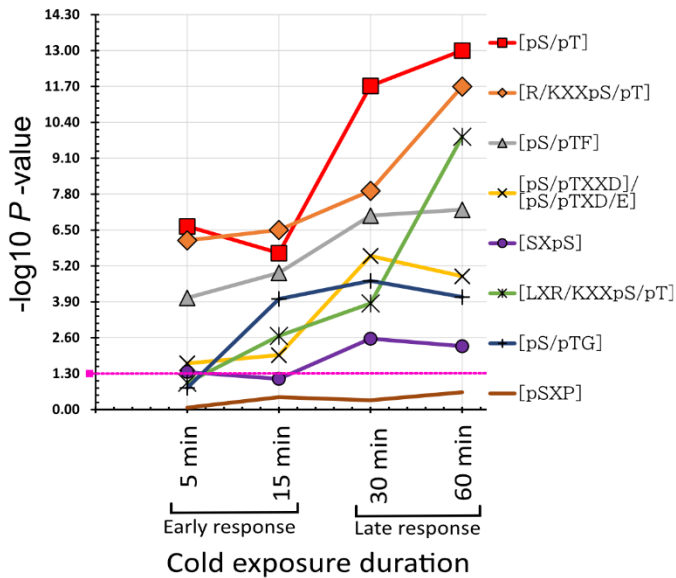
C
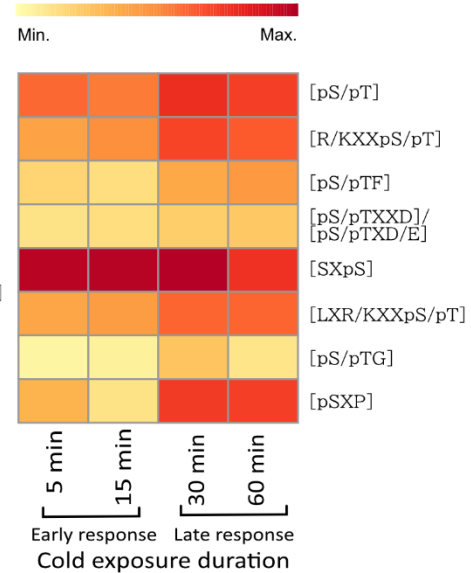
Figure 2.7. Cold-responsive phosphorylation kinase motifs. (A) Kinase motifs and major motif groups and their corresponding/putative upstream kinases. The numbers of corresponding motifs from the differentially expressed phosphopeptides (DEPS) are listed. (B) Temporal changes in the motif dynamics in response to cold. The p-values were obtained by Fisher's exact test using enriched motif counts in DEPS and the major motif groups mentioned in (A). (C) Time-dependent change in the relative abundance in the corresponding phosphopeptides of each major motif.
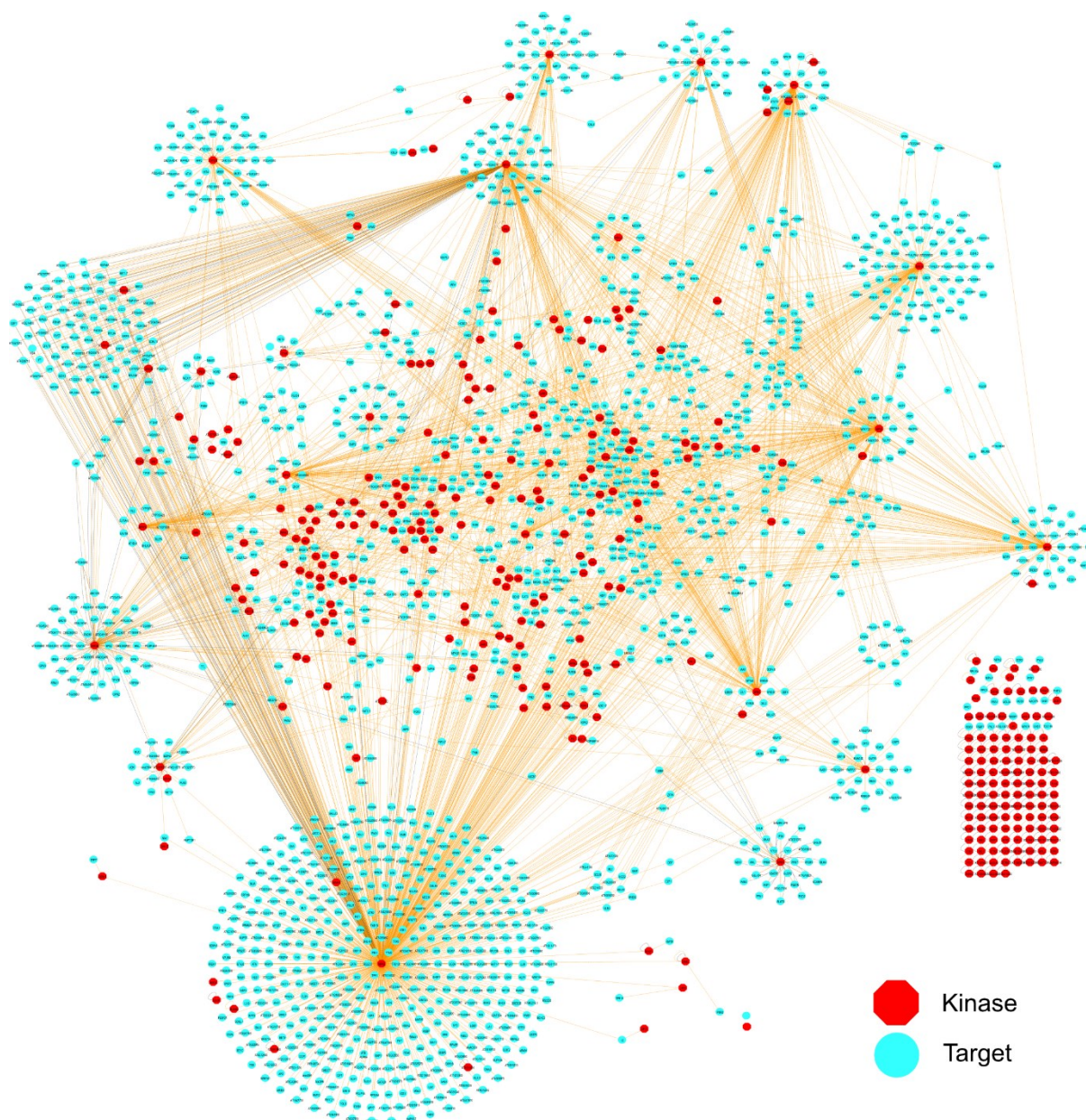
Figure 2.8. *Arabidopsis* **kinase-substrate interaction network.** This network was constructed using available information from the PhosphAT database and other literature cited in the text. The subnetwork of *Arabidopsis* cold-responsive kinase-substrate interaction in Figure 2.9 was extracted based on this network

Figure 2.9. Cold-responsive kinase–substrate network in *Arabidopsis thaliana*. The network was constructed based on the identified kinase and substrates from this study and their corresponding interactions from the database-derived kinase–substrate interactions. The unique shapes of the nodes in this figure indicate a specific/unique group of kinases involved in the early cold response. Blue nodes indicate the kinases identified in this study; red nodes indicate the upstream kinases of the substrates identified in this study. Yellow and magenta borders indicate the phosphorylated kinases and substrates identified in this study, respectively.

Figure 2.10. Coordinated regulation of related receptor kinase (RKs) gene family members (RLKs, RLCKs) in response to cold. The RLK/RLCKs phosphorylated inside their kinase domains are highlighted in blue. The closely related kinases may work in coordination under cold. The tree was made from protein sequence alignment using MEGA10 software.

41

Figure 2.11. Coordinated regulation of related MAPK gene family members in response to cold.
(A) MAP4K phylogenetic tree. (B-C) MAP3K and MAP3K RAF kinase phylogenetic tree. Kinases identified in this study are highlighted in blue. The closely related kinases may work in coordination under cold. The tree was made from protein sequence alignment using MEGA10 software.
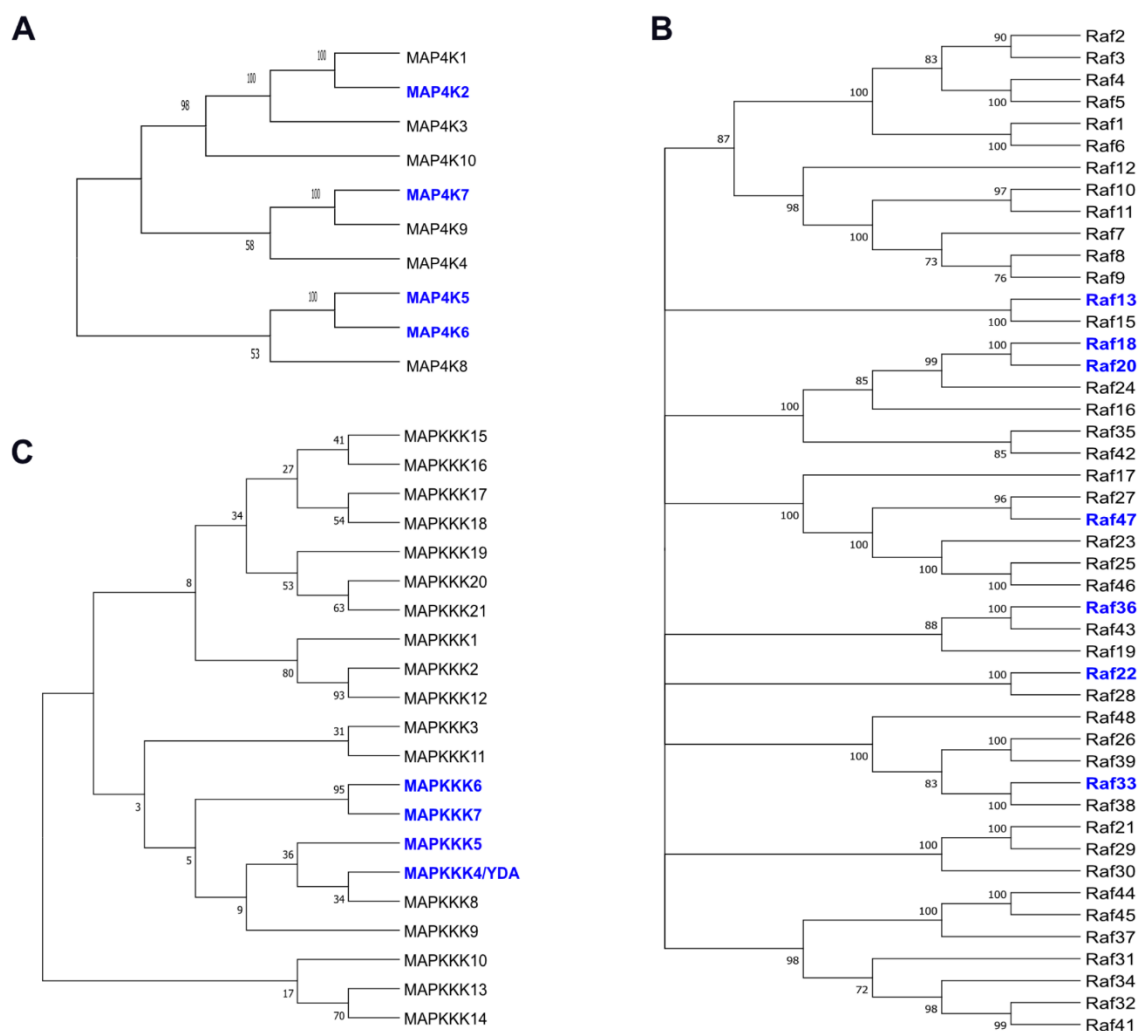
Table 1. Phosphopeptides described in the results and discussion sections.

TAIR Accession	TAIR Symbols	Protein Description	Localization	Bin Names of Functional Categories	Phosphopeptides	Phospho-residue	Phospho-sites	KMC Clusters
AT1G59610	DRP2B	dynamin-like 3	PM	Vesicle trafficking	RYS[+80]DPAQNGEDSSGSGGSSR	S	883	E,C*
AT1G10290	DRP2A	dynamin-like protein 6	G,PM	Vesicle trafficking	RYS[+80]DPAQNGDAASPGSGSNRR	S	877	A*
AT1G13980	GN	sec7 domain-containing protein	G,PM	Vesicle trafficking	FSQLLS[+80]LDTEEPR	S	961	C*
AT5G06140	SNX1	sorting nexin 1	C,PM	Vesicle trafficking	NISGSMQS[+80]PR	S	16	C*
AT3G11820	SYP121	syntaxin of plants 121	PM	Vesicle trafficking	TLDRLIS[+80]TGESER	S	190	C*
AT5G08080	SYP132	syntaxin of plants 132	PM	Vesicle trafficking	GQS[+80]SREGDVELGEQQGGDQGLEDFFKK	S	16	D*
AT5G61210	SNAP33	soluble N-ethylmaleimide-sensitive factor adaptor protein 33	PM	Vesicle trafficking	TTS[+80]EPSLADMTNPFGGER	S	47	E,C*
AT5G58440	SNX2A	sorting nexin 2A	G,EM	Vesicle trafficking	SPS[+80]SSSSDYIK	S	146	A*
AT1G08190	VPS41	vacuolar protein sorting 41	G,EM	Vesicle trafficking	EDNNRSS[+80]FSQR	S	860	B*
AT5G06560	MYOB7	myosin-binding protein (Protein of unknown function 2C DUF593)	EM	unknown	FKNDTADGYAMS[+80]PR	S	385	E,A*
AT4G27500	PPI1	proton pump interactor 1	ER,PM	unknown	KKTGGNTETETEEVPEAS[+80]EEEIEAPVQEEKPQK	S	540	E,C*
AT1G72160	PATL3	Sec14p-like phosphatidylinositol transfer family protein	PM	Solute transport	SMIPQNLGS[+80]FKEESSKLSDLSNSEK	S	108	E,C*
AT2G41560	ACA4	autoinhibited Ca^{2+}-ATPase 2C isoform 4	V,PM	Solute transport	SSVS[+80]IVKNR	S	28	A*
AT1G27770	ACA1	autoinhibited Ca^{2+}-ATPase 1	PM	Solute transport	FTANLS[+80]KR	S	46	A*
AT4G04340	AtOSCA1.1	ERD (early-responsive to dehydration	PM	Solute transport	RNT[+80]PAPSR	T	750	B*

TAIR Accession	TAIR Symbols	Protein Description	Localization	Bin Names of Functional Categories	Phosphopeptides	Phospho-residue	Phospho-sites	KMC Clusters
		stress) family protein						
AT4G22120	AtOSCA1.2	ERD (early-responsive to dehydration stress) family protein	PM	Solute transport	NTPAPSIIS[+80]GDDSPSLPFSGK	S	757	C*
AT5G23660	SWEET12	bidirectional sugar transporter SWEET12-like protein	PM	Solute transport	LGTLTS[+80]PEPVAITVVR	S	248	A*
AT1G08930	ERD6	Major facilitator superfamily protein	ER,PM	Solute transport	SLS[+80]IRER	S	17	A*
AT3G18830	PLT5	polyol/monosaccharide transporter 5	PM	Solute transport	TVPNPEVEIGS[+80]NKQWKEGDTQSS	S	527	D*
AT1G20840	TMT1	tonoplast monosaccharide transporter1	V,PM	Solute transport	LYGTHENQSYLARPVPEQNS[+80]SLGLR	S	277	E,A*
AT1G20840	TMT1	tonoplast monosaccharide transporter1	V,PM	Solute transport	YYLKEDGAES[+80]R	S	446	B*
AT4G35300	TMT2	tonoplast monosaccharide transporter2	V,PM	Solute transport	IYLHQEGFPGS[+80]RR	S	448	E,A*
AT4G35300	TMT2	tonoplast monosaccharide transporter2	V,PM	Solute transport	HGS[+80]TMSR	S	287	D*
AT1G75220	ERDL6	Major facilitator superfamily protein	V,PM	Solute transport	RPFIHTGS[+80]WYR	S	23	D*
AT2G18960	AHA1	H^{+}-ATPase 1	PM	Solute transport	T[+80]LHGLQPKEDVNIFPEKGSYR	T	881	D*
AT2G18960	AHA1	H^{+}-ATPase 1	PM	Solute transport	GLDIDTAGHHYT[+80]V	T	948	D*
AT2G18960	AHA1	H^{+}-ATPase 1	PM	Solute transport	EDVNIFPEKGS[+80]YRELSEIAEQAK	S	899	E,D*
AT3G47950	AHA4	H^{+}-ATPase 4	PM	Solute transport	GLDIETIQQAYT[+80]V	T	959	E,A*
AT3G54820	PIP2-5	plasma membrane intrinsic protein 2%3B5	PM	Solute transport	ALGS[+80]FRSQPHV	S	279	E,D*
AT2G39010	PIP2-6	plasma membrane	PM	Solute transport	AYGS[+80]VRS[+80]QLHELHA	S;S	279;282	D*

44

TAIR Accession	TAIR Symbols	Protein Description	Localization	Bin Names of Functional Categories	Phosphopeptides	Phospho-residue	Phospho-sites	KMC Clusters
		intrinsic protein 2E						
AT4G35100	PIP2-7	plasma membrane intrinsic protein 3	PM	Solute transport	ALGSFRS[+80]NATN	S	276	C*
AT2G36910	ABCB1	ATP binding cassette subfamily B1	PM	Solute transport	NSVSS[+80]PIMTR	S	634	A*
AT1G30400	ABCC1	multidrug resistance-associated protein 1	V,PD	Solute transport	SIT[+80]LENKR	T	1485	A*
AT1G59870	ABCG36	ABC-2 and Plant PDR ABC-type transporter family protein	PM	Solute transport	SLS[+80]TADGNRRGEVAMGR	S	825	B*
AT3G53480	ABCG37	pleiotropic drug resistance 9	PM	Solute transport	MNLS[+80]YWR	S	1187	C*
AT5G01240	LAX1	like AUXIN RESISTANT 1	PM	Solute transport	QAEESIVVS[+80]GEDEVAGR	S	14	E,A*
AT5G01240	LAX1	like AUXIN RESISTANT 1	PM	Solute transport	KVEDS[+80]AAEEDIDGNGGNGFSMK	S	27	B*
AT5G47910	*RBOHD*	*respiratory burst oxidase homologue D*	*PM*	*Redox homeostasis*	*VFS[+80]RRPSPAVR*	*S*	*148*	*B**
AT5G47910	RBOHD	respiratory burst oxidase homologue D	PM	Redox homeostasis	TSS[+80]AAIHALKGLK	S	163	C*
AT5G47910	RBOHD	respiratory burst oxidase homologue D	PM	Redox homeostasis	ILSQMLS[+80]QK	S	347	B*
AT3G15220	AT3G15220	Protein kinase superfamily protein	MT, CT	Protein modification	RQEVS[+80]PNRISQR	S	364	D,*
AT5G14720	AT5G14720	Protein kinase superfamily protein	PM	Protein modification	YLEQTSAKQPGS[+80]PETNVDDLLQTPPATSR	S	613	E,C*
AT4G24100	AT4G24100	Protein kinase superfamily protein	PM	Protein modification	SDS[+80]NGNVEPVASERER	S	654	E,D*
AT4G10730	AT4G10730	Protein kinase superfamily protein	PM	Protein modification	KSAS[+80]VGNWILDSK	S	579	C*

TAIR Accession	TAIR Symbols	Protein Description	Localization	Bin Names of Functional Categories	Phosphopeptides	Phospho-residue	Phospho-sites	KMC Clusters
AT1G63 700	YDA	Protein kinase superfamily protein	PM	Protein modification	S[+80]LPCLDSED ATNYQQK	S	692	D*
AT5G66 850	MAPKK K5	mitogen-activated protein kinase kinase kinase 5	PM	Protein modification	SPS[+80]AFTAVP R	S	90	C*
AT3G07 980	MAP3K E2	mitogen-activated protein kinase kinase kinase 6	V	Protein modification	KIS[+80]GQLDYV K	S	925	E,D*
AT3G13 530	M3KE1	mitogen-activated protein kinase kinase kinase 7	PM	Protein modification	S[+80]GQLDPNNP IFGQNETSSLSMI DQPDVLK	S	788	C,A*
AT5G19 010	MPK16	mitogen-activated protein kinase 16	PM	Protein modification	VAFNDTPTAIFW TDY[+80]VATR	Y	189	D,A*
AT1G18 150	MPK8	Protein kinase superfamily protein	PM	Protein modification	AAAAVASTLESE EADNGGGYS[+80]AR	S	539	D*
AT2G31 010	Raf13	Protein kinase superfamily protein	PM	Protein modification	KLSNTSHS[+80]E PNVATVFWR	S	335	D*
AT1G16 270	Raf18	kinase superfamily with octicosapeptide	PM	Protein modification	NT[+80]LVSGGVR GTLPWMAPELLN GSSSKVSEK	T	1024	E*,D*
AT2G24 360	Raf22	Protein kinase superfamily protein	PM	Protein modification	HYS[+80]LSVGQS VFRPGR	S	81	A*
AT5G50 000	Raf33	Protein kinase superfamily protein	PM	Protein modification	LLDWGEEGHRS[+80]EAEIVSLR	S	120	C*
AT5G58 950	Raf36	Protein kinase superfamily protein	PM	Protein modification	SVS[+80]PSPQMA VPDVFK	S	101	C*
AT3G58 760	Raf47	Integrin-linked protein kinase family	PM	Protein modification	SSGS[+80]FNR	S	468	A*
AT4G35 310	CPK5	Calcium-dependent protein kinase 5	PM	Protein modification	NSLNIS[+80]MRD A	S	552	A*
AT1G49 580	CRK8	Calcium-dependent protein kinase (CDPK) family protein	PM	Protein modification	TES[+80]GIFR	S	360	A*

TAIR Accession	TAIR Symbols	Protein Description	Localization	Bin Names of Functional Categories	Phosphopeptides	Phospho-residue	Phospho-sites	KMC Clusters
AT4G04720	CPK21	calcium-dependent protein kinase 21	PM	Protein modification	T[+80]MFANIDTDK	T	387	A*
AT2G17290	CPK6	Calcium-dependent protein kinase family protein	C,PM	Protein modification	NSLNIS[+80]MRDV	S	540	E,D*
AT5G12480	CPK7	calmodulin-domain protein kinase 7	PM	Protein modification	FNSLS[+80]LKLMR	S	520	E,C*
AT3G10660	CPK2	calmodulin-domain protein kinase cdpk isoform 2	ER,EM	Protein modification	VSSAGLRT[+80]ESVLQRK	T	171	C*
AT3G19100	CRK2	Protein kinase superfamily protein	PM	Protein modification	DAVLQNDDSTPAHPGKS[+80]PVR	S	37	D*
AT5G58380	CIPK10	SOS3-interacting protein 1	C,PM	Protein modification	KS[+80]NGDTLEYQK	S	421	B*
AT3G09830	PCRK1	Protein kinase superfamily protein	PM	Protein modification	IVEASSGNGS[+80]PQLVPLNSVK	S	377	A*
AT2G01820	TMK3	Leucine-rich repeat protein kinase family protein	PM	Protein modification	LAPDGKYS[+80]IETR	S	745	A*
AT5G18610	PBL27	Protein kinase superfamily protein	PM	Protein modification	LGPVGDKTHVS[+80]TR	S	244	B*
AT1G66150	TMK1	transmembrane kinase 1	PM	Protein modification	EASFKKAIDT[+80]T[+80]IDLDEET[+80]LASVHTVAELAGHCCAR	T;T;T	825;826; 833	C*
AT2G39660	BIK1	botrytis-induced kinase1	PM	Protein modification	LDTQYLPEEAVRMASVAVQCLS[+80]FEPKSRPTMDQVVR	S	333	C*
AT3G53380	LECRK81	Concanavalin A-like lectin protein kinase family protein	PM	Protein modification	QIEHDKS[+80]PEATVAAGTMGYLAPEYLLTGR	S	530	C*
AT4G23250	EMB1290	cysteine-rich receptor-like protein kinase 17	PM	Protein modification	IFGVDQTVANT[+80]AR	T	518	D*

TAIR Accession	TAIR Symbols	Protein Description	Localization	Bin Names of Functional Categories	Phosphopeptides	Phospho-residue	Phospho-sites	KMC Clusters
AT2G37710	LECRK41	receptor lectin kinase	PM	Protein modification	LYDHGSDPQTT[+80]HVVGTLGYLAPEHTR	T	506	D*
AT5G16590	LRR1	Leucine-rich repeat protein kinase family protein	PM	Protein modification	WVSSITEQQS[+80]PSDVFDPELTR	S	562	E,B*
AT5G41210	GSTT1	glutathione S-transferase THETA 1	Per	Protein modification	REMGTLSKPGLQS[+80]KI	S	243	E,C*
AT1G72710	CKL2	casein kinase 1-like protein 2	PM	Protein modification	NSGQIFNS[+80]GSLAK	S	353	C*
AT4G26540	RGI3	Leucine-rich repeat receptor-like protein kinase family protein	PM	Phytohormone action	NLTS[+80]ANVIGTGSSGVVYR	S	762	B*
AT2G13790	SERK4	somatic embryogenesis receptor-like kinase 4	PM	Phytohormone action	LMNYNDS[+80]HVTTAVR	S	451	B*
AT5G38990	AT5G38990	Malectin/receptor-like protein kinase family protein	PM	Phytohormone action	VGPTSAS[+80]QTHVSTVVK	S	683	C*
AT5G59700	AT5G59700	Protein kinase superfamily protein	PM	Phytohormone action	ANPKSQQGLAEFRT[+80]EIEMLSQFR	T	525	D*
AT1G06390	ASK9	GSK3/SHAGGY-like protein kinase 1	PM	Phytohormone action	VLVKGEPNIS[+80]YICSR	S	229	B*
AT1G01740	BSK4	kinase with tetratricopeptide repeat domain-containing protein	PM	Phytohormone action	SYS[+80]TNLAFTPPEYLR	S	210	E,C*
AT4G18710	ASK7	Protein kinase superfamily protein	PM	Phytohormone action	QLVKGEANISY[+80]ICSR	Y	200	D*
AT1G70940	PIN3	Auxin efflux carrier family protein	PM	Phytohormone action	ELHMFVWSSNGS[+80]PVSDR	S	366	D*
AT2G01420	PIN4	Auxin efflux carrier family protein	PM	Phytohormone action	MVVSDQPRKS[+80]NAR	S	395	E,C*

TAIR Accession	TAIR Symbols	Protein Description	Localization	Bin Names of Functional Categories	Phosphopeptides	Phospho-residue	Phospho-sites	KMC Clusters
AT2G01420	PIN4	Auxin efflux carrier family protein	PM	Phytohormone action	KS[+80]GGDDIGGLDSGEGEREIEK	S	395	C*
AT1G23080	PIN7	Auxin efflux carrier family protein	PM	Phytohormone action	LRCNS[+80]TAELNPK	S	431	E,C*
AT1G23080	PIN7	Auxin efflux carrier family protein	PM	Phytohormone action	SFYGGGGTNMTPRPSNLTGAEIYSLNTT[+80]PR	T	242	C*
AT4G33240	FAB1A	1-phosphatidylinositol-3-phosphate 5-kinase FAB1A	G,EM	Multi-process regulation	NVS[+80]LEKLSDEKVK	S	1143	C*
AT1G71010	FAB1C	FORMS APLOID AND BINUCLEATE CELLS 1C	C,EM	Multi-process regulation	VQS[+80]FDSAIR	S	1184	A*
AT1G49340	PI4KA1	Phosphatidylinositol 3- and 4-kinase family protein	PM	Multi-process regulation	LIS[+80]GAFSQAPQPEDDSFNEMLIAR	S	1111	D*
AT1G60890	AT1G60890	Phosphatidylinositol-4-phosphate 5-kinase family protein	PM	Multi-process regulation	AFS[+80]VGEKEVDLILPGTAR	S	662	C*
AT3G01310	AT3G01310	Phosphoglycerate mutase-like family protein	G,PM	Multi-process regulation	QGS[+80]GIIGTFGQSEELR	S	358	B*
AT1G22620	SAC1	Phosphoinositide phosphatase family protein	G,EM	Multi-process regulation	ASQLSHANTAREPS[+80]LRDLR	S	456	A*
AT2G18730	DGK3	diacylglycerol kinase 3	PM	Lipid metabolism	FVAS[+80]RPSTADSKTMR	S	18	A*
AT3G08510	PLC2	phospholipase C 2	PM	Lipid metabolism	RLS[+80]LSEEQLEK	S	346	D
AT5G60900	RLK1	receptor-like protein kinase 1	PM	Enzyme classification	GAFGIVYKGYLEVAGGSEVT[+80]VAVKK	T	559	D*
AT1G17580	XI-1	myosin 1	C,CT	Cytoskeleton organization	QQTLTIS[+80]PTTR	S	1052	E,D*

TAIR Accession	TAIR Symbols	Protein Description	Localization	Bin Names of Functional Categories	Phosphopeptides	Phospho-residue	Phospho-sites	KMC Clusters
AT3G19960	ATM1	myosin 1	PM	Cytoskeleton organization	S[+80]LPADYRFDGSPVSDRLENSSGASVR	S	14	E,C*
AT5G20490	XI-K	myosin family protein with DiI	G,EM	Cytoskeleton organization	ENS[+80]GFGFLLTRK	S	1516	C*
AT1G08730	XI-C	Myosin family protein with DiI domain-containing protein	C,CT	Cytoskeleton organization	KLHVASLVVQT[+80]GLR	T	823	C*
AT1G24764	ATMAP70-2	microtubule-associated proteins 70-2	MT	Cytoskeleton organization	GTSKS[+80]FDGGTR	S	464	C*
AT4G27060	TOR1	ARM repeat superfamily protein	C,MT	Cytoskeleton organization	EASDGSTLS[+80]PDSASKGK	S	370	E,A*
AT2G01750	MAP70-3	microtubule-associated proteins 70-3	PM	Cytoskeleton organization	MS[+80]EKLKLTENLLDS[+80]K	S;S	125;137	E,C*
AT4G29810	ATMKK2	MAP kinase kinase 2	PM	Cell cycle organization	IISQLEPEVLS[+80]PIKPADDQLSLSDLDMVK	S	56	D*
AT5G55230	ATMAP65-1	microtubule-associated proteins 65-1	MT	Cell cycle organization	RLS[+80]LNANQNGSR	S	532	C*

Cold-responsive phosphopeptides are highlighted in the text. Bin names are extracted from MAPMAN4.0 functional classification of proteins. K-means cluster E represents peptides phosphorylated during at least three time points of cold exposure; cluster number next to E represents the clusters where the phosphopeptide intensity was highest. Asterisk (*) indicates statistical significance ($p < 0.05$) by Student's t-test. Localizations—PM: plasma membrane, G: Golgi, ER: endoplasmic reticulum, V: vacuole, Per: peroxisome, CT: cytoskeleton, MT: microtubule, EM: endomembrane system, PD: Plasmodesmata, C: Cytosol. For more detailed information, see Table S2.1. Detailed explanations on the K-means cluster names are in Figure 2.2.

Supplementary information

Supporting tables:

Table S2.1. Identified cold-responsive phosphopeptides in the microsomal membrane fraction (MMF). (A) Class-I phosphopeptides based on Mascot variable localization confidence score ≥ 0.75. **(B)** All phosphopeptides identified in the study using Skyline-Daily software.

Table S2.2. Identified proteins from microsomal membrane fraction (MMF). Data were generated using Progenesis software for proteomics data analysis. The data show no significant changes in protein abundance within a short duration of cold exposure.

Table S2.3. An updated *Arabidopsis* kinase-substrate interaction network from published literature. (A) Binary interaction between kinase and corresponding substrates was used to construct the kinase-substrate network. **(B)** Sub-network data were used to build the cold-responsive kinase-substrate network shown in Figure 2.9. **(C)** The number of binary interactions between a kinase and its corresponding substrates.

Chapter 3

A single seed treatment mediated through reactive oxygen species increases germination, growth performance, and abiotic stress tolerance in *Arabidopsis* and rice

Summary

Hydroxyl radical (•OH) is considered to be the most damaging among reactive oxygen species. Although a few studies have reported on its effects on growth and stress adaptation of plants, no detailed studies have been performed using •OH in germination and early seedling growth under abiotic stresses. Here I report a single seed treatment with •OH on germination and seedling growth of *Arabidopsis* and rice under non-stressed (ambient) and various abiotic-stressed conditions (chilling, high temperature, heat, and salinity). The treatment resulted in faster seed germination and early seedling growth under non-stressed conditions, and, interestingly, these effects were more prominent under abiotic stresses. In addition, *Arabidopsis* seedlings from treated seeds showed faster root growth and developed more lateral roots. These results show a positive and potential practical use for •OH in model and crop plants for direct seeding in the field, as well as improvement of tolerance against emerging stresses.

Introduction

Plants are sessile organisms and are continuously exposed to various biotic and abiotic stresses throughout their lifetimes. Moreover, alterations of the rhythm of seasonal changes by global climate change aggravate the severity of these stresses on plants. Simultaneous exposure to different abiotic and biotic stresses have much more devastating effects on plant growth and development and resulting in yields lower than the plants exposed to an individual stress in the field (Downing, 1993; Silva et al., 2012; Suzuki et al., 2014; Perdomo et al., 2015). Different abiotic stresses such as cold/chilling (Hatfield and Egli, 1974; Duke et al., 1977; Leopold, 1980), salinity (Khan et al., 1997; Gill et al., 2003; Zhang et al., 2014; Kan et al., 2016), osmotic (Pratap and Sharma, 2010; Mickky and Aldesuquy, 2019), drought and/or water deprivation, and high temperature (Wright, 1931; Pagamas and Nawata, 2007) negatively affect the seed germination, seedling establishment, survival of the young seedlings (Boyer and Westgate, 2004; Maraghni et al., 2010; Prasad et al., 2011). Multiple abiotic stresses have a significant impact on crop production and food security all over the world (Downing, 1993; Mittler, 2006; Lobell and Field, 2007; Silva et al., 2012; Suzuki et al., 2014). Numerous approaches have been developed over the last few decades to improve plant performance against multiple abiotic stresses in different climatic conditions around the world (Suzuki et al., 2014; Pandey et al., 2017)

In the last couple of decades, several strategies have been developed to fight against biotic and abiotic stresses, including strategies using conventional breeding, genetic engineering, and selection of resistant varieties, some of which are tightly associated with mitigating the impact of stresses arising from global climate changes. However, some of these methods are time-consuming, expensive, and controversial. For example, genetically modified organisms have the potential for increasing tolerance against stresses, but their use is unpopular with growers and consumers. Additionally, the gaps in knowledge on the application between the labs and field, and from model plant to crop plant transitions require extensive studies (Zhang et al., 2004; Savvides et al., 2016; Ahanger et al., 2017).

Alongside the methods mentioned above, a growing number of alternative approaches are emerging to deal with multiple abiotic stresses. For example, priming treatments, in which plants are pre-treated under stressed conditions or with endogenous, natural, or synthetic chemicals to prepare them against upcoming stresses, have gained popularity (Chen and Arora, 2011; Chen et al., 2012; Savvides et al., 2016). Among the different kinds of priming treatments, the most promising and commonly used chemicals are polyamines, hormones such as salicylic acid, reactive sulfur species such as NaHS, reactive nitrogen species such as nitric oxide, and reactive oxygen species (ROS) such as hydrogen peroxide (H_2O_2) (Tanou et al., 2009; Gill and Tuteja, 2010a; Parra-Lobato and Gomez-Jimenez, 2011; Hossain et al., 2015). Exogenous application of these chemicals has been found to be effective against different abiotic stresses (Tanou et al., 2009; Li et al., 2012b). However, most of these treatments are focused on a single abiotic stress at a single stage of growth and development.

ROS, including singlet oxygen ($^1O_2$), superoxide (O_2^-), hydrogen peroxide (H_2O_2), and the hydroxyl radical (•OH), are involved in almost every stage of growth, development, and differentiation (Bethke and Jones, 2001; Kobayashi et al., 2007; Queval et al., 2007; Miller et al., 2009; Kimura et al., 2012). Researchers have reported that exogenous application of H_2O_2 enhances stress tolerance in both model and crop plants by increasing the endogenous concentration to an optimum level (Savvides et al., 2016; Mittler, 2017). Before the discovery of the positive roles of H_2O_2, ROS were considered toxic byproducts of oxygen metabolism. In particular, •OH is still considered a dangerous compound in the cell that damages DNA and proteins and is responsible for cell death (Richards et al., 2015; Mittler, 2017). However, similar to H_2O_2, several positive roles of •OH in cell growth, elongation, germination, and stress signaling processes have been reported (Richards et al., 2015). •OH has been found to accelerate the elongation and growth of coleoptiles and roots in maize seedlings (Schopfer, 2001; Schopfer et al., 2002; Liszkay et al., 2004). It was also found to contribute to the elongation of radicles and the acceleration of germination in cress seeds (Muller et al., 2009b). However, no papers have reported the application of •OH to improve seed germination and early seedling growth under stressful environments in crop plants.

Recently, my collaborators of this study filed a patent #CA2949750 (Olkowski et al., 2014) on the catalytic seed treatment phenomenon, which may be operating through the Fenton/Haber Weiss reaction and generating •OH to enhance seed germination and lateral root growth. Because •OH is highly reactive and short-lived, it cannot be added directly in the same manner as H_2O_2. Therefore, in this study, the Fenton /Haber-Weiss reaction was used for •OH treatment. Furthermore, many physiological and biochemical studies have confirmed that this reaction is equivalent to •OH treatment (Deng et al., 2010; Galano et al., 2010; Khorobrykh et al., 2011; Vreeburg et al., 2014; Matros et al., 2015). In this study, *Arabidopsis* was used as a model system to investigate the mechanism of action, and rice was also studied to validate the breadth of this phenomenon in other crops. The single seed treatment with •OH (with H_2O_2 as a substrate and Fe or Cu as a catalyst) had multiple positive effects: accelerated germination and early hypocotyl growth in the short term, increased lateral root numbers, and improved tolerance during the germination process to several abiotic stresses in both *Arabidopsis* and rice. The overall findings from this work will help to improve plant performance against a wide range of abiotic stresses through a simple, single application of •OH based on the Fenton/Haber Weiss reaction in a cost-, time- and labor-effective manner.

Materials and methods

Plant materials

Seeds of *Arabidopsis thaliana* ecotype Columbia-0 (Col-0) and *Oryza sativa* cv. Nipponbare were used for experiments. *Arabidopsis* seeds were purchased from Lehle Seeds (Round Rock, USA)

and multiplied in my lab. Rice seeds were purchased from Noken Co. (Kyoto, Japan). Seeds were stored at 4°C in a dry container until use.

Seed treatment with reactive oxygen species

A combination of H_2O_2 and a metal catalyst, $FeSO_4 \cdot 7H_2O$, or $CuSO_4 \cdot 5H_2O$, was used to generate •OH based on the Fenton reaction/Haber Weiss (see formula below). The metal catalysts were used in a ratio of 1:200 with H_2O_2. •OH catalyzed by $FeSO_4 \cdot 7H_2O$ and $CuSO_4 \cdot 5H_2O$ is denoted •OH(Fe) and •OH(Cu), respectively. Seeds were also treated with the same concentration of H_2O_2 without any metal catalyst to compare against the effect of •OH. All solutions were prepared at pH 4.9 using 0.1 M sodium citrate buffer.

$$H_2O_2 + Fe\,(II) \rightarrow Fe\,(III) + \text{•OH} + OH^-$$

$$H_2O_2 + Cu\,(I) \rightarrow Cu\,(II) + \text{•OH} + OH^-$$
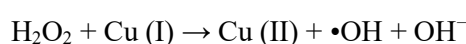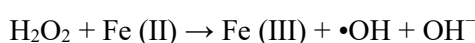
After surface sterilization, *Arabidopsis* seeds were treated with •OH(Fe/Cu) (0, 3, 6, and 25 mM H_2O_2 in the ratio with Fe/Cu mentioned above) or a similar concentration of H_2O_2 without any metal catalyst in 1.5 ml microtubes. The tubes were incubated for 1, 4, 8, and 24 h in the dark at room temperature (23°C) before seeding. Rice seeds were submerged in •OH(Fe) (0, 25, 50, 75, and 100 mM H_2O_2 in the ratio with Fe mentioned above) in 50 ml Falcon tubes and incubated at room temperature on a rotary shaker at 80 rpm for 6 h in the dark. The seeds were then planted in a designated medium without washing off the treatment solution except for one batch of •OH(Fe)-treated *Arabidopsis* seeds, in which the seeds were washed with ultrapure water after incubation (indicated as •OH(Fe)+W). All seeds were germinated under the ambient condition.

Germination and growth assay in ambient conditions

Arabidopsis seeds were germinated on 0.8% agar (Wako, Japan) medium with a modified Hoagland solution (Uemura et al., 1995). For each treatment condition, at least 80–100 seeds were sown on the agar medium without clustering in a 9 cm square petri dish. The agar plates were placed vertically inside a growth chamber (CLE-303, Tomy Digital Biology, Tokyo, Japan) at 23°C under dark conditions. For rice, at least 30 seeds were germinated with 5 ml of water in a 9 cm petri dish and kept at 30°C under dark inside a growth chamber (E-8 growth chamber, Conviron, Winnipeg, Manitoba, Canada). All experiments were repeated more than three times in duplicate. A seed was considered germinated when the radicle emerged by protruding the seed coat. Germination data were collected by taking photographs at different time points to determine the time required for 50% germination (*t50*). The *t50* was considered as the speed of germination, which has been used as a determining factor for seed vigor in different studies (Hacisalihoglu et al., 1999; Mastouri et al., 2010). Final germination numbers for both *Arabidopsis* and rice plants were counted 48 h after transfer to the growth chamber.

The root growth of *Arabidopsis* at 23°C was marked every 24 h from day 5 to day 9 after the seeds were placed on agar media. The lateral roots were counted at day 10. All roots, including taproots and lateral roots, were measured for more than 30 plants from at least five replicates. All photographs were taken using high-resolution cameras (Canon 80D, 100D, and M5) and analyzed using the open-source image analysis software ImageJ (version 1.51, https://imagej.nih.gov/ij/). For rice, the radicle length of 48-h-old seedlings was measured.

Seed treatment on germination under different abiotic stresses

For chilling stress, *Arabidopsis* seeds treated with or without •OH(Fe) solution were planted on agar as described above and placed vertically inside a growth chamber (CLE-303, Tomy Digital Biology, Tokyo, Japan) at 11°C in the dark. Photographs were taken every 12 h after transfer to the chamber.

To study the germination performance under high temperature, *Arabidopsis* seeds with or without •OH(Fe) treatment were planted on agar plates and kept vertically in a growth chamber at 30°C. Data were taken at several different time points after transfer to the chamber.

To expose seeds to heat stress, a slightly modified version of the basal heat stress method used by Silva-Correia (2014) (Silva-Correia et al., 2014) was applied: treated and untreated *Arabidopsis* seeds were washed and kept at 50°C in a heat block (ALB-120, Iwaki Asah Techno Glass, Japan) for 65 min and then transferred to 23°C conditions. Photographs were taken every 12 h. Maximum germination was measured at 96 h after transfer to the chamber.

Treated and untreated *Arabidopsis* seeds were germinated on agar in the presence of 120 mM and 150 mM NaCl and kept vertically in a growth chamber. Photographs were taken every 12 h after transfer to the growth chamber. For rice seeds, treated or untreated seeds were germinated in water containing different concentrations of NaCl ranging from 25 to 200 mM.

Statistical analysis of data using the four parameter Hill function (4PHF)

Statistical analysis was carried out using the "Germinator_curve-fitting 1.31.xls" Microsoft Excel solver, a part of the "Germinator" software package developed by Joosen et al. (Joosen et al., 2010). This solver was developed based on the four parameter Hill function (4PHF), a mathematical model described by El-Kassaby et al. (El-Kassaby et al., 2008) to describe germination properties from curve fitting. The solver can extract valuable information from a germination curve that is biologically relevant to the germination characteristics of a seed population using the following equation:

$$y = y_0 + ax^b/(c^b + x^b)$$

where y is the cumulative germination percentage at time x (h), y_0 is the intercept on the y-axis (≥0), a is the maximum cumulative germination percentage (≤100), b controls the shape and steepness of the germination curve, and c is the time to reach 50% germination by viable seeds (*t50*). A detailed

description of how this solver performs the statistical analysis can be found in the article by Joosen et al. (Joosen et al., 2010) and also on the website (https://www.wur.nl/en/Research-Results/Chair-groups/Plant-Sciences/Laboratory-of-Plant-Physiology/Wageningen-Seed-Lab/Resources/Germinator.htm).

From this 4PHF, germination performance was measured by extracting information such as maximum germination (*gMAX*), mean germination time (*MGT*), time for 50% viable seed germination (*t50*), germination uniformity (*U_{b-a}*), and area under the germination curve (*AUC*). The germination uniformity (*U*) can be set to different ranges of germination; for example, U_{75-25} is the uniformity from 25% to 75% germination of the seeds. *AUC* is the area between the germination curve and the *x*-axis (the germination time).

El-Kassaby et al. (El-Kassaby et al., 2008) defined the differences between areas under the curve of cold-stratified and unstratified seeds (*$\Delta AUC = AUC_{\text{stratified seeds}} - AUC_{\text{unstratified seeds}}$*) as the dormancy index (*DI*), which can be used as a quantitative measure of changes in seed vigor due to specific treatments. Using a similar idea to *DI*, I used *ΔAUC* to quantify the effect of the ROS treatment under ambient and stress conditions. In this study, *ΔAUC* under ambient conditions (23ºC for *Arabidopsis* and 30ºC for rice) was defined as the germination speed index (*GSI*) and under stress conditions as the stress index (*SI*) as defined by Joosen et al. (Joosen et al., 2010). *GSI* and *SI* were measured by the averaged differences between the *AUC* of the ROS-treated seed germination curve (*AUC_{ROS}*) and *AUC* of the control seed germination curve (*AUC_{Control}*) under different stress conditions (*$\Delta AUC = \Delta AUC_{\text{ROS}} - \Delta AUC_{\text{Control}}$*). In this experiment, *AUC* was counted from the initial germination time *t = 0* to the maximum germination time for all experiments. This germination curve fitting summarized the data with different biologically relevant information regarding seed germination using Student's *t*-test and Tukey's HSD.

Results

Hydroxyl radical/ROS treatment accelerates germination and early seedling growth

In preliminary experiments with different "concentration × incubation period" combinations, the optimum treatment conditions for *Arabidopsis* were found to be 8 h of incubation in 0.03 mM Fe/Cu and 6 mM H_2O_2 solution. Under these conditions, it took the shortest time to reach 50% germination in most cases (Figure 3.1). To nullify the effect of the seed surface-bound treatment solution on germination and other developmental changes, •OH(Fe)-treated seeds were washed after eight-hour incubation. The germination of the washed seeds maintained the similar tendency to the •OH(Fe)-treated seeds. Furthermore, to determine the effect of light on germination, seeds were germinated both under a 16-h light and 8-h dark cycle and under continuous dark. *Arabidopsis* seeds germinated faster under continuous dark than under the light-dark-cycling conditions. In the dark, seeds treated with the

optimized treatment solution reached 50% germination 10+ h earlier than seeds germinated under the light and dark conditions (Figure 3.2). Thus, for all subsequent studies, the seeds were germinated in the dark.

The maximum germination of *Arabidopsis* seeds at ambient temperature reached over 95% in all treatments and control groups, and the treatment increased the speed of germination significantly (Figure 3.3A). To extract more biologically relevant information from the germination data, the 4PHF was applied by inputting the germination data at different time points into the "Germinator curve-fitting 1.31.xls" solver (Joosen et al., 2010). The solver returned similar results to the manual germination data analysis with a characteristic germination curve (Figure 3.4). This curve provided significant biological information such as *t50*, *AUC*, *gMAX*, *MGT*, and U_{7525} (Figure 3.3B, C, and 3.5).

Because mean germination time does not provide clear information on the imbibition initiation time and specific germination percentage, the time to reach 50% germination (*t50*) was used to describe seed vigor (Soltani et al., 2015). *t50* is also a sensitive measure of seed quality and viability under field conditions (Mastouri et al., 2010). Germination speed was significantly (*P < 0.05*) faster in the •OH(Fe)-treated group than the control. The *t50* for the •OH(Fe)-treated seeds was 5 h shorter than the control (Figure 3.3B). There was a slight difference in *t50* between the •OH(Fe/Cu)- and H_2O_2-treated seeds, which was not statistically significant (Figure 3.3B). The germination speed was further quantified from the differences in the *AUCs* of the control and all the other ROS treatments (•OH(Fe/Cu), •OH(Fe), and then washing, and H_2O_2) (Figure 3.3C and D). This difference was expressed as *ΔAUC*, where *ΔAUC = AUC* of any treatment group – *AUC* of the control group. The *ΔAUC* of a treatment under the optimum conditions was named the germination speed index, *GSI.* The *GSI* of the •OH(Fe)-treated group was correlated with the actual germination percentage of the •OH(Fe)-treated seeds. The *GSI* of the •OH(Fe) or •OH(Cu)-treated seeds at different time points was higher than that of the H_2O_2-treated seeds, and the extent of the effect was similar in the Fe and Cu systems (Figure 3.3D). Interestingly, in all these data, I observed that the washed seeds, •OH(Fe)+W, showed a similar effect as the •OH(Fe)-treated seeds. When I considered the data from the •OH(Fe)-treated seeds in the statistical analysis, I found a highly significant correlation (r^2 = 0.979, Figure 3.3E). Based on data, showing that both metal catalysts (Fe, Fe+ H_2O_2+W, and Cu) had similar effects on germination, only Fe-catalyzed data were used for further statistical analysis to determine the •OH treatment effects to avoid redundancy.

Early seedling growth was also positively affected by the •OH(Fe) treatment. The radicles were clearly longer in the •OH(Fe)-treated seeds. The differences were visible at 36 h through to 72 h. The opening and greening of the cotyledon started earlier in the •OH(Fe)-treated seeds than the control (Figure 3.6A).

The treatment effect is sustained beyond germination

The difference in early seedling growth after 72 h indicated the •OH(Fe) treatment had a relatively long-term effect on seedling growth. Even though I observed the growth in both shoot part (hypocotyl and cotyledon) and the root part, in the early stages the growth was more visible and quantifiable in the roots. Therefore, root growth and lateral root numbers were measured to compare the effect between the control and the treated group.

The root growth difference between seedlings from non-treated control and •OH(Fe)-treated seeds was recorded from day 6 to day 9 after transfer into the growth chamber. The difference between the root growth of the control and the treatment group was always significant ($P < 0.05$) from day 6 to day 9 (Figure 3.7A). There was also a significant difference in the total length of roots between the two groups after 9 days of germination (Figure 3.7B).

In addition, I made an interesting observation of lateral root numbers. When the lateral roots per plant were counted on day 10, the •OH(Fe)-treated group had a significantly ($P < 0.05$) larger number of lateral roots than the control group (Figure 3.7C). The treated seedlings had an average number of >12, while the control seedlings had only an average number of 10 lateral roots per plant (Figure 3.7C, S5B). On day 10, the lateral roots in the •OH(Fe)-treated group also looked longer and denser than the control group (Figure 3.6B).

The effect of the hydroxyl radical treatment is prominent under abiotic stress

After observing a clear and significant difference between the water treatment (control) and ROS treatments (•OH and H_2O_2) on *Arabidopsis* seed and seedling performance under ambient conditions, the treatment effects were tested under various abiotic stresses such as chilling, high temperature, heat, and salinity.

The speed of *Arabidopsis* seed germination decreased dramatically under the chilling condition at 11°C, but •OH(Fe) or •OH(Cu) treatment had a prominent effect under this condition (Figure 3.8A). The treated group germinated significantly ($P < 0.05$) faster than both the control and H_2O_2-treated group (Figure 3.8A) and took a significantly shorter time ($P < 0.05$) to reach 50% germination (Table 3.1). The •OH(Fe/Cu)-treated seeds showed a prominent tolerance effect under this condition and showed improved $gMAX$, U_{7525}, MGT, and AUC compared with the control and H_2O_2-treated seeds (Figure 3.9A–D). However, there was no significant difference in U_{7525} between the Fenton- and H_2O_2-treated seeds (Figure 3.9B). The effect of the treatment was also observed in early seedling growth after 6 days with longer radicle and opened cotyledon in the treated group than the controls (Figure 3.10A).

Compared with low temperature, incubation of seeds at high temperature (30°C) increased the germination speed, although it was not as fast as the germination at ambient temperature (23°C) (Figure 3.8B). Even though the •OH(Fe/Cu)-treated seeds took significantly less time than the control seeds,

there was no significant difference between treated seeds with different combinations (•OH(Fe) and H_2O_2) (Table 3.1). The *gMAX* for the •OH(Fe/Cu)-treated was higher than the control group, but there was no significant difference between either control and H_2O_2- treated seeds or •OH(Fe/Cu)-treated and H_2O_2- treated seeds (Figure 3.9E). U_{7525}, *MGT*, and *AUC* of ROS-treated seeds showed a significant difference with that of the control seeds (Figure 3.9F-H). Furthermore, there was a clear difference in seedling growth; cotyledon opening and radicle growth were faster in all ROS-treated groups than the control (Figure 3.10B).

Although the speed of germination was greatly reduced after heat stress at 50°C for 65 min, the ROS treatment improved the germination performance significantly (Figure 3.8C and S6I). The germination rates of the treated seeds reached 50% more than 10 h earlier than that of the control; 61.5 h and 62.1 h for •OH(Fe) and •OH(Cu), respectively, compared with over 71.6 h for the control (Table 3.1). The difference was only a few hours between the •OH(Fe/Cu)-treated and H_2O_2-treated seeds (Table 3.1). *MGT* was also significantly smaller in comparison to the control and H_2O_2-treated seeds (Figure 3.9K). There was no significant difference in germination uniformity (U_{7525}) observed in control *vs.* •OH(Fe/Cu and H_2O_2 *vs.* •OH(Fe/Cu). (Figure 3.9J). Because the experiments were carried out in the dark, the cotyledons were elongated. However, cotyledon -expansion and -greening, hypocotyl, and radical elongation were advanced in all of the treated seeds, and the difference was visible 72 h after transfer to the chamber (Figure 3.10C).

Similar to chilling and heat stress, salinity stress decreased the germination performance, but the •OH treatment improved seed germination (Figure 3.8D). The •OH(Fe/Cu)-treated seeds performed much better than the control and the H_2O_2-treated seeds under salinity stress, and the extent of the effect was larger at 150 mM than at 120 mM NaCl (Table 3.2). At 150 mM NaCl, the •OH(Fe/Cu)-treated seeds reached 50% germination earlier than both the control and the H_2O_2-treated seeds; •OH(Fe/Cu)-treated seeds took around 16 h less than the control and 7 h less than the H_2O_2-treated seeds (Table 3.1). Except for the germination uniformity where the differences were close to each other among the groups, the *gMAX*, *AUC*, and *MGT* were significantly better in the •OH(Fe/Cu)-treated seeds (Figure 3.9M–P). Both the germination and the early seedling growth were accelerated by the •OH(Fe/Cu) treatment under salinity stress: opened and green cotyledon, longer radicles are clearly visible in the treated groups (Figure 3.10D).

The 4PHF can be used to extract biologically relevant information using the surface area under each germination curve, which is expressed as *AUC* in a short form. As mentioned by Joosen et al. (Joosen et al., 2010), the *AUC* can be used to quantify the effect of any treatment under different stress conditions as an index of stress. As described in the methods section, by deducting the *AUC*s extracted from the solver for the control and ROS-treated groups ($\Delta AUC = \Delta AUC_{ROS} - \Delta AUC_{Control}$) under all four abiotic stress conditions, the *SI* was calculated. The data in Figure 3.11A, C, E, and G show clearly that •OH(Fe/Cu)-treated seeds had a larger ΔAUC. There was no difference in the *AUC*s of the •OH(Fe)-

and •OH(Cu)-treated seeds, even though the *AUC* of the •OH(Cu)-treated seeds was slightly larger than that of the •OH(Fe)-treated seeds (Figure 3.11E and G). *SI* for the •OH(Fe)-treated seeds was plotted against the original germination percentage under every stress and a significant correlation ($r = 0.99$) was found for each stress (Figure 3.11B, D, and F): chilling stress, $r^2 = 0.983$; high temperature stress, $r^2 = 0.994$; heat stress, $r^2 = 0.972$; salinity stress, $r^2 = 0.981$. The *SI* for the •OH(Cu)-treated seeds also showed a similar correlation with the germination percentage under every stress (data not shown).

The •OH treatment also improves the performance of a crop plant: rice

The promising effect of the •OH(Fe/Cu) treatment on performance in the model plant *Arabidopsis* seed directed my attention to its use on an important crop plant such as rice. The Fe-based •OH(Fe/Cu) treatment showed a similar effect on rice seeds under non-stressed conditions; it increased the germination rate as well as the speed of germination (Figure 3.12A). The time for 50% germination of the •OH(Fe/Cu)-treated seeds was significantly shorter than for the water control (Figure 3.12B). Furthermore, early growth, as determined by radicle length was significantly larger in the •OH(Fe/Cu)-treated seeds than in the control seeds (Figure 3.12C).

As a case study to investigate the effect of the •OH(Fe/Cu) treatment on rice seed germination under stressed conditions, I applied salinity stress (25–200 mM NaCl) to seeds germinated at 30°C. The results were similar to what I found in the *Arabidopsis* seeds; the •OH(Fe/Cu) treatment accelerated rice seed germination under salinity stress. From 25 to 200 mM NaCl, the •OH(Fe/Cu)-treated seeds performed better than the control in every case (Figure 3.13 and 3.14A). Furthermore, the effect at higher NaCl concentrations (100–200 mM) was more prominent; the seeds germinated faster according to the 48-h germination rate and the time to 50% germination (Figure 3.14A and B). In addition, similar to what I observed in the *Arabidopsis* seed germination, *ΔAUC* was also larger at 100 mM and 150 mM NaCl (Figure 3.14C).

Under abiotic stress conditions, in both *Arabidopsis* and rice, the seeds in the control group could never reach a similar germination percentage to the treated group (Fig 3 A to D, 3.9; Figure 3.14). For example, in rice when the stress level was high (200 mM NaCl), the treated seeds reached over 95% germination, where the controls were below 70% at the 48th hour (Figure 3.14). Furthermore, by the time the control groups reached their full germination potential, the treated groups already started other growth and developmental stages such as hypocotyl and radicle growth, opening- and greening- in cotyledons (Figure 3.10).

Discussion

A cost-effective, non-laborious single seed treatment that improves germination, growth performance, and tolerance against multiple abiotic stresses, and could contribute to an increase in crop production, may provide an essential tool for the adaptation to the emerging/ongoing threat of global

climate change to agriculture. In this study, I demonstrated that a single seed (*Arabidopsis* and rice) treatment with H_2O_2 and a metal catalyst such as Fe or Cu, which quickly produces hydroxyl radicals (•OH) in the system, resulted in faster germination under both ambient and different abiotic stress conditions. It also improved the growth performance of young seedlings (root growth and lateral root numbers). In addition, interestingly, the treatment improved seed and seedling performance under abiotic stress conditions, including chilling, high temperature, heat, and salinity stresses. The positive effects of this treatment on rice seedlings indicate a potential use for this treatment in major crops.

The •OH treatment accelerated germination speed (*t50*) in both *Arabidopsis* and rice seeds under ambient temperature (23°C and 30°C, respectively) (Figure 3.3A and 5A). The *ΔAUC* or germination speed index (*GSI*) significantly correlated ($r^2 > 0.9$) with the germination percentage at different time points, indicating that the acceleration of germination was due primarily to the treatment effect of ROS and the metal catalyst in the treatment solution rather than random chance. This correlation fits with the study by El-Kassaby et al.(El-Kassaby et al., 2008), who used a similar approach to quantify the effect of cold stratification on seed germination and dormancy breaking using the term dormancy index (*DI*). The positive effect of the •OH treatment was further proved by washing the seeds after •OH(Fe)-treatment, where the washed seeds [•OH(Fe)+W] also showed similar germination profile as the unwashed seeds (Figure 3.3A). Furthermore, the speed of germination is a critical factor that provides a sensitive measurement of seed vigor (Hacisalihoglu et al., 1999). Thus, the shorter *t50* and larger *GSI* determined in this study imply that the treatment increases seed vigor. This is consistent with several previously reported studies, where the exogenous application of •OH on seeds, directly via Fenton reagents (Muller et al., 2009b) and indirectly via nano-bubble water containing •OH (Liu et al., 2016), improved germination.

In addition to the effect observed under ambient temperature conditions (at 23°C for *Arabidopsis* and at 30°C for rice), one of the most interesting findings of this study was the improvement of seed germination and early growth under different stress conditions. In *Arabidopsis*, the treatments with ROS (•OH and H_2O_2) showed superior performance to the controls under all stress conditions employed. The faster germination, larger *AUC* and *SI*, and accelerated seedling growth (longer hypocotyl and radical and early cotyledon-expansion and -greening) indicate that the treatment improves stress tolerance in germinating seeds and young seedlings. Although several previous studies have shown that pre-soaking/treating seeds with H_2O_2 improves germination, growth performance, and stress tolerance by enhancing the performance of the antioxidative machinery, maintaining turgor pressure, inducing stress protein expression, and osmotic readjustment (Wahid et al., 2007; Liheng et al., 2009; Gondim et al., 2010), there is, to my knowledge, no evidence that exogenous •OH treatment results in similar and in most cases superior improvements under abiotic stress.

The effect also continued beyond the germination stage to the early radicle growth stage in both *Arabidopsis* and rice. The effect of the treatment at much later stages was shown by an increase in daily

root growth and in the number of lateral roots in *Arabidopsis*. Several reports have shown that exogenous application of •OH accelerates elongation growth in maize coleoptiles (Schopfer, 2001; Schopfer et al., 2002). These studies reported that the auxin-mediated ROS generation facilitates this extension growth. The final ROS that is generated by the action of auxin is •OH, which acts on the cell wall to breakdown polysaccharide crosslinking and loosens the tightness of the cell wall. Renew et al. also reported that the plasma membrane-bound NADPH oxidase (NOX) enzyme generates apoplastic superoxide radicals ($O_2^{•-}$). $O_2^{•-}$ is a precursor of H_2O_2, and apoplastic metal catalysts (Fe/Cu) can easily convert H_2O_2 into •OH and then facilitate elongation growth similarly to the exogenous application (Fry, 1998; Foreman et al., 2003). Exogenous application of H_2O_2 can also restore the formation of lateral roots in the mutants that do not produce lateral roots (Orman-Ligeza et al., 2016). Unlike previous studies, only the seeds were treated in this study, and no other treatment was applied to plants in later stages. Because ROS mediate signal transduction in plants (Mittler, 2006; Miller et al., 2009; Baxter et al., 2014; Mittler and Blumwald, 2015; Mittler, 2017), it is possible that the treatment with ROS (•OH and H_2O_2) might affect a signaling mechanism that the plants carry from the germination stage to later stages, such as lateral root formation. In addition, I cannot rule out the possibility that the accelerated seed germination and root growth might partially come from the seed coat and cell wall weakening by the action of exogenous •OH (Muller et al., 2009b).

Moreover, apoplastic •OH is involved in the salt overly sensitive (SOS) signaling pathway for adaptive growth under salinity stress, where •OH is generated by plasma membrane-bound NOX (Laohavisit et al., 2013). Under salt stress, Na^+ uptake increases the cytosolic Ca^{2+} level, which activates the membrane-bound NOX to convert $O_2^{•-}$ into •OH via H_2O_2 (Demidchik et al., 2010). As I discussed in the previous sections, •OH can facilitate germination (Muller et al., 2009b) and elongation growth (Fry, 1998; Schopfer, 2001; Schopfer et al., 2002; Renew et al., 2005). Thus, it is possible that the seed treatment in this study using ROS (•OH via H_2O_2) triggered the SOS signaling and elongation growth mechanism to facilitate germination and early seedling growth under salt stress conditions in both *Arabidopsis* and rice.

In plant cells, H_2O_2 can react with the cell wall, cell membrane, organellar membrane-bound, or cytosolic soluble metal ions and converts into •OH in a downstream reaction (Nagasaki-Takeuchi et al., 2008; Pospisil, 2009; Schwarzlander and Finkemeier, 2013). Thus •OH may play an important, positive role that contrasts with its well-established damaging properties. Hence, exogenous application of •OH at an optimum concentration may provide a head start to the supply of •OH in seed germination and early seedling growth processes. Another possible explanation of the effect could be that the treatment provides a cue to seeds to advance their physiological state. This advanced physiological state allows the embryo to start developmental processes, such as germination, earlier than the controls, which might be similar to the priming effect. The same explanation may fit with the improved stress tolerance, with the embryo sensing the exogenous ROS as a stress and activating the stress tolerance machinery in

advance. A report showed that, during priming, the initial soaking agents can generate mild to moderate stress, which can enhance tolerance to abiotic stress by activating stress-responsive genes and proteins (Kubala et al., 2015). A seed proteomic study under chilling stress (See chapter 4) showed that the •OH-treated seeds had increased abundance of dehydroascorbate reductase, ascorbate peroxidase, reduced glutathione, glutathione S-transferase, and other ROS-scavenging proteins. This indicates that similar to exogenous H_2O_2 treatment, •OH activates the ROS-scavenging system under stress conditions. However, further detailed studies are required to elucidate the mechanism.

Decades of research showed that ROS works mostly in a dose-dependent manner; a high concentration of ROS can cause cell death or oxidative stress, low concentration can be cytostatic that can slow down growth and development. On the other hand, a balanced scale of ROS can work as a signaling molecule for growth, development, and stress (Mittler, 2006; Mittler, 2017). Although individual abiotic stresses differ significantly in their signaling and response systems, they share a number of common features in signaling pathways and resultant physiological responses via crosstalk. One such common component is ROS (Mastouri et al., 2010). This was further shown by the observations in this study that ROS treatment of seeds improved germination and early growth performance under chilling, high temperature, heat, and salinity stress, possibly via a common mechanism in which ROS plays a central role. I successfully developed a seed treatment method that is easy to apply and non-laborious involving an endogenous rather than a synthetic chemical, which improves seed and seedling performance under both ambient and stress conditions. The accelerated germination, larger roots, increased lateral roots, and enhanced stress tolerance enables plants to establish under various environmental conditions. This study opens up a new application and positive roles of •OH, which is well known as a dangerous byproduct of aerobic respiration. Further technological advancements in imaging, detecting, and tracking •OH inside plant cells will reveal how, when, and where •OH works under different conditions. In addition, a comprehensive molecular study to elucidate which genes and proteins are involved in the improved seed and seedling performance due to •OH treatment will provide a better understanding of the mechanisms to improve crop management. Finally, treatment at the seed stage will save farmers time, labor, and money, and with further field trials, this treatment could be a potential solution to improve crop performance in the face of upcoming unfavorable climate conditions.
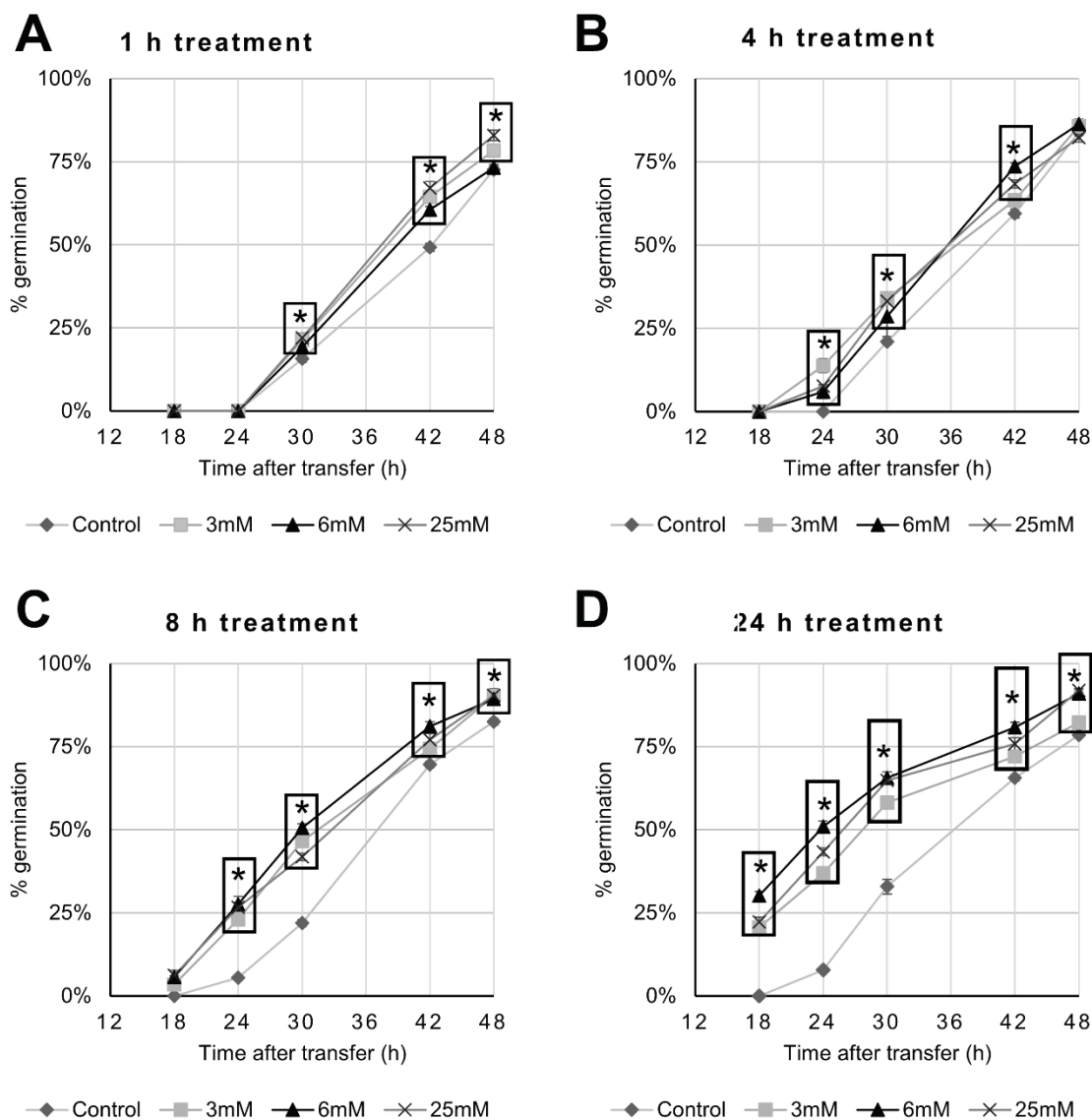
Figure 3.1. **Optimization of the treatment conditions for *Arabidopsis* seeds using different concentrations of the •OH(Fe)-solution and incubation period**. The concentration of H_2O_2 was at 0, 3, 6, or 25 mM with the fixed ratio of $FeSO_4 \cdot 7H_2O$ and H_2O_2, 1:200. Incubation/ incubation period is (A) 1 hour, (B) 4 hours, (C) 8 hours, and (D) 24 hours. The asterisk indicates a significant *P < 0.05*, Student's t-test) difference between control and other treatments.
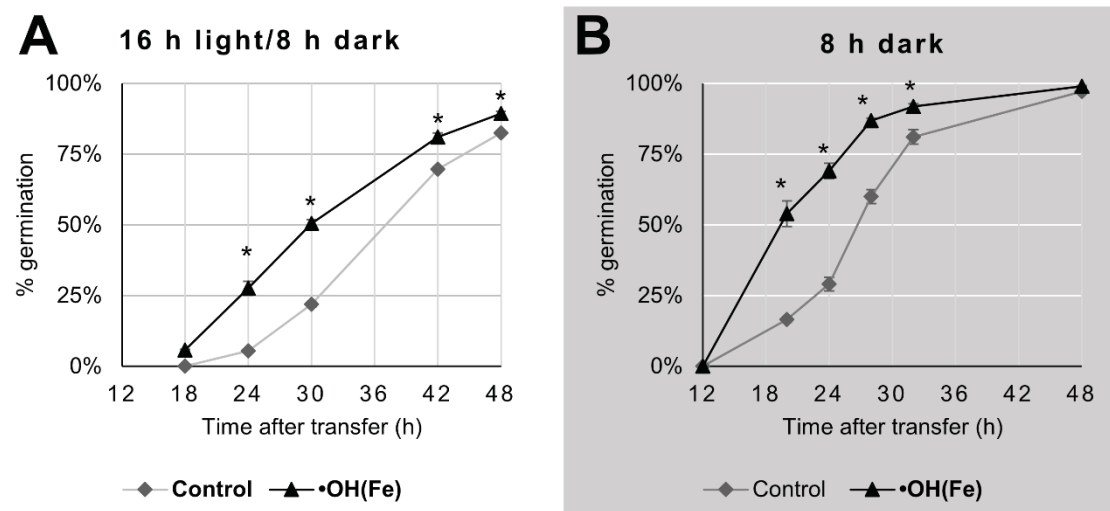
Figure 3.2. **Optimization of the light conditions for *Arabidopsis* seed germination** after the •OH(Fe)-treatment for 8 hours. The concentration of H_2O_2 was at 6 mM with a ratio of $FeSO_4 \cdot 7H_2O$ and H_2O_2, 1:200. (A) 16-hour photoperiod and (B) continuous dark.
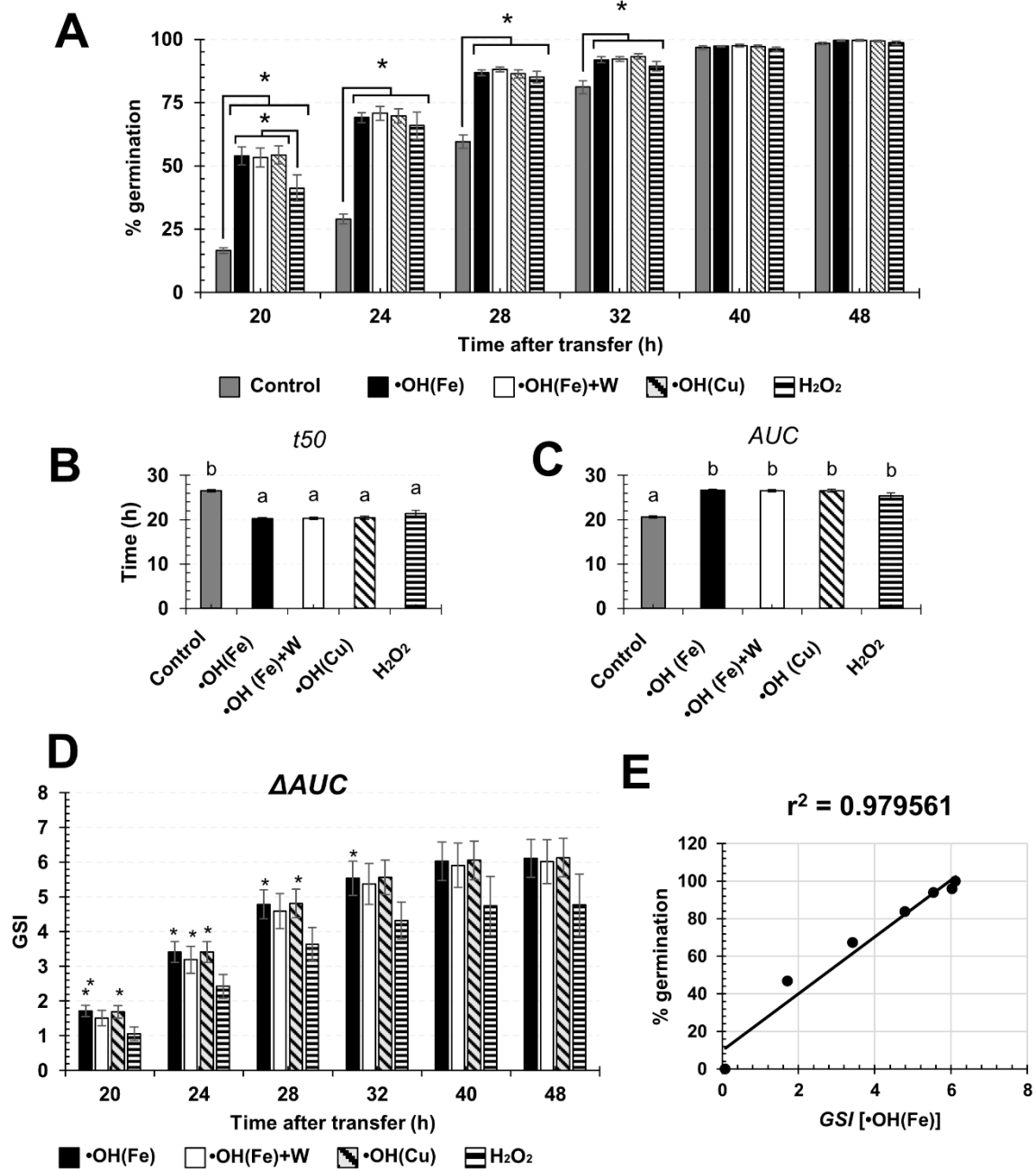
Figure 3.3. **Effect of the treatment on germination and early seedling growth of *Arabidopsis* at the ambient temperature (23ºC).** (A) Germination rate at different time points, (B) time for 50% germination (*t50*) for all the seed groups, (C) area under curve (*AUC*s) for all the seed groups at 48th hour, (D) germination speed index (*GSI*) and (E) correlation of germination speed index (*GSI*) generated by subtracting *AUC* for the control seeds from *AUC*s for the •OH(Fe/Cu), •OH(Fe)+W, and H$_2$O$_2$-treated seeds and the germination percentage at different time points. The asterisk indicates a significant $P < 0.05$) difference between conditions obtained by the Student's t-test. Letters (a–b) represent statistically different subsets (Tukey HSD, $P < 0.05$).
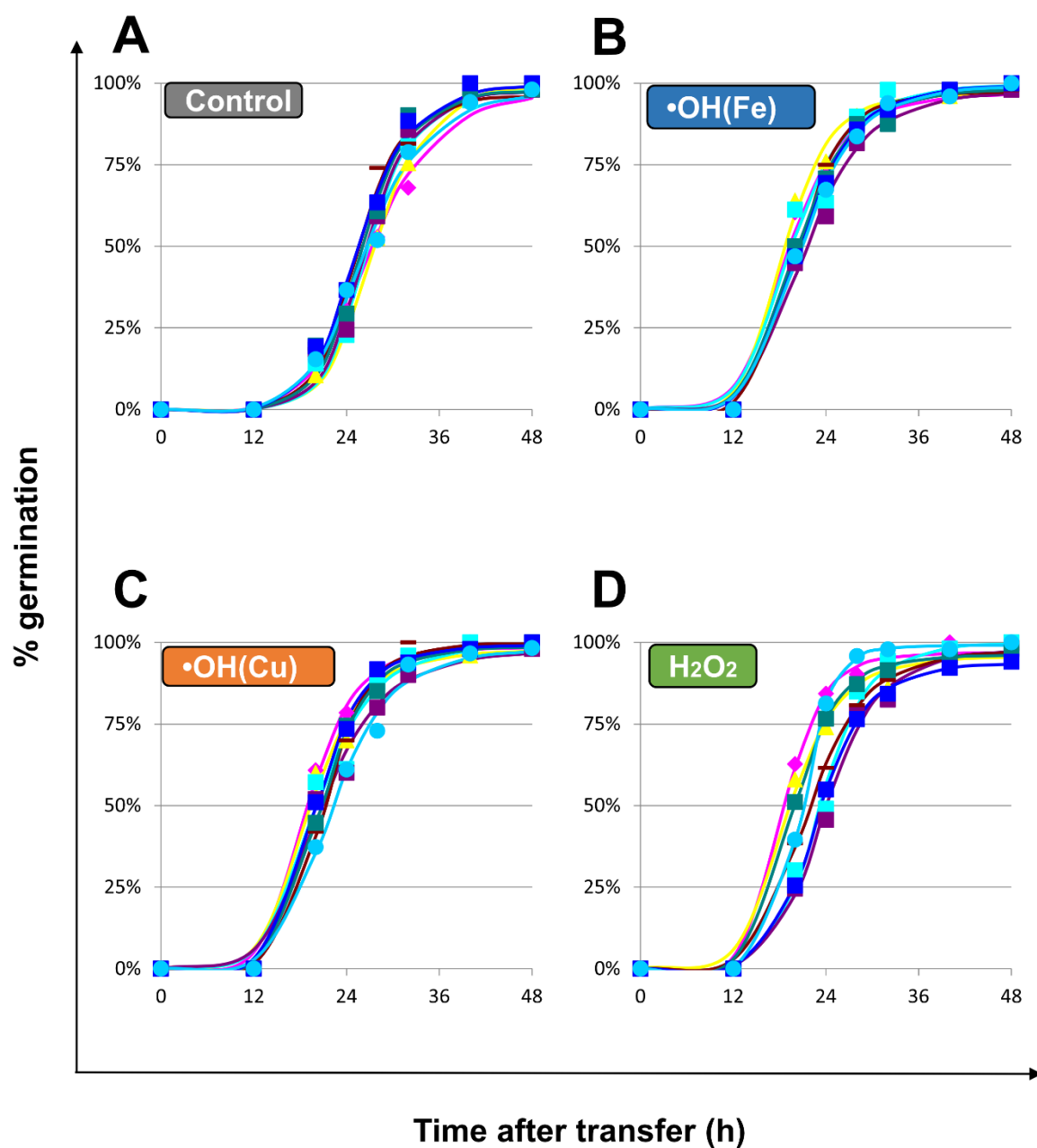
Figure 3.4. **Germination curves of *Arabidopsis* seeds treated under various conditions**. The curve graphs were generated using 4PHF formula from the Germinator package. Individual line/curve in each graph represents a duplication from an individual replicate (A) Control seeds (non-treated), (B) •OH(Fe)-treated seeds, (C) •OH(Cu)-treated seeds, and (D) H_2O_2-treated seeds.
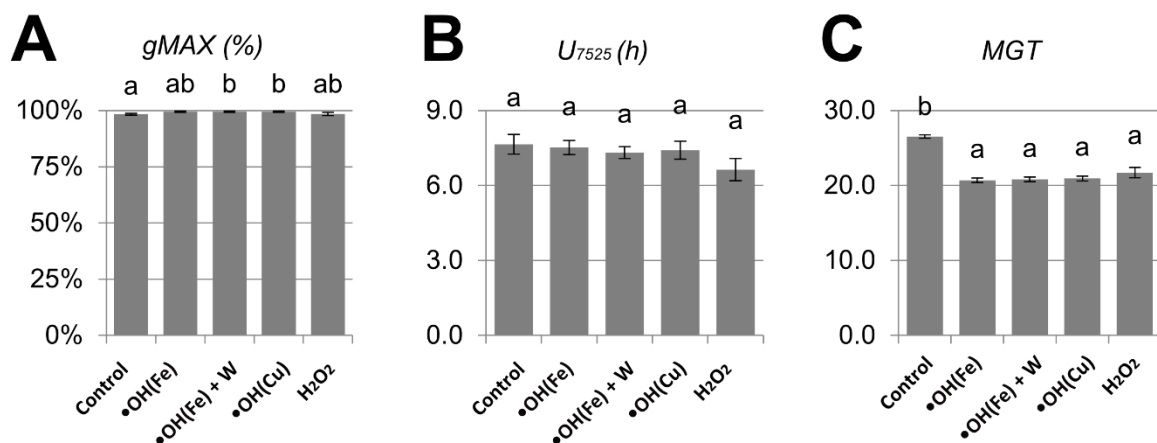
Figure 3.5. **Germination related characteristics of *Arabidopsis* seeds extracted from the Germinator package using 4PHF**. (A) Maximum germination percentage (*gMAX*) after 48 hours, (B) uniformity of germination from 25% to 75% (U_{7525}), and (C) mean germination time (*MGT*). Letters (a–b) represent statistically different subsets (Tukey HSD, *P < 0.05*).

69
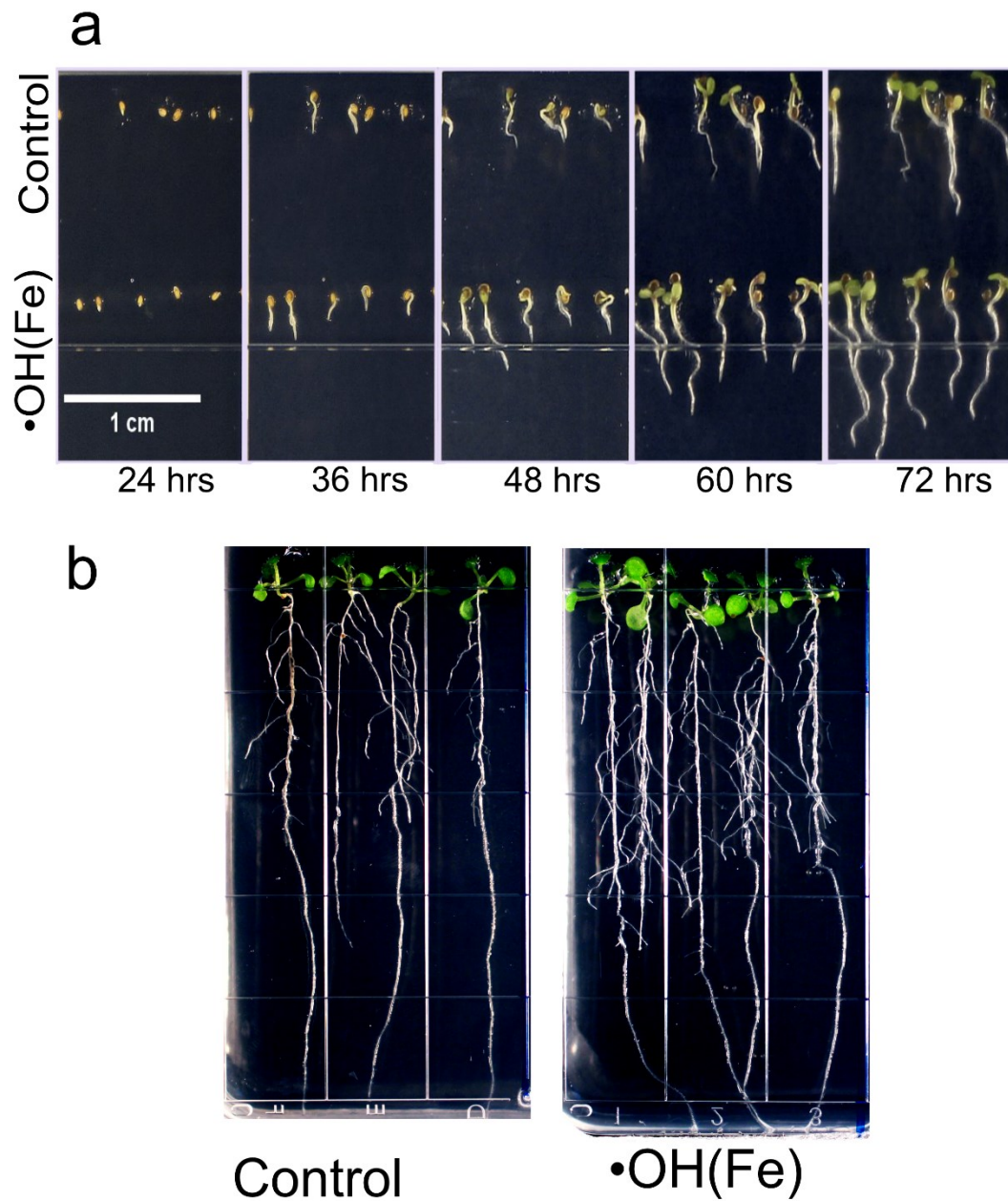
Figure 3.6. **Treatment effect beyond germination.** (A) The differences between the control and the •OH(Fe)-treated groups in growth patterns in the early stage. (B) The differences between the control and the •OH(Fe)-treated groups in lateral roots on day 10.
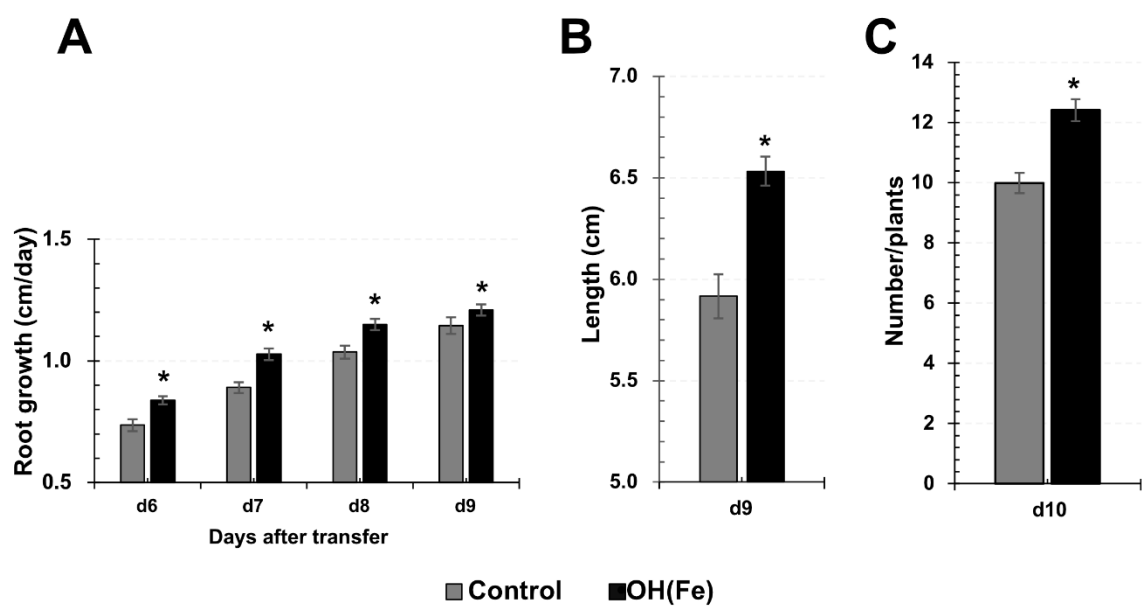
Figure 3.7. **Effect of the treatment on *Arabidopsis* seedling growth.** (A) Daily root growth from day 6 to day 9, (B) total root length after 9 days, and (C) the number of lateral roots per plant after 10 days. The asterisk indicates a significant $P < 0.05$) difference between conditions obtained by the Student's t-test.
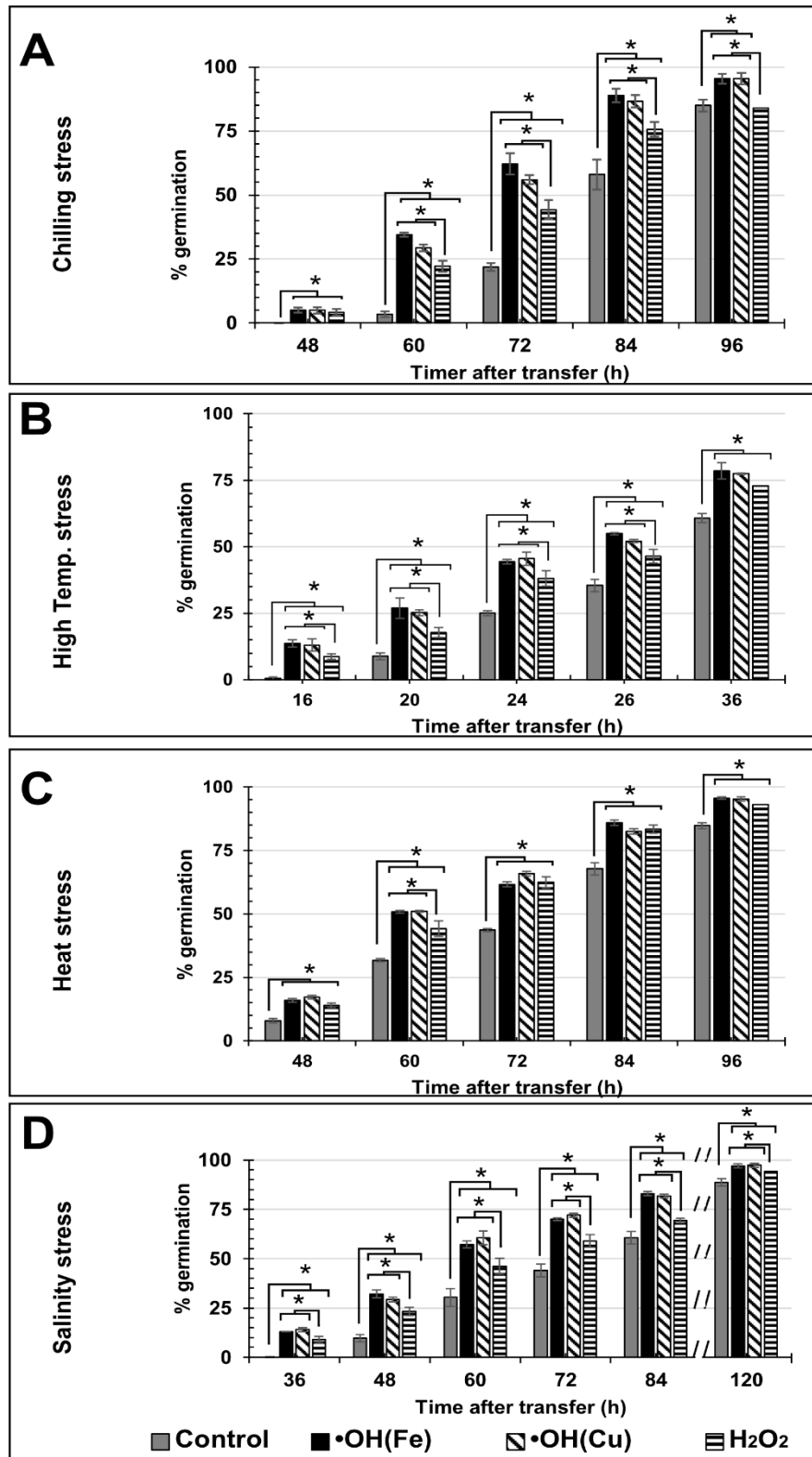
Figure 3.8. **Germination and early growth performance in *Arabidopsis* under different abiotic stresses.** Graphs show the seed germination rate, and the photographs show early seedling growth. (A) Chilling stress (11°C), (B) high-temperature stress (30°C), (C) heat stress (50°C, 1 h), and (D) salinity stress (150 mM NaCl). The asterisk indicates a significant ($P < 0.05$) difference between conditions obtained by the Student's t-test.

Treatments	Chilling(11ºC)		High temperature (30ºC)		Heat (50ºC for 65 min)		Salinity (150 mM NaCl)	
	$t50$ (h) ±SE	$P < 0.05$	$t50$ (h) ±SE	$P < 0.05$	$t50$ (h) ±SE	$P < 0.05$	$t50$ (h) ±SE	$P < 0.05$
Control	80.7±1.3	c	29.6±0.5	b	71.6±0.5	c	73.3±2.5	c
•OH(Fe)	66.1±0.8	a	24.7±0.3	a	61.5±0.2	a	56.9±0.9	a
•OH(Cu)	68.0±0.5	a	25.0±0.3	a	62.1±0.2	b	56.5±1.1	a
H_2O_2	72.2±1.4	b	26.7±0.8	a	63.6±0.8	b	64.1±2.3	b

Table 3.1. **Comparison of the 50% germination time (t50)** among four different stresses generated using 4PHF from the Germinator package (asterisk indicates the germination temperate 23ºC). Letters in the P < 0.05 columns indicate the significant differences from Tuckey's HSD test.

Treatment	120 mM NaCl		150 mM NaCl	
	t50 (h) ±SE	$P < 0.05$	t50 (h) ±SE	$P < 0.05$
control	50.6±0.7	b	73.3±2.5	c
•OH(Fe)	45.5±1.0	a	56.9±0.9	a
•OH(Cu)	46.0±0.6	a	56.5±1.1	a
H_2O_2	45.8±0.9	a	64.1±2.3	b

Table 3.2. **Comparison of the 50% germination time (*t50*)** of *Arabidopsis* seeds subjected to various treatments under salinity stress conditions, 120 and 150 mM NaCl generated using 4PHF from the Germinator package. Letters in the *P < 0.05* columns indicate the significant differences from Tuckey's HSD test.
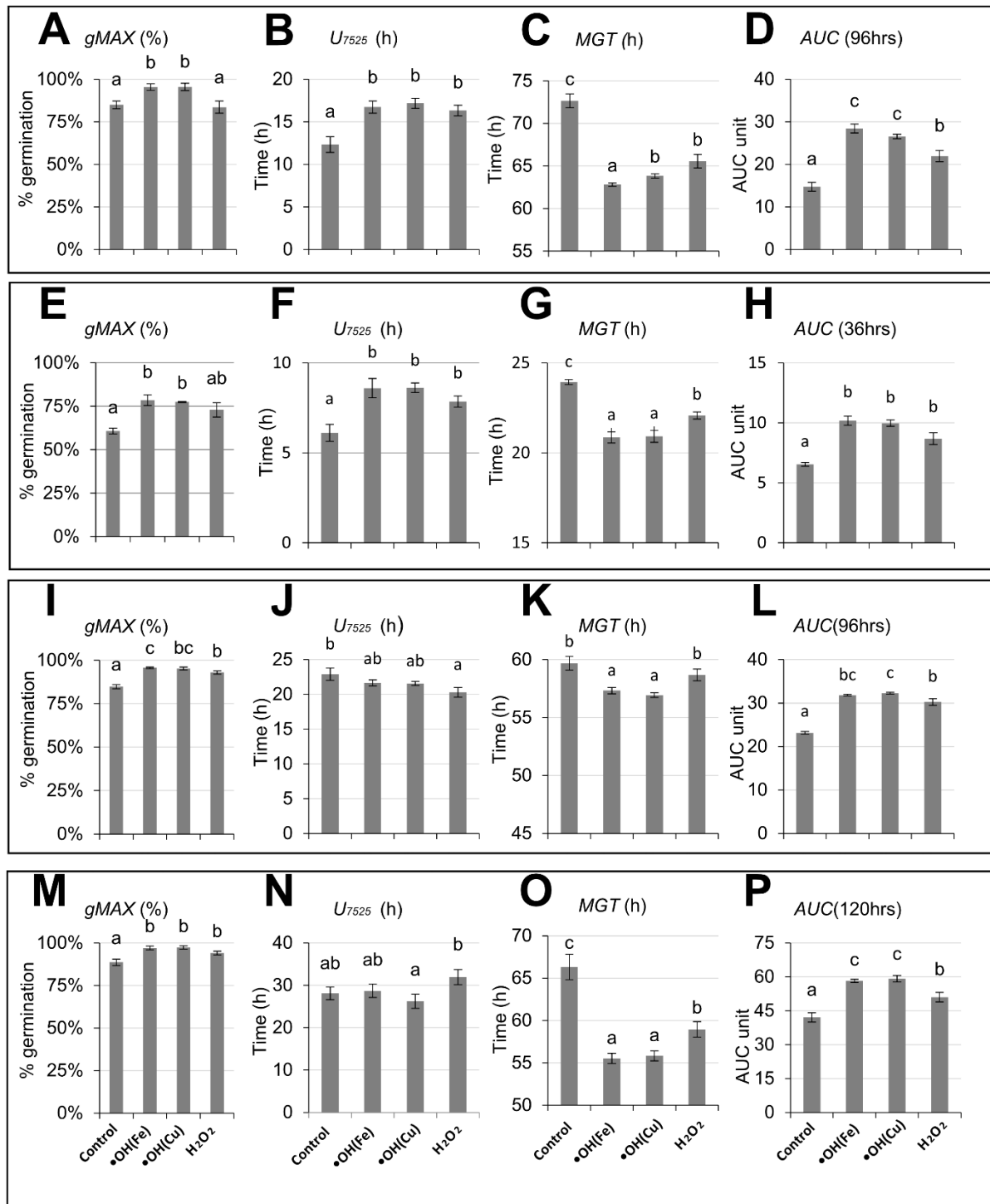
Figure 3.9. Germination related characteristics (maximum germination, *gMAX*; uniformity from 25% to 75% germination, U_{7525}; mean germination time, *MGT*) of *Arabidopsis* seeds extracted from the germinator package using 4PHF. (A-D) Chilling stress (11ºC), (E-H) High temperature (30ºC), (I-L) Heat stress (50ºC for 1 hour), and (M-P) salinity stress (150 mM NaCl).
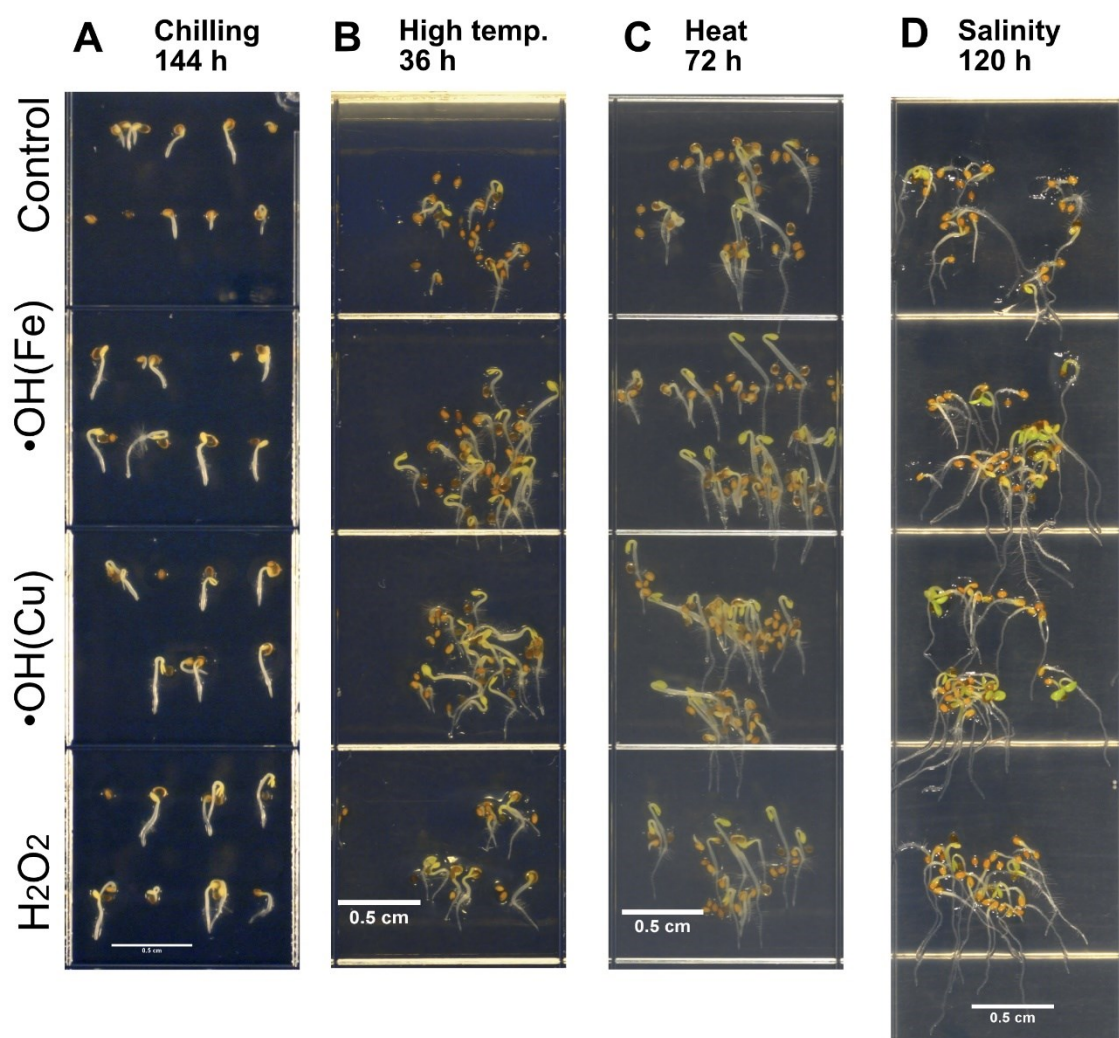
Figure 3.10. **Visual differences between the control and the •OH(Fe)-treated groups under different abiotic stresses.** (A) Chilling stress (11°C) for 144 hours, (B) high-temperature stress (30°C) for 36 hours, (C) heat stress (50°C, 1 hour) then returned to ambient conditions for 72 hours, and (D) salinity stress (150 mM NaCl) for 120 hours.
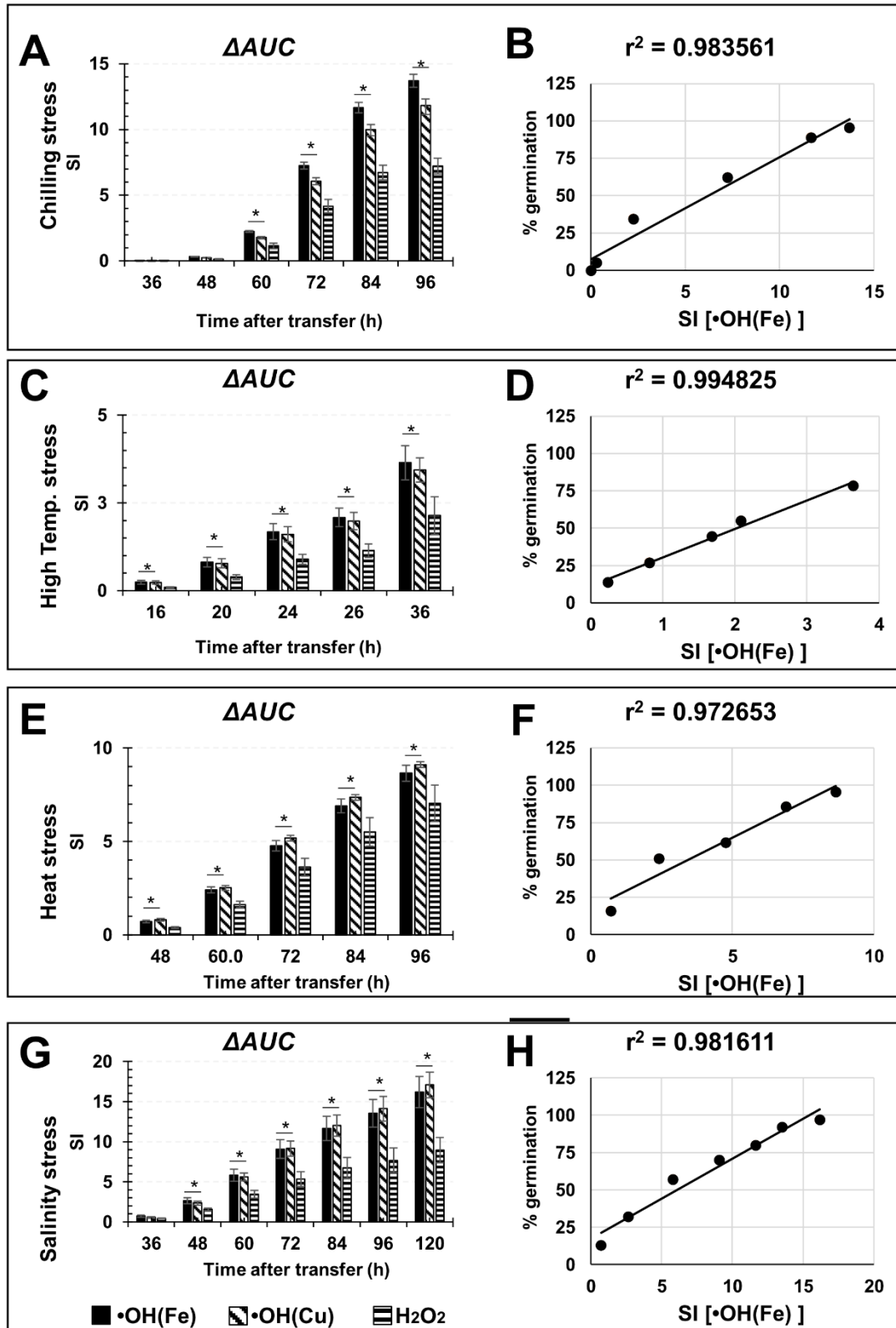
Figure 3.11. **Seed germination indices (*ΔAUC* and *SI* for *Arabidopsis* seeds germinated under abiotic stresses.)** *ΔAUC* and *SI* were calculated at different time points, as described in the text. (A and B) Chilling stress (11°C), (C and D) High-temperature stress (30°C), (E and F) heat stress (50°C, 1 hour), and (G and H) salinity stress (150 mM NaCl). The asterisk indicates a significant $P < 0.05$) difference between •OH(Fe/Cu) and H_2O_2 obtained by the Student's t-test.

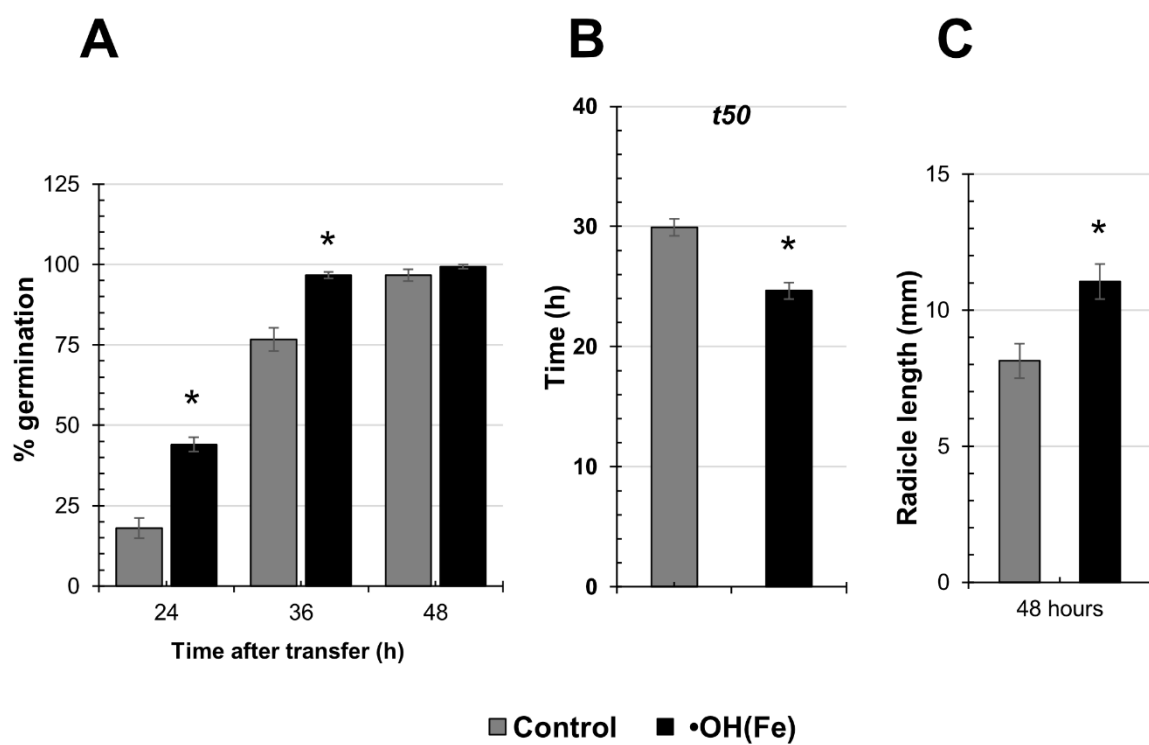**Figure 3.12**. **Effect of the •OH(Fe)-treatment in rice seeds.** (A) Germination, (B) time for 50% germination *t50*, and (C) radicle growth at 48th hours. The asterisk indicates a significant *P < 0.05*, Student's t-test) difference between control and other treatments.
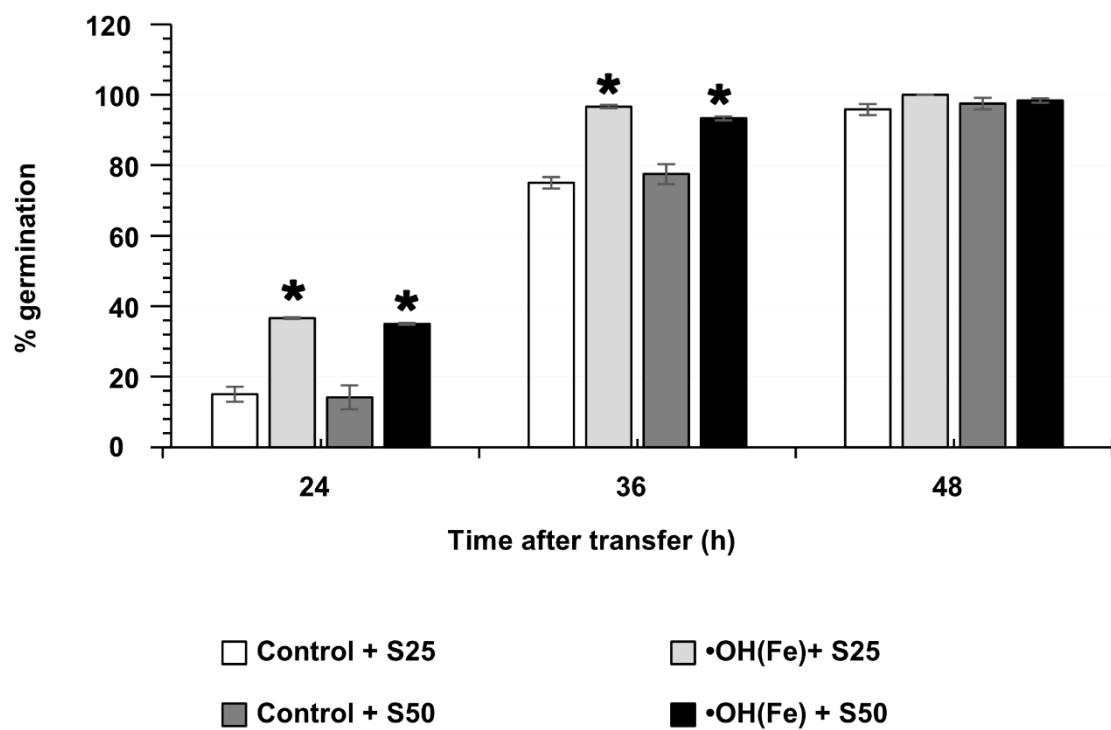
Figure 3.13. **Effect of the •OH(Fe)-treatment in rice seeds under 25 mM and 50 mM NaCl stress germinated at 30ºC.** The asterisk indicates a significant $P < 0.05$, Student's t-test) difference between control and other treatments.
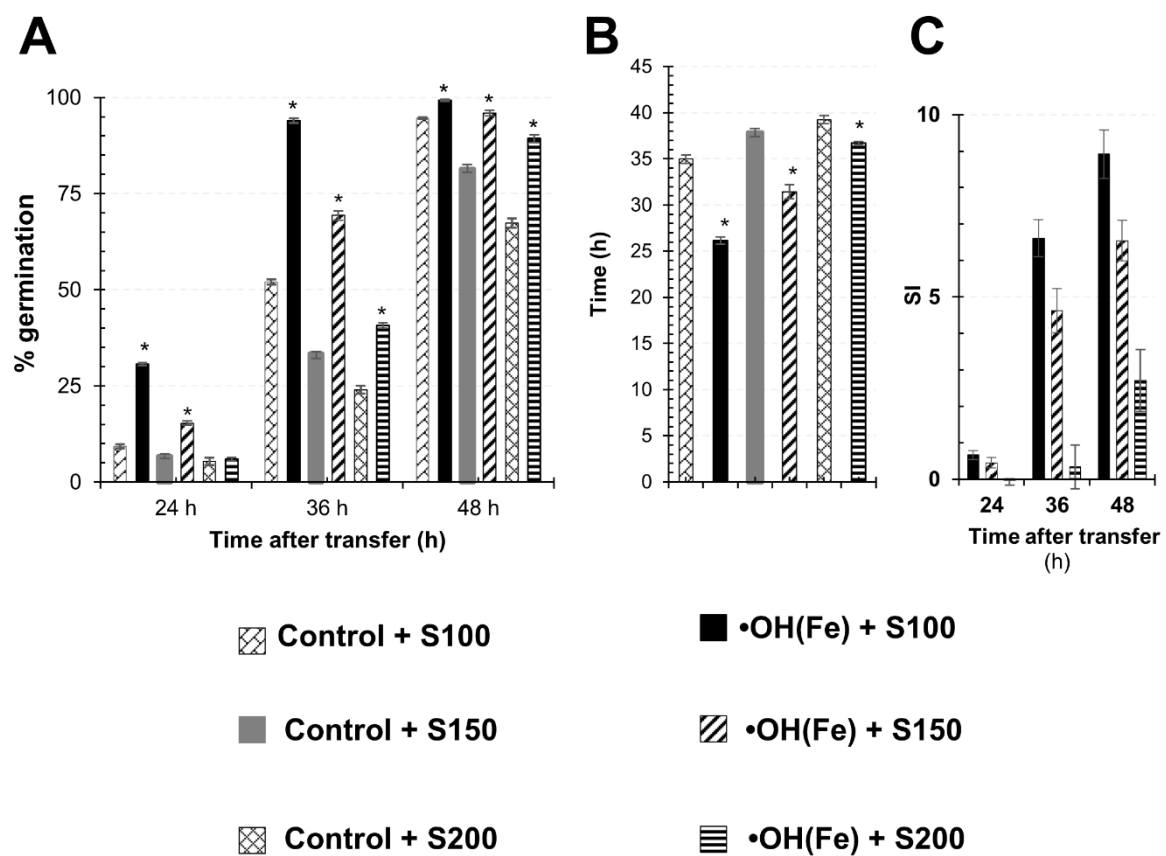
Figure 3.14. **Improvement of salinity stress tolerance by the •OH(Fe)-treatment in rice.** (A) Germination rate at different NaCl concentrations, (B) time to reach 50% germination *t50*, and (C) *SI* at different time points under different NaCl concentrations. The asterisk indicates a significant *P < 0.05*) difference between conditions obtained by the Student's t-test. Seeds were incubated with 100 mM (S100), 150 mM (S150), and 200 mM (S200) NaCl.

Chapter 4

A proteomic study of hydroxyl radical (•OH) treated *Arabidopsis* seeds under chilling stress

Summary

Reactive oxygen species (ROS) play an essential role in plant growth, development, and stress response. Hydroxyl radical (•OH) is one of the short-lived ROS and is well known for its destructive properties. However, new evidence is emerging on the positive role of •OH in growth and development. In Chapter 3, I showed the positive effects of •OH under a wide range of abiotic stresses. In this Chapter, to determine molecular mechanisms, I conducted a large-scale proteomic study of germinating seeds pretreated with •OH under chilling stress. A large number of proteins showed differences when compared to water and/or H_2O_2 treated seeds. I found that 116 proteins were exclusively up-accumulated under chilling stress in •OH treated seeds. GO analysis showed that proteins that were exclusively accumulated in •OH treated group were mostly antioxidation-related (such as glutathione reductase1/GR1, dehydroascorbate reductase/DHAR, and ascorbate peroxidase/APX), chaperones (such as heat-shock protein60/HSP60, chaperonin 60 subunit beta1/CPN60B1/LEN1, and Calreticulin/CRT), late embryogenesis related (LEA) proteins, proteins involved stress response, toxin catabolism, and embryo development. This proteomic study sheds light on the potential positive roles of •OH that may improve chilling stress tolerance in germinating seeds and seedlings.

Introduction

ROS are the byproducts of aerobic respiration in living organisms and consist of several members such as singlet oxygen ($^1O_2$), superoxide (O_2^-), hydrogen peroxide (H_2O_2), and the hydroxyl radical (•OH). Among all the ROS, H_2O_2 has the longest lifetime and can permeate through biological membranes and received vast experimental attention. ROS are well-established regulators of plant growth, development and play a role as signaling molecules in stressful environments (Bethke and Jones, 2001; Kobayashi et al., 2007; Queval et al., 2007; Miller et al., 2009; Kimura et al., 2012). Decades of studies showed that H_2O_2 is involved in cell signaling, stress resistance, environmental response, and cell death (Balazadeh et al., 2011; Li et al., 2011). For example, H_2O_2 pretreatment increased salt tolerance in wheat (Wahid et al., 2007) and chilling tolerance in tomato (İşeri et al., 2013). On the other hand, with the shortest lifetime of approximately 10^{-9} s and the ability to react and damage anything in its vicinity, •OH got the least attention and marked as the most destructive of all the ROS. However, studies showed that •OH also plays different positive roles in stress signaling (Laohavisit et al., 2013), germination and plant growth (Schopfer et al., 2002; Muller et al., 2009a), and cell death (Demidchik et al., 2010). Furthermore, most of the studies using H_2O_2 exogenously hardly consider the possibility of the conversion of H_2O_2 into •OH inside the cell by bivalent metal catalysts. Therefore, more studies require to look beyond the effect of H_2O_2 in ROS treatment studies to enhance the understanding of ROS actions in the plant cell.

In Chapter 3, I demonstrated the physiological evidence of the positive effect of the exogenous application of •OH in *Arabidopsis* and rice. I showed that the exogenous application of •OH could accelerate germination, early seedling growth under optimum and suboptimum conditions such as chilling, high temperature, heat stress, and salinity stress. In this Chapter, I took the opportunity of the analytical power of mass spectrometry-based proteomics to find out the possible mechanism of how the exogenous •OH increased seed germination and early growth under chilling stress.

Materials and methods

Seed treatment solutions

The •OH was generated based on Fenton and Haber-Weiss reaction (see the formula below) using 6 mM H_2O_2 and FeSO$_4$·7H$_2$O in a 200:1 ratio. To keep the Fenton and Haber-Weiss reaction stable, pH of the solution was adjusted to 4.9 using 0.1 M sodium citrate buffer. Six mM H_2O_2 and water without any metal catalysts were used as controls to compare against the •OH.

$$H_2O_2 + Fe\,(II) \rightarrow Fe\,(III) + •OH + OH^-$$
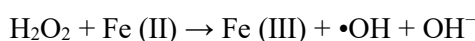
Seed materials and stress conditions

Surface sterilized *Arabidopsis thaliana* ecotype Columbia-0 (Col-0) seeds (25 mg) were treated using the solutions mentioned above. The seeds were incubated for 8 hours, according to the optimum incubation period (Chapter 3). After treatment, seeds were placed on 0.8% agar (Wako, Japan) medium with a modified Hoagland solution (Uemura et al., 1995) and transferred to 11ºC. Seed samples were collected every 24 hours for four days. Another batch of seed sample was collected after seven days of cold exposure. After collection, seeds were frozen in liquid nitrogen and proceed to seed protein extraction or stored at -80ºC for future use. The sample groups were named as follows:

Cold treatment duration	Water treated	•OH treated	H_2O_2 treated
After 8h incubation, no cold exposure	C_0h	•OH_0h	H_2O_2_0h
24 h cold exposure	C_24h	•OH_24h	H_2O_2_24h
48 h cold exposure	C_48h	•OH_48h	H_2O_2_48h
72 h cold exposure	C_72h	•OH_72h	H_2O_2_72h
96 h cold exposure	C_96h	•OH_96h	H_2O_2_96h
7 days cold exposure	C_7d	•OH_7d	H_2O_2_7d

Protein extraction and storage protein depletion

Frozen seeds from each sample group were ground into a fine powder using chilled mortar and pastel. The thawed powder was homogenized using 0.8 ml of extraction buffer containing 500 mM sorbitol, 50 mM 3-(n-morpholino) propane sulfonic acid-potassium hydroxide (MOPS-KOH) (pH 7.6), 5.0 mM ethylene glycol-bis(β-aminoethyl ether)-*N*,*N*,*N′*,*N′*-tetraacetic acid (EGTA) (pH 8.0), 5.0 ethylenediaminetetraacetic acid (EDTA) (pH 8.0), 2.0 mM phenylmethylsulfonyl fluoride (PMSF), 4.0 mM salicylhydroxamic acid (SHAM), 2.5 mM dithiothreitol (DTT) and 1x protease inhibitor cocktail (Sigma-Aldrich P9599). After the homogenate was transferred to an 1.0 ml centrifuge tube, protein was extracted using 15 min vigorous shaking followed by centrifugation at 15000 x g for 10 min at 4ºC. The supernatant was collected into a clean tube for storage protein depletion. The storage protein depletion was carried out using the method described by Krishnan et al., with a few modifications (Krishnan et al., 2009). Storage proteins were depleted by adding 10 mM $CaCl_2$ into the supernatant and vigorous shacking at 4ºC for 10 min. The tubes were centrifuged at 15000 x g for 10 min, and the supernatant was collected as the storage protein depleted sample. Protein concentration was measured using Bradford (Bio-Rad, Hercules, CA, United States) assay (Bradford, 1976).

Sample preparation for nano-LC-MS/MS analysis

In-solution protein digestion

Ten micrograms of protein were resuspended in 6 M Tris-UTU buffer (100 mM tris aminomethane, 6 M urea, 2 M thiourea, pH 8.5) where the final concentration of the UTU was below 2 M. The diluted protein was reduced at room temperature for 30 min in 10 mM reduction buffer (10 mM DTT in 50 mM ammonium bicarbonate (ABC) buffer). Reduced proteins were alkylated in the dark at room temperature for 20 min in 50 mM iodoacetamide (IAA) alkylation buffer (50 mM IAA in 50 mM ABC buffer). The reduced-alkylated proteins were pre-digested using lysyl endopeptidase in an enzyme to protein ratio of 1:100 (w/w) and incubate for 3 h at room temperature in the dark. The pre-digested samples were digested again using modified sequencing grade trypsin at a 1:150 (w/w) enzyme to protein ratio and incubated overnight at room temperature. The trypsin digestion was stopped by adding trifluoroacetic acid (TFA) to a final concentration of 0.2 to 0.5 % (v/v) to bring pH $\leq$ 3.0 using a 10% TFA stock solution. Any insoluble debris from the trypsin digest was removed by centrifugation at 15000 x g for 2 min at room temperature. The digested peptide samples were cleaned and desalted using SPE C-TIP (AMR, Tokyo, Japan), and the final volume was adjusted to 15 µl.

Nano-LC-MS/MS analysis of the seed protein

Digested peptide solutions were subjected to nano-LC-MS/MS analysis. Peptide solutions were trapped and concentrated in a trap column (L-column Micro 0.3 x 5 mm; CERI, Japan) using an ADVANCE UHPLC system (MICHROM Bioresources, Auburn, CA, USA). After elution from the trap column with 0.1% (v/v) formic acid in acetonitrile, concentrated peptides were separated with a Magic C18 AQ nano column (0.1 x 150 mm; MICHROM Bioresources) using a linear gradient of acetonitrile (from 5% [v/v] to 45% [v/v]) at a flow rate of 500 nL/min. The ionization of peptides was performed at a spray voltage of 1.6 kV using an ADVANCE spray source (AMR, Tokyo, Japan). Mass analysis was performed using an LTQ Orbitrap XL mass spectrometer (Thermo Fisher Scientific, Waltham, MA, USA) equipped with Xcalibur software (version 2.0.7, Thermo Fisher Scientific). Under the data-dependent scanning mode, full scan mass spectra were obtained in the range of 400 to 1800 m/z with a resolution of 60,000. Collision-induced fragmentation was applied to the ten most intense ions at a threshold above 500.

Protein identification and quantification

Progenesis QI for proteomics (Nonlinear Dynamics, New Castle, UK) software was used for semi-quantitative analysis of the seed protein sample from all the conditions. Thermo raw files were used in the software according to the manufacturer's instructions. The peak list was generated as mascot generic format (mgf) and searched to identify proteins using the MASCOT search engine (ver. 2.6., Matrix Science, London, UK) against the *Arabidopsis* protein database araport11 (Cheng et al., 2017). Two

missed cleavages were allowed. Fixed and variable modifications were set as carbamidomethylation of cysteines and oxidation of methionine, respectively. Peptide mass tolerance was 5 ppm, MS/MS tolerance was 0.6 Da, and peptide charges were set to +2, +3, and +4. Mascot decoy database was used for false discovery rate (FDR), and proteins with 5% FDR were extracted for final integration to the Progenesis QI for proteomics software. Proteins with at least two peptides were selected as a confident identification.

Bioinformatics and statistics

The abundance for any given protein was compared between the water-treated (C) and hydroxyl radical (•OH) or hydrogen peroxide (H_2O_2) treated seeds at each time point. A significant change in abundance (increase or decrease) was considered if the P-value was ≤ 0.05 from a two-sample Student's t-test. Proteins significantly up- or down-accumulated ($P \leq 0.05$) at least in two replicates at any time point were selected for further bioinformatics analysis. Statistical analysis was carried out in the R programming language platform and Microsoft excel.

MapMan 4 was used for the functional annotation and classification of the identified proteins (Schwacke et al., 2019). Gene ontology of biological processes (GOBP) analysis was carried out using DAVID: BP_Direct (v6.8: https://david.ncifcrf.gov/) (Huang da et al., 2009; Huang et al., 2009). The GOBP was reduced and visualized using the REViGO online platform (http://revigo.irb.hr/) (Supek et al., 2011). The protein-protein interaction network was created using the string-db online platform (https://string-preview.org/). A high confidence interaction score ≥ 7.0 was used for plotting the protein-protein protein interaction.

Results and discussions

Overview of the proteomic data

The storage protein depletion method used in this study reduced the number of storage proteins from the selected protein set. A total of 818 proteins were identified from the storage protein depleted samples, where less than ten were from different storage protein members (Table S4.1). Therefore, similar to other cereal crop seeds, $CaCl_2$ can also be used as a potential storage protein removing agent from *Arabidopsis* seeds.

The changes in protein abundance profile under cold stress from different treatment conditions were compared using principal component analysis (PCA) (Figure 4.1A). The PCA analysis showed that all the biological replicates clustered close to each other while each condition is separated from each other. Interestingly, there was a clear time-dependent shift in protein abundance, which seems to be resulting from the duration of cold exposure. Seed proteins under optimum temperature (C_/•OH_ /H_2O_2_0h) stayed close to each other. Seeds exposed to cold for 24 h and 48 h (C_/•OH_ /H_2O_2_24h and C_/•OH _/H_2O_2_48h) showed a small shift in protein abundance from the optimum condition. On

the other hand, with the extended cold exposure such as 72 h and 96 h, protein abundance shifted further away from the 24 h and 48 h clusters. More interestingly, in 72 h and 96 h clusters, •OH treated seeds showed a clear separation from the water treated and H2O2 treated seeds. It can be hypothesized that the •OH treatment affected the seeds differently than the water and H_2O_2 treatment. Seven days old germinating seeds are further ahead in their growth and developmental stage. Therefore, the protein abundance profile from 7 days of cold exposure was analyzed separately from the early cold exposed seeds. The PCA analysis showed that both •OH and H_2O_2 treated seeds cluster close to each other and further away from the water treated seeds (Figure 4.1B).

Differential protein abundance profile

The difference in these different treatments became clear when statistically significant differentially abundant proteins were compared (Figure 4.2). Of these, 140 and 124 proteins showed increased abundance in •OH, and H_2O_2 treated seeds under cold stress, respectively, with only 53 proteins shared between these two sets (Figure 4.2A; Table S4.1). Similarly, 88 and 38 protein abundance were found to be decreased under cold stress in •OH and H_2O_2 treatment groups, respectively, with only 12 shared protein (Figure 4.2B; Table S4.1).A small number of differentially expressed proteins that were shared between •OH and H_2O_2 indicate that they have specific target proteins, and the mode of action of these two ROS might be different from each other to some extent. Interestingly, the protein abundance profile was different in long cold exposure, where a smaller number of protein significantly increased in •OH treated group (64 protein increased) than the H_2O_2 treated group (106 protein increased) and sharing only 39 proteins between these two groups (Figure 4.2C; Table S4.1).

To further identify which protein abundance increased exclusively in response to •OH under cold stress, proteins from •OH treated seeds were also compared with the H_2O_2 treatment group, and 49 proteins increased significantly. Altogether, exclusively •OH responsive 116 proteins from •OH vs. water treatment (C) and •OH vs. H_2O_2 treatment were further analyzed to understand deeper biological processes associated with •OH treatment of seeds.

Functional analysis of tentative •OH target proteins under cold stress

Exclusively up-accumulated 116 proteins in •OH treated group were subjected to gene ontology analysis to examine potential biological processes (GOBP) that might be involved in the stress tolerance under cold, reported in Chapter 3 (Figure 4.3). The gene ontology revealed interesting biological processes that may be influenced by the •OH treatment and help to maintain growth and increase stress tolerance under cold. The most notable biological processes that were enriched in •OH treated seeds are, for example, proteins involved in different abiotic stress response, proteins that contribute to the redox homeostasis, oxidation-reduction process, glutathione metabolic process, toxin catabolic process, protein folding/re-folding, gametophyte development, and embryo development ending seed dormancy

(Figure 4.3, Table S4.1). Besides, predicted protein-protein interaction analysis of these 116 proteins produced many connected clusters (Figure 4.4), suggesting that some orchestrated responses are induced in the germinating seedling in response to •OH.

•OH treatment increased proteins related to ROS/redox homeostasis

In this study, •OH treatment increased the abundance of proteins related to the ROS scavenging system and redox homeostasis under cold stress in germinating seeds (Table S4.1). Redox homeostasis related proteins such as ascorbate peroxidase 1 (APX1), copper/zinc superoxide dismutase 1 and 2 (CSD1, CSD2), glutathione reductase (GR1), NADPH-dependent thioredoxin reductase 2 (NTR2), and NAD(P)-linked oxidoreductase superfamily protein (LGALDH) were exclusively up-accumulated in •OH treated group. Another two ROS scavengers, such as glutathione s-transferase dehydroascorbate reductase 1 and 3 (GST-DHAR 1, GST-DHAR 3), were up-accumulated in both •OH and H_2O_2 treated group. These findings indicate that the ROS treatment, especially •OH, activated the antioxidant machinery in the treated seeds. It can be hypothesized that the activated antioxidants played a crucial role by protecting against the chilling induced oxidative stress in the germinating seeds. Almost all abiotic stresses are accompanied by oxidative stress due to ROS accumulation in the cell (Demidchik, 2015). Individual or combined or synergistic stress and stress duration can be more severe to plants due to excessive ROS (Prasad et al., 2005; Zhao et al., 2009; Gill and Tuteja, 2010b; Zhang et al., 2012). Excessive ROS over the basal level in the cell damages lipids, carbohydrates, DNA, and proteins, ultimately damages the cell membrane and causes cell death (Gill and Tuteja, 2010b; Mittler, 2017). Therefore, regardless of any individual or multiple abiotic stresses or stress duration, controlling cellular ROS/Redox to a basal level is one of the major keys to enhance abiotic stress tolerance in plants (Savvides et al., 2016). Studies showed that plants pretreated or primed with different chemicals such as H_2O_2, sodium nitroprusside (SNP), melatonin (Mel), and polyamines had a lower ROS (H_2O_2) in the system and enhanced tolerance against different abiotic stresses (Uchida et al., 2002; Wahid et al., 2007; Farooq et al., 2009b; Savvides et al., 2016). The stress tolerance or reduction in the oxidative damage in those above mentions studies was either by the activated antioxidant action or by direct scavenging of ROS by the chemical agents themselves. Unlike all the previous studies, in this study, •OH, which is well known for its damaging capacities, was used for treating the seeds and observed increased antioxidative enzyme activities. These findings suggest that the •OH, similar to most studied priming or treating agent (e.g., H_2O_2), also plays important positive roles in improving stress tolerance, such as chilling in this study.

Furthermore, the glutathione (GSH) metabolic and biosynthesis process was also enriched in the •OH treated group. This enriched GSH indicates that, along with the members of the antioxidant machinery mentioned earlier, nonenzymatic GSH might be playing a major regulatory role in increasing tolerance to chilling and chilling induced oxidative stress in the germinating seedling. In this study,

several members of glutathione *S*-transferase (GST) family proteins were increased in •OH treated group (Figure 4.3). GSH is one of the potent nonenzymatic antioxidants that is involved in multiple metabolic processes such as protection of oxidative denaturation of proteins under stress conditions, protection of biomembrane, removal of toxins/toxic byproducts from the cell, and also one of the substrates of GST (Hasanuzzaman et al., 2017). Glutathione can also act as a redox sensor and directly participates in the ROS scavenging and improve resistance against oxidative stress (Mahmood et al., 2010). The GSH and its antioxidant properties against abiotic stress tolerance are well established, but the molecular mechanism of its stress defense is still not well understood. The glutathione homeostasis or the ratio of reduced and oxidized glutathione (GSH/GSSG) and its redox status plays a significant role in growth, development, and stress signaling in plants (May et al., 1998; Noctor and Foyer, 1998; Hasanuzzaman et al., 2017). Interestingly, GR1, which was increased in •OH treated group under cold stress (Table S4.1), maintains the balanced status of GSH/GSSG in the cell along with glutathione peroxidase (GPX). Therefore, the increase in the GSH and GSH related proteins under chilling stress shows a clear connection between •OH treatment and stress tolerance in germinating seeds. Therefore, GSH metabolism may be directly connected to the chilling tolerance increase by •OH in germinating seeds.

Chaperons and other stress-responsive proteins

Severe abiotic stress conditions lead to protein denaturation, dysfunction, and aggregation, ultimately affecting plant growth development and survival (Singh et al., 2019). Therefore, maintaining protein homeostasis by preventing protein degradation or removing dysfunctional proteins is one of the critical stress tolerance mechanisms that plants have evolved (Singh et al., 2019). Molecular chaperones, containing some heat shock proteins (HSPs), play an essential role in maintaining protein integrity by preventing degradation, folding of misfolded proteins, disaggregation of aggregated proteins folding-refolding of naïve proteins (Singh et al., 2019). In this study, several members of chaperone proteins increased their abundance only in •OH treated group, such as chaperonin 60 beta (CPN60B1 or LEN1), chaperonin 60 subunit beta 2 (CPN60B2), chaperonin 10 (CPN10), and heat shock protein 60-3A (HSP60-3A) (Table S 4.1). Two other chaperone proteins outside major HSPs were also found only in the •OH treated group, such as calreticulin 1a and 1b (CRT1a, CRT1b) (Table S 4.1). Chaperonin, for example, CPN60 were reported to be involved in different abiotic stress and development. These proteins play an essential role in the folding of many chloroplast proteins such as Rubisco (Boston et al., 1996). Transgenic *Nicotiana* containing an antisense CPNB resulted in abnormal phenotypes showing stunted growth, leaf chlorosis, and flowering delay (Zabaleta et al., 1994). *Arabidopsis cpn60* mutants failed to develop chloroplast and embryo, and ultimately failed to establish seedlings (Apuya et al., 2001). The deletion of LEN1 leads to cell death in *Arabidopsis* (Ishikawa et al., 2003). Apart from classical chaperones, two members of late embryogenesis abundant (LEA) protein were also found

to be increased in •OH treated group under chilling stress (Table S 4.1). LEA proteins function in growth and development and abiotic stress tolerance (Chen et al., 2019). Studies also showed that disordered LEA could also act as molecular chaperones (Kovacs et al., 2008); for example, LEA protein prevents protein aggregation under water stress (Goyal et al., 2005), play a role in protein stabilization under desiccation stress and involved in desiccation tolerance (Chakrabortee et al., 2007). Increased accumulation of these chaperone proteins in this study might be preventing the protein degradation or denaturation under chilling stress and oxidative stress from the exogenously applied •OH itself.

A larger number of proteins increased in response to •OH are involved in different abiotic stress responses, including cold. The increase of these stress response proteins by •OH treatment could indicate a direct activation of the stress tolerance mechanism in the seeds and seedlings, working along with the induced antioxidant machinery. Any abiotic stress also produces different toxic substances in the cell as a byproduct of different metabolic pathways (Zhu, 2016). One of the biological processes that enriched in response to •OH treatment is the "toxin catabolic process" involved in removing or destroying toxic substances from the cell (Figure 4.3, Table S4.1). The increase in the proteins involved in toxic catabolism indicates that •OH treatment of the seeds reduces or mitigates cellular toxicity. However, further detailed studies are required to know what molecular mechanisms are involved in these positive effects of •OH treatment despite being well known notorious ROS.

This proteomic study of ROS treatment, especially •OH treatment, mediated chilling stress tolerance is one of the first steps towards understanding and establishing positive roles •OH in plant system. It is tempting to say that the exogenous application of •OH may provide mild oxidative stress that alerts the germinating embryo to activate different stress tolerance and protective mechanisms. The activation of antioxidative machinery may reduce the generation of H_2O_2 and other ROS, which, in return, might be preventing the more deleterious effect of •OH.
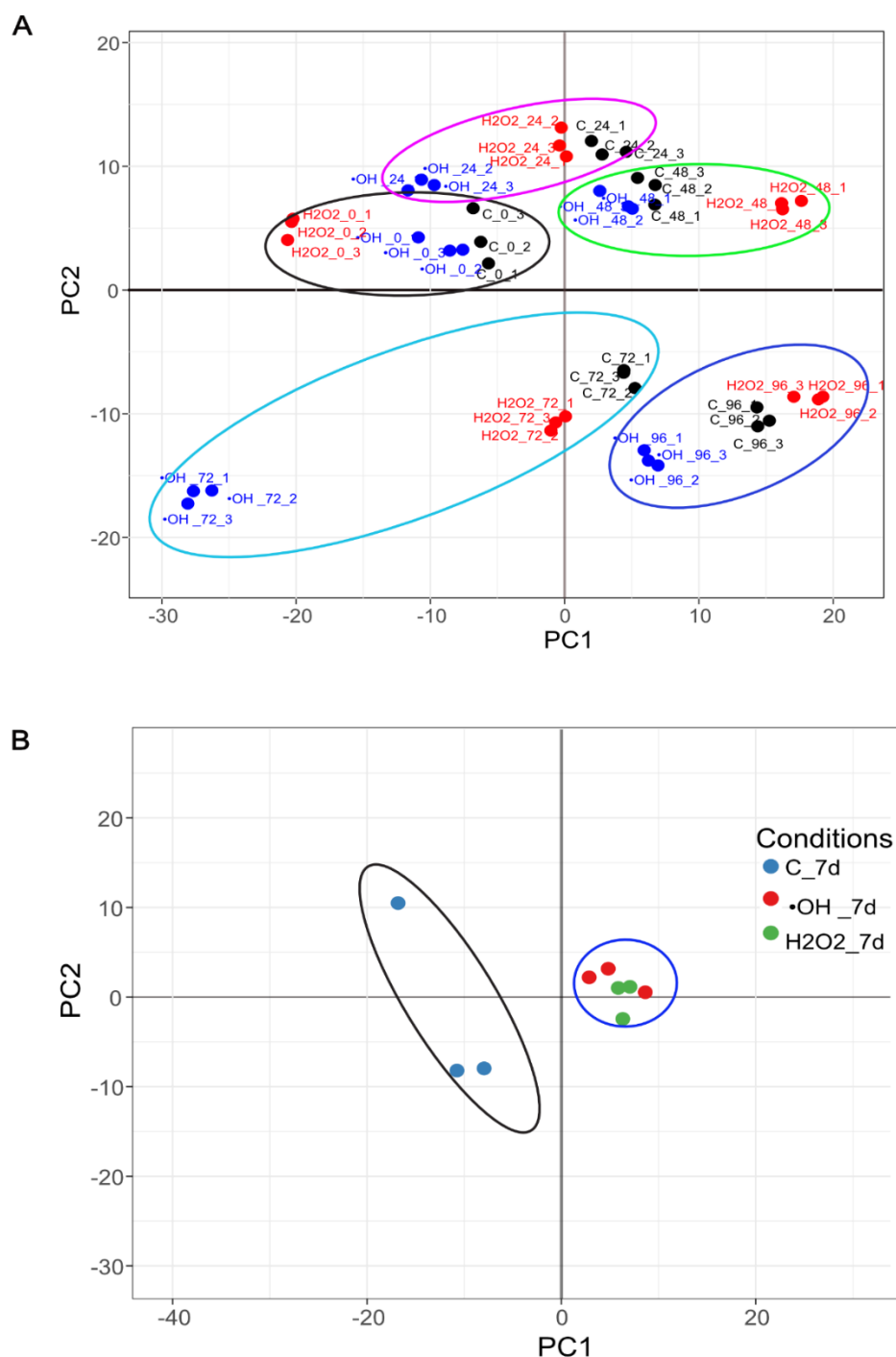
Figure 4.1: **Quantitative analysis of the proteomic data identified in this study. (A)** PCA analysis showing the distribution pattern of the seed proteins from different treatment groups over the cold exposure duration. The elliptic circles are showing the clusters of specific time points. The proteins from 72 h and 96 h cold exposed samples moved further away from the proteins from shorter-treated or non-stressed samples. **(B)** The PCA analysis of the seven days cold exposed seed proteins. It shows that proteins from both •OH and H_2O_2 treated samples cluster close to each other but further away from water control.
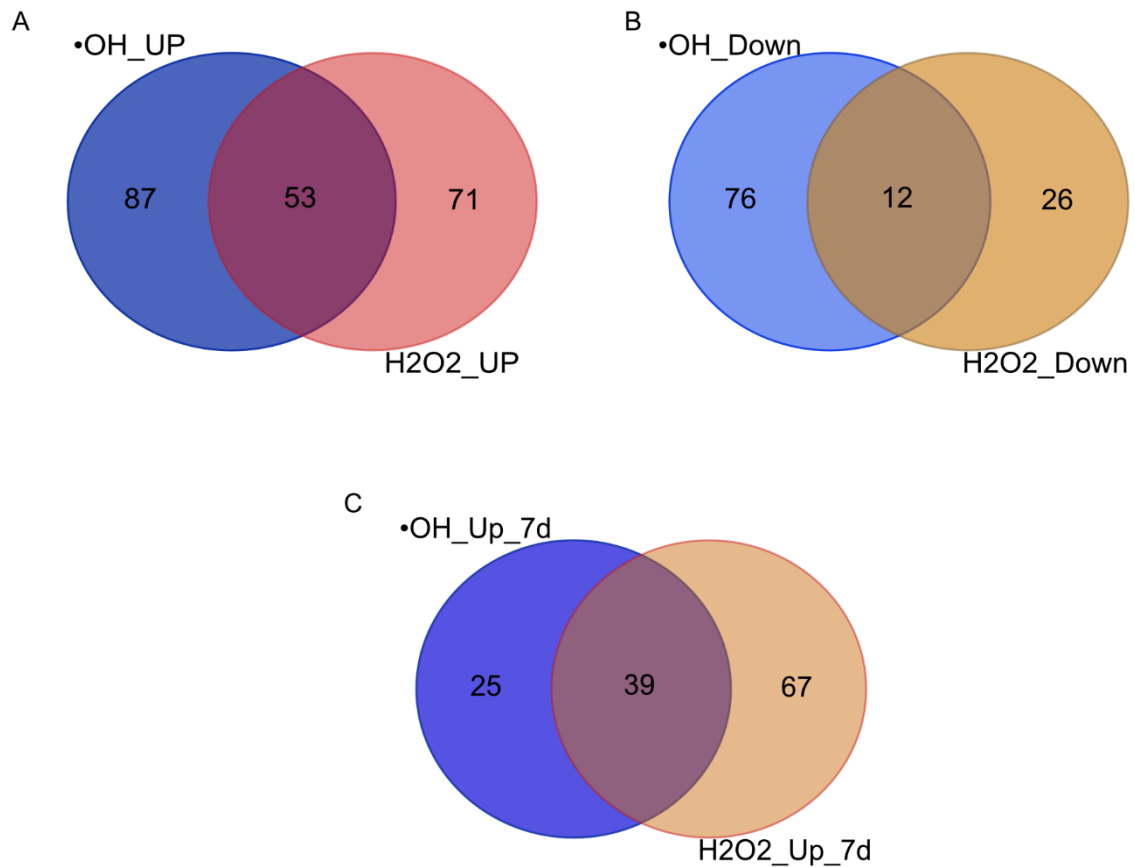
Figure 4.2: **Responses of seed proteins to •OH and H₂O₂ treatment.** (A-B). Protein abundance changes within 96 hours of cold exposure. **(A)** The up-accumulated proteins in the •OH and H₂O₂ treated group show that only 53 proteins are shared between these two ROS treated groups**. (B)** The number of down-accumulated proteins was higher in the •OH treated group than in the H₂O₂ treated group. **(C)** The comparison of the •OH and H₂O₂ treated groups after seven days of cold exposure. The number of significantly accumulated proteins were lower in the •OH treated group than in the H₂O₂ treated group
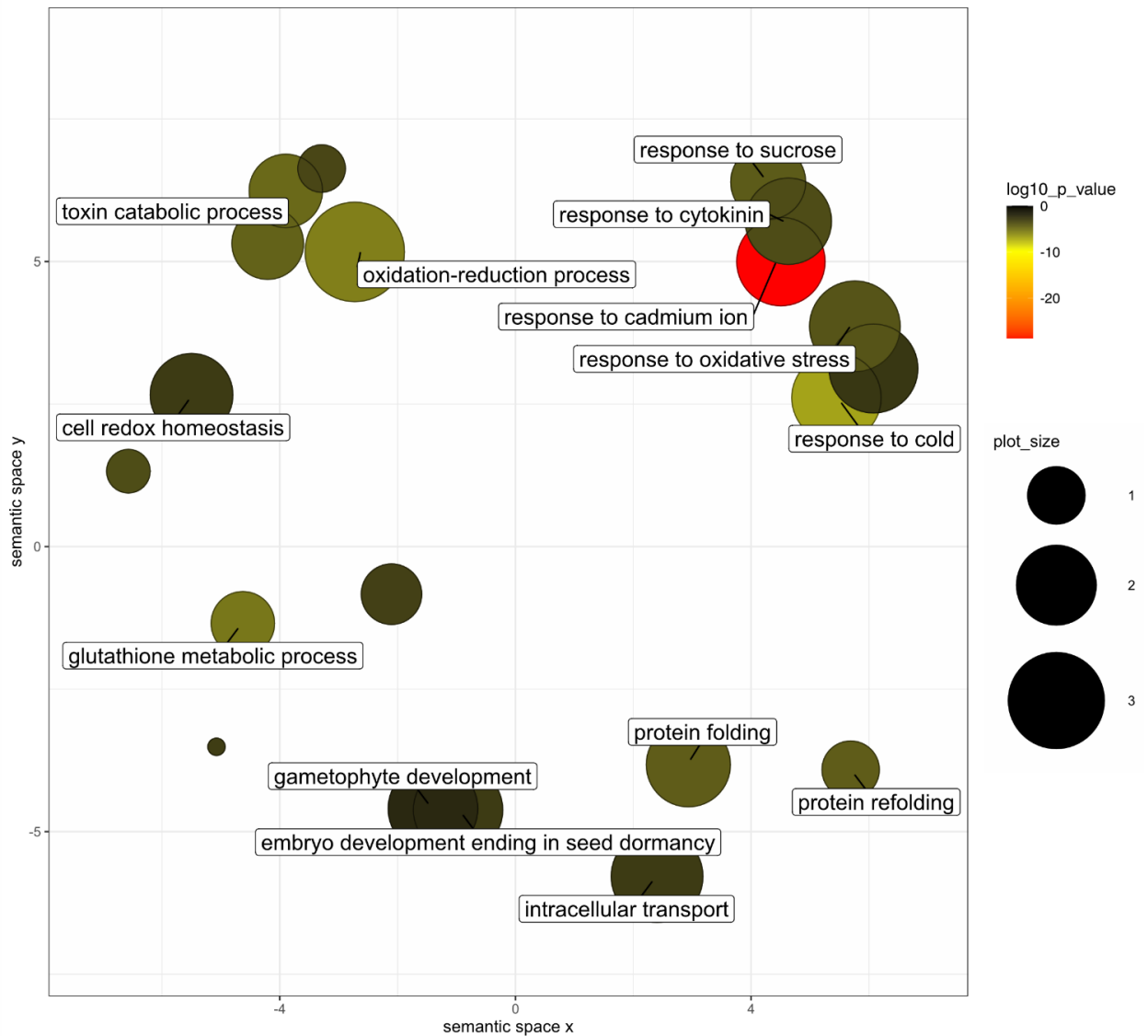
Figure 4.3: GO analysis of the uniquely up-accumulated proteins in the •OH treated group after cold exposure. GO terms were evaluated by the DAVID program and visualized with REViGO. Each circle color and size show the *P*-value and frequency (%), respectively
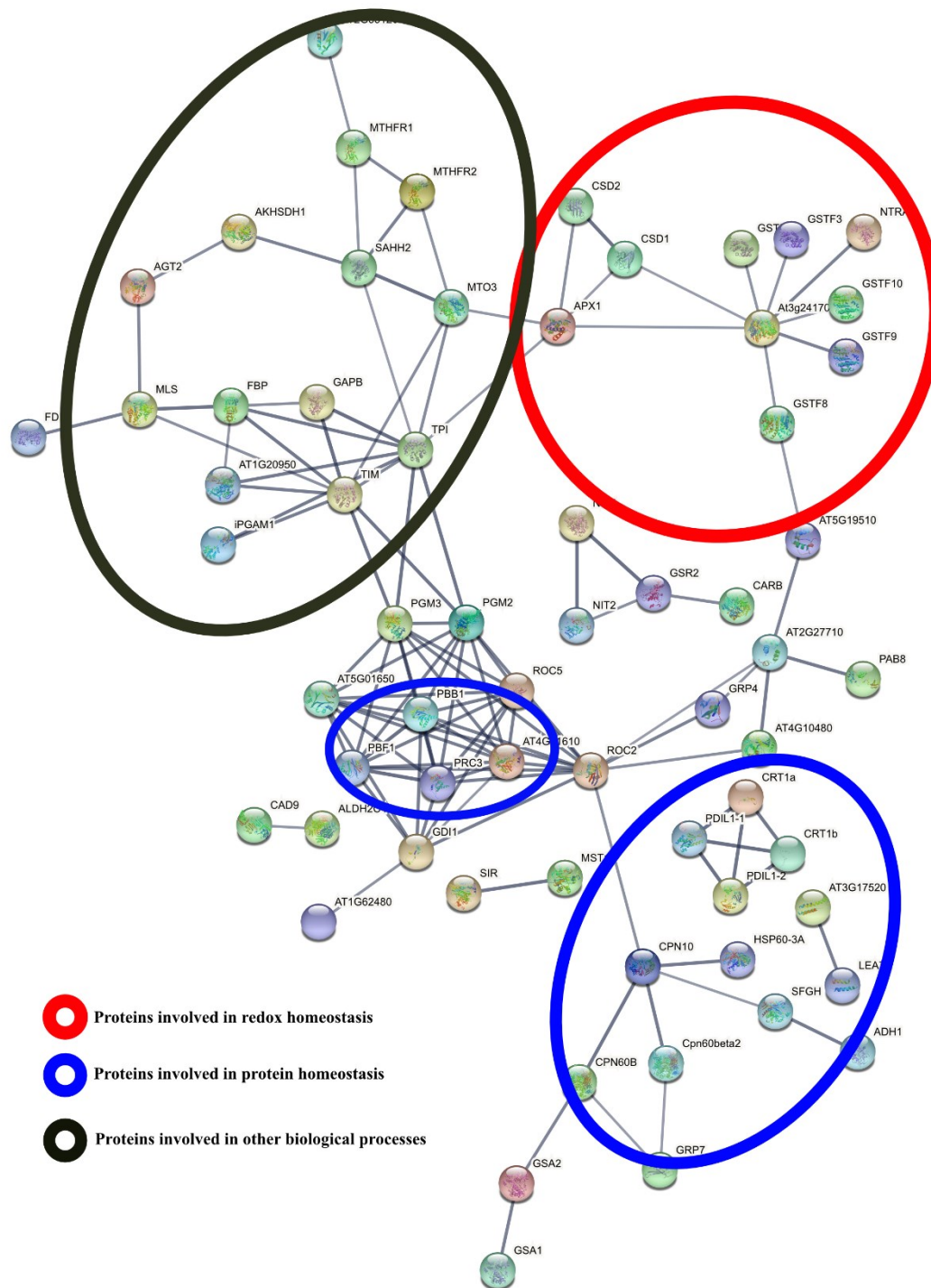
Figure 4.4: Protein-protein interaction network (PIN) of the uniquely up-accumulated proteins in the •OH treated group. The PIN was generated using the String online platform; only the highly confident interactions are mapped here. The colored circles show proteins with similar functions interacting and clustering close to each other.

Supplementary information

Supporting table

Table S4.1: Proteins identified in the seed proteomic study using LC-MS/MS analysis. The files are output from the Progenesis data analysis software. **(A)** All the proteins identified in seed samples. **(B)** Proteins with at least two unique peptides used for further downstream analysis. **(C)** Exclusively up-accumulated proteins in •OH treatment group.

Chapter 5

General Discussion

In the last couple of decades, global warming has driven world climate change to a more extreme and devastating state than in the 19th century or prior centuries—the effect of this unprecedented climate disaster threatening the global food and ecosystem security now more than ever. Recent research and climate modeling show that the world will face a significant threat to feed the ever-growing population in the upcoming future. Therefore, it is an utmost demand to improve crop and plant performance and production against the emerging and upcoming abiotic stresses. Surprisingly, plants have survived and evolved through several major climate change events for a half a billion years since its emergence from the aquatic habitats to land. Therefore, plants themselves possess all the clues on how to improve in the fast-changing climates than they ever experienced. How plants percept and understand the changes in their surrounding environment and prepare themselves to survive holds a primary key for scientists to accelerate the development of practical methods to improve plant performance against abiotic stresses. However, despite decades of research and attempt to develop resistant crop and plant varieties, progress is still slow because of the lack of understanding and gaps in knowledge of abiotic stress perception and response mechanisms in plants. Therefore, the main objectives of my thesis were to understand how plants sense cold stress (Chapter 2) and develop a practical method to improve abiotic stress resistance in the model plant *Arabidopsis thaliana* and rice (Chapter 3 and 4).

In Chapter 2, I worked on understanding the early cold response events in the model plant *Arabidopsis thaliana.* In this chapter, I mainly focused on temporal protein phosphorylation events in the microsomal membrane fraction (MMF). Plant PM is the outermost living part of the cell, which, combined with the cell wall and extracellular space, forms the first checkpoint to sense, generate, and transfer external signals to the nucleus; it also serves as the controlled gate from solute transport inside the cell (Chen and Weckwerth, 2020). Further, protein phosphorylation is one of the most common and crucial PTMs (Pawson and Scott, 1997). Approximately one-third of proteins can be phosphorylated (Hubbard and Cohen, 1993), and according to the "PTM viewer" database, nearly 76% (last updated on October 2020) of the reported plant proteins contain phosphorylation sites (Willems et al., 2019). Reversible protein phosphorylation-dephosphorylation is involved in a wide range of cellular processes, transmembrane signaling, structural and functional protein modification, modulation of protein activity and localization (Jorgensen and Linding, 2008; Batalha et al., 2012). Plant proteins go through cascades of protein phosphorylation and form complex signaling pathways that regulate essential biological processes, including external environmental response (Mishra et al., 2006; Li et al., 2015; Chen and Weckwerth, 2020). Therefore, studying membrane protein phosphorylation events and identifying protein kinases and their phosphorylated targets under a brief period of cold exposure will provide

insights into early cold signaling events. Furthermore, to my knowledge, before this study, there was no large-scale analysis of membrane phosphoproteomics focusing on the early cold response in plants.

To understand phosphoregulation in the earliest cold response within minute windows (5 min to 60 min), I performed a large-scale mass spectrometry-based phosphoproteomic analysis of the *Arabidopsis* microsomal membrane proteins. I detected nearly 1900 phosphosites from over 850 proteins, where around 1000 phosphosites showed temporal phosphorylation in response to cold (Table S2.1). The PCA analysis (Figure 2.1B) showed close clustering of replicates by conditions and time; the frequency distribution of phosphorylated residues (S, 85%, T, 12%, and Y, 2%) showed similarity with previously reported distribution from different plant phosphoproteomics study (Nakagami et al., 2010; Umezawa et al., 2013; Wu et al., 2017; Hsu et al., 2018; Haj Ahmad et al., 2019; Ishikawa et al., 2019a; Ishikawa et al., 2019b). Further, studies showed that the protein abundance does not change within a time frame of minutes after stress/treatment exposure; instead, the changes I observe in the protein intensity come from the phosphorylation status change (Stecker et al., 2014; Wu et al., 2014; Haj Ahmad et al., 2019). For further confirmation, I also analyzed the protein abundance using the same protein samples collected within 60 min of cold exposure and did not find any statistically significant change in protein abundance (Table S2.2). Therefore, it is reasonable to say that the differential changes in the phosphopeptides in my study are due to the cold-responsive change in protein phosphorylation rather than de novo protein synthesis. These results ensure the validity of the phosphoproteomic data used to study early cold response in *Arabidopsis*.

From the in-depth analysis of the phosphoproteomic data, I revealed that the plant response to a brief drop in temperature is a rather complicated process. Phosphorylation of ion channel or transporter proteins for Ca^{2+} (OSCAs, ACAs), K^+ (POTs), and Na^+/K^+ (NHXs), which are involved in maintaining ionic homeostasis inside the cell, indicated that plant cell tries to maintain its ionic balance in a steady-state under cold. Ca^{2+} is established as signaling molecules in signal transduction pathways involved in abiotic stress response, including cold (Knight et al., 1996b; Knight and Knight, 2000; Marti et al., 2013; Yuan et al., 2018; Hiraki et al., 2019). Even though before this study, there is no large scale phosphoproteomic study showing phosphorylation in the Ca^{2+} channels and other components of Ca^{2+} mediated signal transduction pathway in early cold response, a few studies showed that change in Ca^{2+} signature is one of the earliest response events under cold stress (Knight et al., 1996b; Knight and Knight, 2000; Marti et al., 2013; Yuan et al., 2018; Hiraki et al., 2019). Furthermore, the increase in Ca^{2+} influx into the cytoplasm in response to cold can create signals that get sensed and interpreted by Ca^{2+}/CaM/CBL proteins (Luan, 2009; Mao et al., 2016). Ca^{2+} can also recruit or activate signaling components such as RLKs, CDPK/CaMKs, MAPKs, and ROS in response to cold stress or under cold acclimation (Zeng et al., 2015). In the present study, I also found that a large number of proteins are connected to Ca^{2+} or Ca^{2+} related signaling pathways, indicating that the Ca^{2+} signature and all the other Ca^{2+} signaling components respond to a very early stage of cold exposure (Tables 2.1, S2.1).

My data also indicated that plant kinome gets perturbed by cold exposure and kinases such as RLKs, MAPKs, CDPKs/ CaMKs/, CKs, and GSKs are an active part of the cold sensing and signaling. The kinase motif analysis (Figure 2.7), kinase-substrate network (Figure 2.8, Table S2.3), clearly showed that a large number of kinases and their substrates were phosphorylated under brief cold exposure. Recent phosphoproteomic studies of cold stress in plants also showed that under cold acclimation or longer exposure (days to weeks), similar kinds of kinases were phosphorylated (Gao et al., 2017; Pi et al., 2017; Hsu et al., 2018; Liu et al., 2019). Furthermore, several components of the canonical cold-responsive MAP kinase pathway (Teige et al., 2004; Furuya et al., 2013), such as MKK2, MAPK6, and other MAP kinases such as MAPK8, MAPK16 were also phosphorylated within 60 min of cold exposure (Tables 2.1, S2.1 and (Miki, 2015)). It clearly indicates that the MAPK pathway gets activated within a very short time after cold sensing by plants, even before the cold acclimation or stress-related physiological or molecular changes start to initiate in the plant cell. Not only just Ca^{2+} and kinase-related signaling components get phosphorylated in response to the early cold, but also components of phosphoinositide, ABA, auxin, BR, and ROS mediated signaling pathways were also found to be involve in the early cold response (Tables 2.1, S2.1). Similar to this study, these were also phosphorylated under cold acclimation or cold-stress response in other plants (Gao et al., 2017; Pi et al., 2017; Hsu et al., 2018; Liu et al., 2019).

Proteins involved in intracellular trafficking/vesicle trafficking were found to be phosphorylated in response to the early cold exposure. Several phosphorylated cytoskeleton-related myosin-binding (MyoB) and myosin-like proteins were found in this study (Tables 2.1, S2.1A). Myosin-like proteins also increased under cold stress in rice and perennial grasses (Yan et al., 2006; Xuan et al., 2013). However, before this study, no report showed the phosphorylation in MyoB or Myosin-like proteins in response to early cold exposure. A microtubule related protein, 65-kDa microtubule-associated protein 1 (MAP65-1), was phosphorylated in the microtubule interacting region at pS532 (Tables 2.1, S2.1A). Phosphorylation of the microtubule interacting regions diminishes the binding properties (Nick, 2013). These microtubule cytoskeleton proteins play essential roles as stress sensors (Nick, 2013) and cytoplasmic streaming mediated intracellular trafficking (Caviston and Holzbaur, 2006; Peremyslov et al., 2015), as well as signal transduction (Pickard, 2003). Therefore, it might be possible that these phosphorylated proteins play essential roles in sensing and signaling early cold exposure. Few other proteins involved in vesicle trafficking were also phosphorylated, such as DRP2A, BRP2B, GNOM, SNX1, SNX2A, and VPS41. Several studies showed their transcript or protein abundance changes in response to longer duration (several hours to days) of cold stress (Minami et al., 2009; Ashraf and Rahman, 2019; Miki et al., 2019; Li et al., 2020). However, before this study, it was unclear whether they also respond to early cold exposure at the protein phosphorylation level. I believe findings from my phosphoproteomic study will provide additional knowledge to the vesicle trafficking under cold stress.

Plant cells consistently maintain ionic and cellular homeostasis through different transporter and channel proteins located in the membranes by balancing the influx and efflux of different ions, toxic byproducts, and carbohydrates (Conde et al., 2011). I observed that transport-related proteins were among the largest groups of proteins that phosphorylated under a brief cold exposure (Table S2.1). It indicates that the plant cell transport system gets highly involved in early cold response events. Previous studies also showed transporter phosphorylation as one of the rapid adaptation responses to abiotic stress (Chen and Hoehenwarter, 2015). Two PM H$^+$-ATPase (AHA1 and AHA2) were phosphorylated in this study (Tables 2.1, S2.1A), and previously it was shown that AHAs increase in abundance under cold acclimation (Minami et al., 2009). However, whether the increase in abundance was related to protein phosphorylation modification or not was not shown. Therefore, it could be possible that phosphorylation plays an essential role in controlling the function of AHA proteins under cold stress and activates within minutes of cold sensing. Like AHAs, several sugar transporters were also phosphorylated within 60 min of cold exposure in my study. Soluble sugars are one of the major cryoprotectants and can protect plants from freezing damage and maintain cellular integrity and functions (Guy et al., 1992). A phosphoproteomic study of *Arabidopsis* showed that TMT1 and TMT2 were phosphorylated under cold acclimation, and in this study, I observed the phosphorylation increases within a few minutes of cold exposure. I also reported phosphorylation in a few other sugar transporters such as SWEET12, ERD6, and ERDL6 in response to cold. Therefore, it is reasonable to say that sugar transport activity, an adaptive freezing tolerance mechanism, starts within the earliest exposure to cold, even before the CA process.

In addition to the transporters mentioned above, I also observed phosphorylation in several aquaporins members such as PIP2-5, -6, and -7. Even though aquaporins are known for gated water transport across the PM, PIP1-4, and PIP2-5 were also connected to cold acclimation and freezing tolerance (Rahman et al., 2020). However, phosphorylation of these PIPs was not reported under cold exposure. Interestingly, it was also shown to be involved in phosphorylation controlled diffusion H$_2$O$_2$ out of the cell in maize plants under chilling stress (Aroca et al., 2005). ROS needs to continuously generate and be scavenged or diffuse out of the cell for a balanced cellular function (Mittler, 2017). Therefore, PIPs detected in this study might be potentially involved in diffusing H$_2$O$_2$ from the cell to maintain a balanced and optimum ROS level.

ROS generating respiratory burst oxidase homolog D (RBOHD) was also phosphorylated as shown in this study, which has been never reported in response to a brief cold exposure (Tables 2.1, S2.1A). In my study, RBOHD was phosphorylated in pS8, pS148, pS163, and pS347 within 15 min of cold exposure (Tables 2.1, S2.1A). RBOHD can generate ROS via Ca^{2+} dependent and independent phosphorylation by CDPKs/CIPKs and BIK1 kinase, respectively (Kadota et al., 2014; Li et al., 2014). Calcium-dependent protein kinase 5 (CPK5) and BIK can phosphorylate and regulate RBOHD at the same amino acid positions (pS148, pS163, and pS347) (Boudsocq et al., 2010; Kadota et al., 2014;

Kadota et al., 2015), which are the same positions I observed as cold responding phosphorylated sites in this study. Interestingly, in my data, I detected both CPK5 and BIK phosphorylated in response to a brief cold (Tables 2.1, S2.1A). Furthermore, the phosphosites showed increased phosphorylation contain the characteristic RXXS/LXRXXS motif, a potential target motif of CDPKs (Tables 2.1, S2.1A). This rapid phosphorylation of ROBHD and its kinases indicates ROS signaling involvement in early cold response. Maintaining ROS homeostasis is essential for cells to survive any external stress (Mittler, 2017). As mentioned above, ROBHD and its upstream ROS generating kinases (CPK5 and BIK1) get phosphorylated immediately after cold exposure, which might generate excess ROS and interfere with proper ROS signaling. Interestingly, I also found that the negative regulator of RBOHD, MPK8 was activated in (Tables 2.1, S2.1A). The MKK3-MPK8 pathway can negatively regulate ROS accumulation by controlling the RbohD gene expression in response to mechanical wounding (Takahashi et al., 2011). The above findings show that the ROBOHD mediated ROS signaling gets activated immediately after cold exposure, and PIPs and MPK8 keep the excess ROS at a balanced state.

ROS, including singlet oxygen ($^1O_2$), superoxide (O_2^-), hydrogen peroxide (H_2O_2), and the hydroxyl radical (•OH), are involved in almost every stage of growth, development, differentiation, and cell death (Bethke and Jones, 2001; Kobayashi et al., 2007; Queval et al., 2007; Miller et al., 2009; Kimura et al., 2012). ROS were only considered toxic byproducts of oxygen metabolism until the discovery of signaling and other positive roles of H_2O_2. Researchers have reported that exogenous application of H_2O_2 enhances stress tolerance in both model and crop plants by increasing the endogenous concentration to an optimum level (Savvides et al., 2016; Mittler, 2017). Even after discovering the positive role of some ROS, •OH is still considered a dangerous compound in the cell that damages DNA and proteins and is responsible for cell death (Richards et al., 2015; Mittler, 2017). Interestingly, scientists have been putting forward the thought that all ROS must play positive roles to some extent. There is also the fact that living cells evolved in a high ROS environment, and different species can withstand a higher ROS level, and those ideas and observations strengthen the idea of "ROS" are beneficial. Besides, the already reported and emerging signaling and regulatory roles of ROS indicate that H_2O_2 and other ROSs, such as •OH, might have beneficial roles (Mittler, 2017). It is also inevitable that •OH generates in the cell in the presence of the endogenous H_2O_2 and metal catalysts such as Fe or Cu (Halliwell and Gutteridge, 2015).

Based on the previous reports showing positive roles of exogenous application of ROS and the active participation of ROS as signaling components in Chapter 2, I hypothesized that similar to H_2O_2, •OH would also provide a positive role under normal and abiotic stress conditions. A few shreds of evidence are already showing the usefulness of the •OH in germination and growth under optimum conditions (Muller et al., 2009b; Liu et al., 2016). To bring the idea into reality, in my study (Chapter 3), I developed a practical, non-laborious, cost-effective approach using Fenton/ Haber-Weiss reaction-based •OH. I found an optimized one-time treatment of seeds with •OH accelerates the germination

speed under optimum and stress conditions in *Arabidopsis* and rice (Figures 3.3, 3.8, and 3.12). The germination speed is one of the critical measures of seed-vigor under field conditions (Hacisalihoglu et al., 1999). Therefore, the increase in germination speed indicates that the •OH may contribute to the enhancement of seed vigor.

The effect of the •OH was not limited to the germination level but also improved early seedling growth in both *Arabidopsis* and rice. Under optimum condition, the effect was even visible in later stages of growth and development, such as increased root growth and a denser and large number of lateral roots in *Arabidopsis* (Figures 3.7, 3.9). Previously, it was shown that exogenous application of •OH on maize coleoptile and roots also increased the elongation growth (Schopfer, 2001; Schopfer et al., 2002; Liszkay et al., 2004). These studies linked the growth to a direct effect of the •OH on the cell wall, where •OH breaks down the polysaccharide crosslinking and loosen the tightness of the cell wall, and the growth is facilitated by the turgor pressure on a less rigid cell. It is tempted to say that a similar mechanism might be working in my study; however, unlike those mentioned above, I used the •OH on seeds and observed the differences in later development stages. Therefore, it is reasonable to say that the •OH treatment effect lasts longer and might generate some signals that carry to the growth stage from the germination stage.

The most significant and exciting finding of this •OH treatment was its prominent and superior to the H_2O_2 effect under various abiotic stresses such as chilling, high temperature, heat, and salinity. The treatment increased the germination and early seedling growth under different abiotic stresses in both *Arabidopsis* (Figures 3.8, 3.10) and rice (Figures 3.12, 3.13). Before this, in my knowledge, no study was conducted using •OH as an exogenous treatment compound to improve stress tolerance. However, one of the precursors of •OH, H_2O_2, was used as a pre-soaking or treating agent to improve stress tolerance and growth performance. In these studies, germination, growth performance, and stress tolerance was linked to the enhanced performance of the antioxidative machinery, maintaining turgor pressure, inducing stress protein expression, and osmotic readjustment (Wahid et al., 2007; Liheng et al., 2009; Gondim et al., 2010). However, these H_2O_2 treatment studies always fail to consider that the endogenous metal catalysts may convert the H_2O_2 into •OH, and the converted •OH could cause the observed performance by the treated plants. Therefore, to determine the underlying molecular mechanisms of the exogenous •OH treatment in the seeds and germinating seedlings, in Chapter 4, I focused on the changes in proteins under chilling stress using mass-spectrometry based seed proteomics.

The first challenge of seed proteomics is the depletion of storage proteins from the sample to reduce the noise and increase the detection of low-abundant proteins involved in other regulatory processes. Previous studies on *Arabidopsis seed* proteins were done using two-dimensional gel electrophoresis and MALDI-TOF mass spectrometry, where it is easy to ignore or avoid the storage proteins for the final analytical sample by excluding them from the two-dimensional gel (Gallardo et al., 2001; Chibani et al., 2006; Higashi et al., 2006; Durand et al., 2019). However, for liquid chromatography (LC) based

proteomics, a few studies used $CaCl_2$ and succeeded in depleting or reducing storage proteins from the seed protein sample and enhanced the detection of important regulatory proteins. Here, I developed a modified method using an optimized amount of $CaCl_2$ to deplete the storage protein and detected over 800 proteins with less than ten storage proteins. The PCA analysis of the proteomic data showed that the protein clusters are based on the biological replicates and separated based on the treatment conditions and duration of the stress (Figure 4.1). These results ensure the sample preparation for the proteomics was reliable for further analysis.

When I compared the statistically significant abundance change, a large number of differentially expressed proteins (DEP) were in the •OH compared to the H_2O_2 (Figure. 4.2). This difference in DEP indicates that the •OH treatment was more effective than the H_2O_2. The proteins that were only and exclusively responded to •OH treatment are the potential ones that might be involved in the observed chilling stress-responsive phenotype in Chapter 3 (Figures 3.8A, 3.10A). Deeper bioinformatic and functional analysis revealed that the exclusively •OH responsive proteins that were up-accumulated under chilling stress are mostly related to redox homeostasis, protein homeostasis, abiotic stress response, and germination and development related proteins (Figure 4.3, Table S4.1). These findings are a surprising but clear indication that •OH treatment enhanced the abundance of proteins crucial for survival and maintaining basal cellular ROS under abiotic stress. Previous studies of exogenous H_2O_2 applications that enhanced different abiotic stress tolerance were also reported to improve antioxidant properties in the plant cell stresses (Uchida et al., 2002; Wahid et al., 2007; Farooq et al., 2009b; Savvides et al., 2016). These findings further strengthen the idea of considering •OH and its positive effect on ROS treatment studies, which may be working further downstream of H_2O_2 applied. Among the antioxidative proteins that were up-accumulated, glutathione (GSH) seems to be more active because several numbers of GSH metabolism and GSH related proteins such as GR1, GST-DHAR1, and GST-F were exclusively found in the •OH treated group.

Apart from the protein involved in maintaining ROS homeostasis, several chaperon proteins, such as CPN60B, CRT1a, CRT1b, and HSP60-3A, also increased their abundance of •OH treated group in response to chilling. These chaperones play an essential role in maintaining protein integrity by preventing degradation, folding of misfolded proteins, disaggregation of aggregated proteins, and folding-refolding naïve proteins (Singh et al., 2019). Proteins that are involved in stress response, toxic catabolism were also increased their abundance. These results further consolidate the idea that •OH and its oxidative power can be utilized and redirect to potential positive and practical use.

In brief, in Chapter 2, I tried to reveal the early signaling and adaptive plant cell responses to cold, and in Chapters 3 and 4, I showed the positive sites and practical use of •OH in improving abiotic stresses. In Chapters 2 and 4, I demonstrated the use of mass spectrometry-based proteomics to study cold stress response events, and mechanisms behind •OH mediated improvement of cold stress. I expect

that my thesis findings will be a valuable resource that will help us further understand the cold response and improve cold-resistant crop varieties.

Chapter 6

Concluding remarks and future perspective

In the present study, I first focused on investigating the early cold response in plants to understand the basic mechanisms involved in cold sensing and signaling events that occur before the prolonged and extreme winters. To understand the basic mechanisms behind the early cold sensing and the stress tolerance by •OH, I studied changes in proteins (PTM and abundance) by employing mass spectrometry-based proteomics/phosphoproteomics methods.

From the phosphoproteomic study of early cold sensing, I revealed that the early response to cold is complex. Early cold response processes involve the maintenance of ion, solute, and protein homeostasis, which was revealed by the phosphorylation of different Ca^{2+}, K^+, Na^+/K^+, and Cl^- channel transporters. Protein transport, trafficking, and microtubule-cytoskeleton mediated cytoplasmic streaming may also be involved in the early cold response events. My data further indicated that plant kinome gets perturbed by cold exposure, and kinases such as RLKs, MAPKs, CDPKs/ CaMKs/, CKs, and GSKs are an active part of the cold sensing and signaling. Ca^{2+}, phosphoinositide, ABA, auxin, and ROS signaling pathways were also active during the early cold response. To sum up, I revealed the identity of several proteins that are potential targets of phosphorylation machinery in early cold response. Furthermore, I showed that many proteins that were not implicated in cold tolerance showed a temporal response. I expect the findings from this study will be a valuable resource for understanding cold perception in plants. Moreover, functional analysis of the identified cold-responsive phosphosites will help scientists to develop better cold resistance varieties. Additionally, further optimization of a contaminant-free MMF extraction from less starting material will save time and increase phosphopeptide detection efficiency. Furthermore, targeted proteomics can be an alternative for validating and narrowing false-positive phosphopeptides from discovery phosphoproteomics.

Subsequently, I focused on the development of a practical and sustainable method to improve abiotic stress tolerance in plants using •OH. The ROS treatment of seeds showed that •OH performed better than H_2O_2 under different abiotic stresses at germination and early stages of growth and development. This is a surprising finding because •OH is usually considered deleterious and has never been studied for abiotic stress improvement. The simplicity of the treatment that only requires one-time application in the seed will save time, cost, and labor. The proteomic study of germinating seeds showed that •OH treatment increases the activity of antioxidation-related proteins, proteins involved in chaperone activity, and different stress-responsive proteins. Therefore, it can be reasonably concluded that •OH also plays a positive role in ROS signaling and improves plant performance under abiotic stresses, which was never demonstrated in any other studies before this to my knowledge. However, further studies focusing on *in-vivo* imaging •OH, functionally connecting •OH responsive proteins to genes, and studying •OH combined stress conditions will provide better insight into the mechanisms and the effectiveness of this treatment.

Acknowledgments

References

Ahanger MA, Akram NA, Ashraf M, Alyemeni MN, Wijaya L, Ahmad P. (2017). Plant responses to environmental stresses-from gene to biotechnology. *AoB Plants,* **9**: plx025.

Albrecht C, Russinova E, Kemmerling B, Kwaaitaal M, de Vries SC. (2008). *Arabidopsis* SOMATIC EMBRYOGENESIS RECEPTOR KINASE proteins serve brassinosteroid-dependent and -independent signaling pathways. *Plant Physiol,* **148**: 611-619.

Apuya NR, Yadegari R, Fischer RL, Harada JJ, Zimmerman JL, Goldberg RB. (2001). The *Arabidopsis* embryo mutant schlepperless has a defect in the *chaperonin-60α* gene. *Plant Physiol,* **126**: 717-730.

Aroca R, Amodeo G, Fernandez-Illescas S, Herman EM, Chaumont F, Chrispeels MJ. (2005). The role of aquaporins and membrane damage in chilling and hydrogen peroxide induced changes in the hydraulic conductance of maize roots. *Plant Physiol,* **137**: 341-353.

Ashraf MA, Rahman A. (2019). Cold stress response in *Arabidopsis thaliana* is mediated by GNOM ARF-GEF. *Plant J,* **97**: 500-516.

Axelsen KB, Venema K, Jahn T, Baunsgaard L, Palmgren MG. (1999). Molecular dissection of the C-terminal regulatory domain of the plant plasma membrane H^+-ATPase AHA2: mapping of residues that when altered give rise to an activated enzyme. *Biochemistry,* **38**: 7227-7234.

Balakrishnan R, Harris MA, Huntley R, Van Auken K, Cherry JM. (2013). A guide to best practices for Gene Ontology (GO) manual annotation. *Database,* **2013**: bat054.

Balazadeh S, Kwasniewski M, Caldana C, Mehrnia M, Zanor MI, Xue GP, Mueller-Roeber B. (2011). ORS1, an H_2O_2-responsive NAC transcription factor, controls senescence in *Arabidopsis thaliana. Mol Plant,* **4**: 346-360.

Batalha IL, Lowe CR, Roque AC. (2012). Platforms for enrichment of phosphorylated proteins and peptides in proteomics. *Trends Biotechnol,* **30**: 100-110.

Baxter A, Mittler R, Suzuki N. (2014). ROS as key players in plant stress signalling. *J Exp Bot,* **65**: 1229-1240.

Benschop JJ, Mohammed S, O'Flaherty M, Heck AJ, Slijper M, Menke FL. (2007). Quantitative phosphoproteomics of early elicitor signaling in *Arabidopsis. Mol Cell Proteomics,* **6**: 1198-1214.

Bergmann DC, Lukowitz W, Somerville CR. (2004). Stomatal development and pattern controlled by a MAPKK kinase. *Science,* **304**: 1494-1497.

Bethke PC, Jones RL. (2001). Cell death of barley aleurone protoplasts is mediated by reactive oxygen species. *Plant J,* **25**: 19-29.

Bielach A, Hrtyan M, Tognetti VB. (2017). Plants under stress: involvement of auxin and cytokinin. *Int J Mol Sci,* **18**: 1427.

Bonangelino CJ, Nau JJ, Duex JE, Brinkman M, Wurmser AE, Gary JD, Emr SD, Weisman LS. (2002). Osmotic stress-induced increase of phosphatidylinositol 3,5-bisphosphate requires Vac14p, an activator of the lipid kinase Fab1p. *J Cell Biol,* **156**: 1015-1028.

Bose J, Pottosin, II, Shabala SS, Palmgren MG, Shabala S. (2011). Calcium efflux systems in stress signaling and adaptation in plants. *Front Plant Sci,* **2**: 85.

Boston RS, Viitanen PV, Vierling E. (1996). Molecular chaperones and protein folding in plants. *Plant Mol Biol,* **32**: 191-222.

Boudsocq M, Willmann MR, McCormack M, Lee H, Shan L, He P, Bush J, Cheng SH, Sheen J. (2010). Differential innate immune signalling via Ca^{2+} sensor protein kinases. *Nature,* **464**: 418-422.

Boyer JS, Westgate ME. (2004). Grain yields with limited water. *J Exp Bot,* **55**: 2385-2394.

Bradford MM. (1976). A rapid and sensitive method for the quantitation of microgram quantities of protein utilizing the principle of protein-dye binding. *Anal Biochem,* **72**: 248-254.

Cao M, Chen R, Li P, Yu Y, Zheng R, Ge D, Zheng W, Wang X, Gu Y, Gelova Z, Friml J, Zhang H, Liu R, He J, Xu T. (2019). TMK1-mediated auxin signalling regulates differential growth of the apical hook. *Nature,* **568**: 240-243.

Carpaneto A, Ivashikina N, Levchenko V, Krol E, Jeworutzki E, Zhu JK, Hedrich R. (2007). Cold transiently activates calcium-permeable channels in *Arabidopsis* mesophyll cells. *Plant Physiol,* **143**: 487-494.

Caviston JP, Holzbaur EL. (2006). Microtubule motors at the intersection of trafficking and transport. *Trends Cell Biol,* **16**: 530-537.

Cecchetti V, Brunetti P, Napoli N, Fattorini L, Altamura MM, Costantino P, Cardarelli M. (2015). ABCB1 and ABCB19 auxin transporters have synergistic effects on early and late *Arabidopsis* anther development. *J Integr Plant Biol,* **57**: 1089-1098.

Chaiwongsar S, Otegui MS, Jester PJ, Monson SS, Krysan PJ. (2006). The protein kinase genes *MAP3Kε1 and MAP3Kε2* are required for pollen viability in *Arabidopsis thaliana*. *Plant J,* **48**: 193-205.

Chaiwongsar S, Strohm AK, Su S-H, Krysan PJ. (2012). Genetic analysis of the *Arabidopsis* protein kinases *MAP3Kε1* and *MAP3Kε2* indicates roles in cell expansion and embryo development. *Front Plant Sci*, **10**: 3-228.

Chakrabortee S, Boschetti C, Walton LJ, Sarkar S, Rubinsztein DC, Tunnacliffe A. (2007). Hydrophilic protein associated with desiccation tolerance exhibits broad protein stabilization function. *Proc Natl Acad Sci U.S.A.,* **104**: 18073-18078.

Champion A, Picaud A, Henry Y. (2004). Reassessing the MAP3K and MAP4K relationships. *Trends Plant Sci,* **9**: 123-129.

Chen K, Arora R. (2011). Dynamics of the antioxidant system during seed osmopriming, post-priming germination, and seedling establishment in Spinach (*Spinacia oleracea*). *Plant Sci,* **180**: 212-220.

Chen K, Fessehaie A, Arora R. (2012). Dehydrin metabolism is altered during seed osmopriming and subsequent germination under chilling and desiccation in *Spinacia oleracea* L. cv. Bloomsdale: possible role in stress tolerance. *Plant Sci,* **183**: 27-36.

Chen Y, Hoehenwarter W. (2015). Changes in the phosphoproteome and metabolome link early signaling events to rearrangement of photosynthesis and central metabolism in salinity and oxidative stress response in *Arabidopsis*. *Plant Physiol,* **169**: 3021-3033.

Chen Y, Li C, Zhang B, Yi J, Yang Y, Kong C, Lei C, Gong M. (2019). The role of the late embryogenesis-abundant (LEA) protein family in development and the abiotic stress response: a comprehensive expression analysis of potato (*Solanum tuberosum*). *Genes,* **10**: 148.

Chen Y, Weckwerth W. (2020). Mass spectrometry untangles plant membrane protein signaling networks. *Trends Plant Sci,* **25**: 930-944.

Cheng CY, Krishnakumar V, Chan AP, Thibaud-Nissen F, Schobel S, Town CD. (2017). Araport11: a complete reannotation of the *Arabidopsis thaliana* reference genome. *Plant J,* **89**: 789-804.

Chibani K, Ali-Rachedi S, Job C, Job D, Jullien M, Grappin P. (2006). Proteomic analysis of seed dormancy in *Arabidopsis*. *Plant Physiol,* **142**: 1493-1510.

Chinnusamy V, Zhu J, Zhu JK. (2007). Cold stress regulation of gene expression in plants. *Trends Plant Sci,* **12**: 444-451.

Chou MF, Schwartz D. (2011). Biological sequence motif discovery using motif-x. *Curr Protoc Bioinformatics,* **35**: 13.15.11-13.15.24.

Choudhary MK, Nomura Y, Wang L, Nakagami H, Somers DE. (2015). Quantitative circadian phosphoproteomic analysis of *Arabidopsis* reveals extensive clock control of key components in physiological, metabolic, and signaling pathways. *Mol Cell Proteomics,* **14**: 2243-2260.

Christie JM, Yang H, Richter GL, Sullivan S, Thomson CE, Lin J, Titapiwatanakun B, Ennis M, Kaiserli E, Lee OR, Adamec J, Peer WA, Murphy AS. (2011). *phot1* inhibition of ABCB19 primes lateral auxin fluxes in the shoot apex required for phototropism. *PLoS Biol,* **9**: e1001076.

Conde A, Chaves MM, Geros H. (2011). Membrane transport, sensing and signaling in plant adaptation to environmental stress. *Plant Cell Physiol,* **52**: 1583-1602.

Cooke FT, Dove SK, McEwen RK, Painter G, Holmes AB, Hall MN, Michell RH, Parker PJ. (1998). The stress-activated phosphatidylinositol 3-phosphate 5-kinase Fab1p is essential for vacuole function in *S. cerevisiae*. *Curr Biol,* **8**: 1219-S1212.

Cramer GR, Urano K, Delrot S, Pezzotti M, Shinozaki K. (2011). Effects of abiotic stress on plants: a systems biology perspective. *BMC Plant Biol,* **11**: 163.

Demidchik V. (2015). Mechanisms of oxidative stress in plants: from classical chemistry to cell biology. *Environ Exp Bot,* **109**: 212-228.

Demidchik V, Cuin TA, Svistunenko D, Smith SJ, Miller AJ, Shabala S, Sokolik A, Yurin V. (2010). *Arabidopsis* root K^+-efflux conductance activated by hydroxyl radicals: single-channel properties, genetic basis and involvement in stress-induced cell death. *J Cell Sci,* **123**: 1468-1479.

Deng S, Yu M, Wang Y, Jia Q, Lin L, Dong H. (2010). The antagonistic effect of hydroxyl radical on the development of a hypersensitive response in tobacco. *FEBS J,* **277**: 5097-5111.

DeWald DB, Torabinejad J, Jones CA, Shope JC, Cangelosi AR, Thompson JE, Prestwich GD, Hama H. (2001). Rapid accumulation of phosphatidylinositol 4,5-bisphosphate and inositol 1,4,5-trisphosphate correlates with calcium mobilization in salt-stressed *Arabidopsis*. *Plant Physiol,* **126**: 759-769.

Di Paolo G, De Camilli P. (2006). Phosphoinositides in cell regulation and membrane dynamics. *Nature,* **443**: 651-657.

Dove SK, Cooke FT, Douglas MR, Sayers LG, Parker PJ, Michell RH. (1997). Osmotic stress activates phosphatidylinositol-3,5-bisphosphate synthesis. *Nature,* **390**: 187-192.

Downing TE. (1993). The effects of climate change on agriculture and food security. *Renew Energy,* **3**: 491-497.

Du Z, Zhou X, Ling Y, Zhang Z, Su Z. (2010). agriGO: a GO analysis toolkit for the agricultural community. *Nucleic Acids Res,* **38**: W64-70.

Duke SH, Schrader LE, Miller MG. (1977). Low temperature effects on soybean (*Glycine max* [L.] Merr. cv. Wells) mitochondrial respiration and several dehydrogenases during imbibition and germination. *Plant Physiol,* **60**: 716-722.

Durand M, Porcheron B, Hennion N, Maurousset L, Lemoine R, Pourtau N. (2016). Water deficit enhances C export to the roots in *Arabidopsis thaliana* plants with contribution of sucrose transporters in both shoot and roots. *Plant Physiol,* **170**: 1460-1479.

Durand TC, Cueff G, Godin B, Valot B, Clement G, Gaude T, Rajjou L. (2019). Combined proteomic and metabolomic profiling of the *Arabidopsis thaliana vps29* mutant reveals pleiotropic functions of the retromer in seed development. *Int J Mol Sci,* **20**: 362.

Durek P, Schmidt R, Heazlewood JL, Jones A, MacLean D, Nagel A, Kersten B, Schulze WX. (2010). Phosphat: the *Arabidopsis thaliana* phosphorylation site database. An update. *Nucleic Acids Res,* **38**: D828-834.

El-Kassaby YA, Moss I, Kolotelo D, Stoehr M. (2008). Seed germination: mathematical representation and parameters extraction. *For Sci,* **54**: 220-227.

Engelsberger WR, Schulze WX. (2012). Nitrate and ammonium lead to distinct global dynamic phosphorylation patterns when resupplied to nitrogen-starved *Arabidopsis* seedlings. *Plant J,* **69**: 978-995.

Farooq M, Aziz T, Wahid A, Lee D, Siddique KHM. (2009a). Chilling tolerance in maize: agronomic and physiological approaches. *Crop Pasture Sci,* **60**: 501.

Farooq M, Basra SMA, Wahid A, Rehman H. (2009b). Exogenously applied nitric oxide enhances the drought tolerance in fine grain aromatic rice (*Oryza sativa* l.). *J Agron Crop Sci,* **195**: 254-261.

Fischer M, Kaldenhoff R. (2008). On the pH regulation of plant aquaporins. *J Biol Chem,* **283**: 33889-33892.

Foreman J, Demidchik V, Bothwell JH, Mylona P, Miedema H, Torres MA, Linstead P, Costa S, Brownlee C, Jones JD, Davies JM, Dolan L. (2003). Reactive oxygen species produced by NADPH oxidase regulate plant cell growth. *Nature,* **422**: 442-446.

Fry SC. (1998). Oxidative scission of plant cell wall polysaccharides by ascorbate-induced hydroxyl radicals. *Biochem J,* **332 (2)**: 507-515.

Furtauer L, Weiszmann J, Weckwerth W, Nagele T. (2019). Dynamics of plant metabolism during cold acclimation. *Int J Mol Sci,* **20**: 5411.

Furuya T, Matsuoka D, Nanmori T. (2013). Phosphorylation of *Arabidopsis thaliana* MEKK1 via Ca^{2+} signaling as a part of the cold stress response. *J Plant Res,* **126**: 833-840.

Furuya T, Matsuoka D, Nanmori T. (2014). Membrane rigidification functions upstream of the MEKK1-MKK2-MPK4 cascade during cold acclimation in *Arabidopsis thaliana*. *FEBS Lett,* **588**: 2025-2030.

Galano A, Macias-Ruvalcaba NA, Medina Campos ON, Pedraza-Chaverri J. (2010). Mechanism of the OH radical scavenging activity of nordihydroguaiaretic acid: a combined theoretical and experimental study. *J Phys Chem B,* **114**: 6625-6635.

Gallardo K, Job C, Groot SP, Puype M, Demol H, Vandekerckhove J, Job D. (2001). Proteomic analysis of *Arabidopsis* seed germination and priming. *Plant Physiol,* **126**: 835-848.

Gallardo K, Job C, Groot SP, Puype M, Demol H, Vandekerckhove J, Job D. (2002). Proteomics of *Arabidopsis* seed germination. A comparative study of wild-type and gibberellin-deficient seeds. *Plant Physiol,* **129**: 823-837.

Gao J, Zhang S, He WD, Shao XH, Li CY, Wei YR, Deng GM, Kuang RB, Hu CH, Yi GJ, Yang QS. (2017). Comparative phosphoproteomics reveals an important role of MKK2 in banana (*Musa* spp.) cold signal network. *Sci Rep,* **7**: 40852.

Gary JD, Wurmser AE, Bonangelino CJ, Weisman LS, Emr SD. (1998). Fab1p is essential for PtdIns(3)P 5-kinase activity and the maintenance of vacuolar size and membrane homeostasis. *J Cell Biol,* **143**: 65-79.

Gill PK, Sharma AD, Singh P, Bhullar SS. (2003). Changes in germination, growth and soluble sugar contents of *Sorghum bicolor* (L.) moench seeds under various abiotic stresses. *Plant Growth Regul,* **40**: 157-162.

Gill SS, Tuteja N. (2010a). Polyamines and abiotic stress tolerance in plants. *Plant Signal Behav,* **5**: 26-33.

Gill SS, Tuteja N. (2010b). Reactive oxygen species and antioxidant machinery in abiotic stress tolerance in crop plants. *Plant Physiol Biochem,* **48**: 909-930.

Gilmour SJ, Hajela RK, Thomashow MF. (1988). Cold Acclimation in *Arabidopsis thaliana*. *Plant Physiol,* **87**: 745-750.

Gondim FA, Gomes-Filho E, Lacerda CF, Prisco JT, Azevedo Neto AD, Marques EC. (2010). Pretreatment with H_2O_2 in maize seeds: effects on germination and seedling acclimation to salt stress. *Braz J Plant Physiol,* **22**: 103-112.

Goyal K, Walton LJ, Tunnacliffe A. (2005). LEA proteins prevent protein aggregation due to water stress. *Biochem J,* **388**: 151-157.

Grunewald W, Friml J. (2010). The march of the PINs: developmental plasticity by dynamic polar targeting in plant cells. *EMBO J,* **29**: 2700-2714.

Guy CL, Huber JL, Huber SC. (1992). Sucrose phosphate synthase and sucrose accumulation at low temperature. *Plant Physiol,* **100**: 502-508.

Hacisalihoglu G, Paine DH, Hilderbrand MB, Khan AA, Taylor AG. (1999). Embryo elongation and germination rates as sensitive indicators of lettuce seed quality: priming and aging studies. *HortScience,* **34**: 1240-1243.

Haj Ahmad F, Wu XN, Stintzi A, Schaller A, Schulze WX. (2019). The systemin signaling cascade as derived from time course analyses of the systemin-responsive phosphoproteome. *Mol Cell Proteomics,* **18**: 1526-1542.

Halliwell B, Gutteridge JM. (2015). Free radicals in biology and medicine. Oxford University Press, USA.

Haruta M, Sabat G, Stecker K, Minkoff BB, Sussman MR. (2014). A peptide hormone and its receptor protein kinase regulate plant cell expansion. *Science,* **343**: 408-411.

Hasanuzzaman M, Nahar K, Anee TI, Fujita M. (2017). Glutathione in plants: biosynthesis and physiological role in environmental stress tolerance. *Physiol Mol Biol Plants,* **23**: 249-268.

Hashiguchi A, Ahsan N, Komatsu S. (2010). Proteomics application of crops in the context of climatic changes. *Food Res Int,* **43**: 1803-1813.

Hatfield JL, Egli DB. (1974). Effect of temperature on the rate of soybean hypocotyl elongation and field emergence. *Crop Sci,* **14**: 423-426.

He K, Gou X, Yuan T, Lin H, Asami T, Yoshida S, Russell SD, Li J. (2007). BAK1 and BKK1 regulate brassinosteroid-dependent growth and brassinosteroid-independent cell-death pathways. *Curr Biol,* **17**: 1109-1115.

Heazlewood JL, Durek P, Hummel J, Selbig J, Weckwerth W, Walther D, Schulze WX. (2008). PhosPhAt: a database of phosphorylation sites in *Arabidopsis thaliana* and a plant-specific phosphorylation site predictor. *Nucleic Acids Res,* **36**: D1015-1021.

Heilmann I. (2016). Phosphoinositide signaling in plant development. *Development,* **143**: 2044-2055.

Higashi Y, Hirai MY, Fujiwara T, Naito S, Noji M, Saito K. (2006). Proteomic and transcriptomic analysis of *Arabidopsis* seeds: molecular evidence for successive processing of seed proteins and its implication in the stress response to sulfur nutrition. *Plant J,* **48**: 557-571.

Hiraki H, Uemura M, Kawamura Y. (2019). Calcium signaling-linked *CBF/DREB1* gene expression was induced depending on the temperature fluctuation in the field: views from the natural condition of cold acclimation. *Plant Cell Physiol,* **60**: 303-317.

Hirano T, Matsuzawa T, Takegawa K, Sato MH. (2011). Loss-of-function and gain-of-function mutations in *FAB1A/B* impair endomembrane homeostasis, conferring pleiotropic developmental abnormalities in *Arabidopsis*. *Plant Physiol,* **155**: 797-807.

Hirano T, Munnik T, Sato MH. (2015). Phosphatidylinositol 3-phosphate 5-kinase, FAB1/PIKfyve kinase mediates endosome maturation to establish endosome-cortical microtubule interaction in *Arabidopsis*. *Plant Physiol,* **169**: 1961-1974.

Ho CY, Alghamdi TA, Botelho RJ. (2012). Phosphatidylinositol-3,5-bisphosphate: no longer the poor PIP2. *Traffic,* **13**: 1-8.

Hooper CM, Castleden IR, Tanz SK, Aryamanesh N, Millar AH. (2017). SUBA4: the interactive data analysis centre for *Arabidopsis* subcellular protein locations. *Nucleic Acids Res,* **45**: D1064-D1074.

Hossain MA, Bhattacharjee S, Armin SM, Qian P, Xin W, Li HY, Burritt DJ, Fujita M, Tran LS. (2015). Hydrogen peroxide priming modulates abiotic oxidative stress tolerance: insights from ROS detoxification and scavenging. *Front Plant Sci,* **6**: 420.

Hou C, Tian W, Kleist T, He K, Garcia V, Bai F, Hao Y, Luan S, Li L. (2014). DUF221 proteins are a family of osmosensitive calcium-permeable cation channels conserved across eukaryotes. *Cell Res,* **24**: 632-635.

Howe E, Holton K, Nair S, Schlauch D, Sinha R, Quackenbush J. (2010). MeV: MultiExperiment Viewer. In: Ochs MF, Casagrande JT, Davuluri RV, eds. *Biomedical Informatics for Cancer Research*. Boston, MA: Springer US.

Hsu CC, Zhu Y, Arrington JV, Paez JS, Wang P, Zhu P, Chen IH, Zhu JK, Tao WA. (2018). Universal plant phosphoproteomics workflow and its application to tomato signaling in response to cold stress. *Mol Cell Proteomics,* **17**: 2068-2080.

Huala E, Dickerman AW, Garcia-Hernandez M, Weems D, Reiser L, LaFond F, Hanley D, Kiphart D, Zhuang M, Huang W, Mueller LA, Bhattacharyya D, Bhaya D, Sobral BW, Beavis W, Meinke DW, Town CD, Somerville C, Rhee SY. (2001). The *Arabidopsis* Information Resource (TAIR): a comprehensive database and web-based information retrieval, analysis, and visualization system for a model plant. *Nucleic Acids Res,* **29**: 102-105.

Huang DW, Sherman BT, Lempicki RA. (2009). Bioinformatics enrichment tools: paths toward the comprehensive functional analysis of large gene lists. *Nucleic Acids Res,* **37**: 1-13.

Huang DW, Sherman BT, Lempicki RA. (2009). Systematic and integrative analysis of large gene lists using DAVID bioinformatics resources. *Nat Protoc,* **4**: 44-57.

Huang F, Zago MK, Abas L, van Marion A, Galvan-Ampudia CS, Offringa R. (2010). Phosphorylation of conserved PIN motifs directs *Arabidopsis* PIN1 polarity and auxin transport. *Plant Cell,* **22**: 1129-1142.

Hubbard MJ, Cohen P. (1993). On target with a new mechanism for the regulation of protein phosphorylation. *Trends Biochem Sci,* **18**: 172-177.

Hunt L, Otterhag L, Lee JC, Lasheen T, Hunt J, Seki M, Shinozaki K, Sommarin M, Gilmour DJ, Pical C, Gray JE. (2004). Gene-specific expression and calcium activation of *Arabidopsis thaliana* phospholipase C isoforms. *New Phytol,* **162**: 643-654.

Hwang JU, Song WY, Hong D, Ko D, Yamaoka Y, Jang S, Yim S, Lee E, Khare D, Kim K, Palmgren M, Yoon HS, Martinoia E, Lee Y. (2016). Plant ABC transporters enable many unique aspects of a terrestrial plant's lifestyle. *Mol Plant,* **9**: 338-355.

İşeri Ö, Körpe D, Sahin F, Haberal M. (2013). Hydrogen peroxide pretreatment of roots enhanced oxidative stress response of tomato under cold stress. *Acta Physiol Plant,* **35**: 1905-1913.

Ishikawa A, Tanaka H, Nakai M, Asahi T. (2003). Deletion of a *chaperonin 60β* gene leads to cell death in the *Arabidopsis lesion initiation 1* mutant. *Plant Cell Physiol,* **44**: 255-261.

Ishikawa S, Barrero J, Takahashi F, Peck S, Gubler F, Shinozaki K, Umezawa T. (2019a). Comparative phosphoproteomic analysis of barley embryos with different dormancy during imbibition. *Int J Mol Sci,* **20**.

Ishikawa S, Barrero JM, Takahashi F, Nakagami H, Peck SC, Gubler F, Shinozaki K, Umezawa T. (2019b). Comparative phosphoproteomic analysis reveals a decay of ABA signaling in barley embryos during after-ripening. *Plant Cell Physiol,* **60**: 2758-2768.

Joosen RV, Kodde J, Willems LA, Ligterink W, van der Plas LH, Hilhorst HW. (2010). GERMINATOR: a software package for high-throughput scoring and curve fitting of *Arabidopsis* seed germination. *Plant J,* **62**: 148-159.

Jorgensen C, Linding R. (2008). Directional and quantitative phosphorylation networks. *Brief Funct Genomic Proteomic,* **7**: 17-26.

Kadota Y, Shirasu K, Zipfel C. (2015). Regulation of the NADPH oxidase RBOHD during plant immunity. *Plant Cell Physiol,* **56**: 1472-1480.

Kadota Y, Sklenar J, Derbyshire P, Stransfeld L, Asai S, Ntoukakis V, Jones JD, Shirasu K, Menke F, Jones A, Zipfel C. (2014). Direct regulation of the NADPH oxidase RBOHD by the PRR-associated kinase BIK1 during plant immunity. *Mol Cell,* **54**: 43-55.

Kan G, Ning L, Li Y, Hu Z, Zhang W, He X, Yu D. (2016). Identification of novel loci for salt stress at the seed germination stage in soybean. *Breed Sci,* **66**: 530-541.

Kang J, Park J, Choi H, Burla B, Kretzschmar T, Lee Y, Martinoia E. (2011). Plant ABC Transporters. *Arabidopsis Book,* **9**: e0153.

Karpievitch YV, Dabney AR, Smith RD. (2012). Normalization and missing value imputation for label-free LC-MS analysis. *BMC Bioinformatics,* **13 Suppl 16**: S5.

Karpievitch YV, Stuart T, Mohamed S. (2020)**.** ProteoMM: multi-dataset model-based differential expression proteomics analysis platform. R package version 1.6.0. ed: Bioconductor.

Karpievitch YV, Taverner T, Adkins JN, Callister SJ, Anderson GA, Smith RD, Dabney AR. (2009). Normalization of peak intensities in bottom-up MS-based proteomics using singular value decomposition. *Bioinformatics,* **25**: 2573-2580.

Kawamura Y, Uemura M. (2003). Mass spectrometric approach for identifying putative plasma membrane proteins of *Arabidopsis* leaves associated with cold acclimation. *Plant J,* **36**: 141-154.

Kersten B, Agrawal GK, Iwahashi H, Rakwal R. (2006). Plant phosphoproteomics: a long road ahead. *Proteomics,* **6**: 5517-5528.

Khan M, Rozhon W, Bigeard J, Pflieger D, Husar S, Pitzschke A, Teige M, Jonak C, Hirt H, Poppenberger B. (2013). Brassinosteroid-regulated GSK3/Shaggy-like kinases phosphorylate mitogen-activated protein (MAP) kinase kinases, which control stomata development in *Arabidopsis thaliana*. *J Biol Chem,* **288**: 7519-7527.

Khan M, Takasaki H, Komatsu S. (2005). Comprehensive phosphoproteome analysis in rice and identification of phosphoproteins responsive to different hormones/stresses. *J Proteome Res,* **4**: 1592-1599.

Khan MSA, Hamid A, Karim MA. (1997). Effect of sodium chloride on germination and seedling characters of different types of rice (*Oryza sativa* L.). *J Agron Crop Sci,* **179**: 163-169.

Khorobrykh SA, Khorobrykh AA, Yanykin DV, Ivanov BN, Klimov VV, Mano J. (2011). Photoproduction of catalase-insensitive peroxides on the donor side of manganese-depleted photosystem II: evidence with a specific fluorescent probe. *Biochemistry,* **50**: 10658-10665.

Kim DH, Eu YJ, Yoo CM, Kim YW, Pih KT, Jin JB, Kim SJ, Stenmark H, Hwang I. (2001). Trafficking of phosphatidylinositol 3-phosphate from the trans-Golgi network to the lumen of the central vacuole in plant cells. *Plant Cell,* **13**: 287-301.

Kim DY, Jin JY, Alejandro S, Martinoia E, Lee Y. (2010). Overexpression of *AtABCG36* improves drought and salt stress resistance in *Arabidopsis*. *Physiol Plant,* **139**: 170-180.

Kim TW, Guan S, Sun Y, Deng Z, Tang W, Shang JX, Sun Y, Burlingame AL, Wang ZY. (2009). Brassinosteroid signal transduction from cell-surface receptor kinases to nuclear transcription factors. *Nat Cell Biol,* **11**: 1254-1260.

Kimura S, Kaya H, Kawarazaki T, Hiraoka G, Senzaki E, Michikawa M, Kuchitsu K. (2012). Protein phosphorylation is a prerequisite for the Ca^{2+}-dependent activation of *Arabidopsis* NADPH oxidases and may function as a trigger for the positive feedback regulation of Ca^{2+} and reactive oxygen species. *Biochim Biophys Acta,* **1823**: 398-405.

Knight H, Knight MR. (2000). Imaging spatial and cellular characteristics of low temperature calcium signature after cold acclimation in *Arabidopsis*. *J Exp Bot,* **51**: 1679-1686.

Knight H, Trewavas AJ, Knight MR. (1996a). Cold calcium signaling in *Arabidopsis* involves two cellular pools and a change in calcium signature after acclimation. *Plant Cell,* **8**: 489-503.

Kobayashi M, Ohura I, Kawakita K, Yokota N, Fujiwara M, Shimamoto K, Doke N, Yoshioka H. (2007). Calcium-dependent protein kinases regulate the production of reactive oxygen species by potato NADPH oxidase. *Plant Cell,* **19**: 1065-1080.

Kodra E, Steinhaeuser K, Ganguly AR. (2011). Persisting cold extremes under 21st-century warming scenarios. *Geophys Res Lett,* **38**: L08705.

Komatsu S, Konishi H, Shen S, Yang G. (2003). Rice proteomics: a step toward functional analysis of the rice genome. *Mol Cell Proteomics,* **2**: 2-10.

Kong Q, Sun T, Qu N, Ma J, Li M, Cheng YT, Zhang Q, Wu D, Zhang Z, Zhang Y. (2016). Two redundant receptor-like cytoplasmic kinases function downstream of pattern recognition receptors to regulate activation of SA biosynthesis. *Plant Physiol,* **171**: 1344-1354.

Kosova K, Vitamvas P, Urban MO, Prasil IT, Renaut J. (2018). Plant abiotic stress proteomics: the major factors determining alterations in cellular proteome. *Front Plant Sci,* **9**: 122.

Kovacs D, Agoston B, Tompa P. (2008). Disordered plant LEA proteins as molecular chaperones. *Plant Signal Behav,* **3**: 710-713.

Krishnan HB, Oehrle NW, Natarajan SS. (2009). A rapid and simple procedure for the depletion of abundant storage proteins from legume seeds to advance proteome analysis: a case study using *Glycine max*. *Proteomics,* **9**: 3174-3188.

Ku NO, Liao J, Omary MB. (1998). Phosphorylation of human keratin 18 serine 33 regulates binding to 14-3-3 proteins. *EMBO J,* **17**: 1892-1906.

Kubala S, Garnczarska M, Wojtyla L, Clippe A, Kosmala A, Zmienko A, Lutts S, Quinet M. (2015). Deciphering priming-induced improvement of rapeseed (*Brassica napus* L.) germination through an integrated transcriptomic and proteomic approach. *Plant Sci,* **231**: 94-113.

Laohavisit A, Richards SL, Shabala L, Chen C, Colaco RD, Swarbreck SM, Shaw E, Dark A, Shabala S, Shang Z, Davies JM. (2013). Salinity-induced calcium signaling and root adaptation in *Arabidopsis* require the calcium regulatory protein annexin1. *Plant Physiol,* **163**: 253-262.

Le Hir R, Spinner L, Klemens PA, Chakraborti D, de Marco F, Vilaine F, Wolff N, Lemoine R, Porcheron B, Gery C, Teoule E, Chabout S, Mouille G, Neuhaus HE, Dinant S, Bellini C. (2015). Disruption of the sugar transporters AtSWEET11 and AtSWEET12 affects vascular development and freezing tolerance in *Arabidopsis*. *Mol Plant,* **8**: 1687-1690.

Lee BH, Henderson DA, Zhu JK. (2005). The *Arabidopsis* cold-responsive transcriptome and its regulation by ICE1. *Plant Cell,* **17**: 3155-3175.

Lee SH, Chung GC, Jang JY, Ahn SJ, Zwiazek JJ. (2012). Overexpression of PIP2;5 aquaporin alleviates effects of low root temperature on cell hydraulic conductivity and growth in *Arabidopsis*. *Plant Physiol,* **159**: 479-488.

Leopold AC. (1980). Temperature effects on soybean imbibition and leakage. *Plant Physiol,* **65**: 1096-1098.

Levitt J. (1980). Responses of plants to environmental stress, volume 1: chilling, freezing and high temperature stresses: Academic Press.

Lewis DR, Wu G, Ljung K, Spalding EP. (2009). Auxin transport into cotyledons and cotyledon growth depend similarly on the ABCB19 Multidrug Resistance-like transporter. *Plant J,* **60**: 91-101.

Li B, Takahashi D, Kawamura Y, Uemura M. (2012a). Comparison of plasma membrane proteomic changes of *Arabidopsis* suspension-cultured cells (T87 Line) after cold and ABA treatment in association with freezing tolerance development. *Plant Cell Physiol,* **53**: 543-554.

Li B, Takahashi D, Kawamura Y, Uemura M. (2020). Plasma membrane proteome analyses of *Arabidopsis thaliana* suspension-cultured cells during cold or ABA treatment: relationship with freezing tolerance and growth phase. *J Proteomics,* **211**: 103528.

Li J, Nam KH, Vafeados D, Chory J. (2001). *BIN2*, a new brassinosteroid-insensitive locus in *Arabidopsis*. *Plant Physiol,* **127**: 14-22.

Li J, Silva-Sanchez C, Zhang T, Chen S, Li H. (2015). Phosphoproteomics technologies and applications in plant biology research. *Front Plant Sci,* **6**: 430.

Li J, Wang X, Zhang Y, Jia H, Bi Y. (2011). cGMP regulates hydrogen peroxide accumulation in calcium-dependent salt resistance pathway in *Arabidopsis thaliana* roots. *Planta,* **234**: 709-722.

Li L, Li M, Yu L, Zhou Z, Liang X, Liu Z, Cai G, Gao L, Zhang X, Wang Y, Chen S, Zhou JM. (2014). The FLS2-associated kinase BIK1 directly phosphorylates the NADPH oxidase RbohD to control plant immunity. *Cell Host Microbe,* **15**: 329-338.

Li L, Wang Y, Shen W. (2012b). Roles of hydrogen sulfide and nitric oxide in the alleviation of cadmium-induced oxidative damage in alfalfa seedling roots. *Biometals,* **25**: 617-631.

Liheng H, Zhiqiang G, Runzhi L. (2009). Pretreatment of seed with H_2O_2 enhances drought tolerance of wheat (*Triticum aestivum* L.) seedlings. *Afr J Biotechnol,* **8**: 6151-6157.

Lin LL, Hsu CL, Hu CW, Ko SY, Hsieh HL, Huang HC, Juan HF. (2015). Integrating phosphoproteomics and bioinformatics to study brassinosteroid-regulated phosphorylation dynamics in *Arabidopsis. BMC Genomics,* **16**: 533.

Lin W, Lu D, Gao X, Jiang S, Ma X, Wang Z, Mengiste T, He P, Shan L. (2013). Inverse modulation of plant immune and brassinosteroid signaling pathways by the receptor-like cytoplasmic kinase BIK1. *Proc Natl Acad Sci U.S.A,* **110**: 12114-12119.

Liszkay A, van der Zalm E, Schopfer P. (2004). Production of reactive oxygen intermediates (O_2^-, H_2O_2, and $\cdot OH$) by maize roots and their role in wall loosening and elongation growth. *Plant Physiol,* **136**: 3114-3123.

Liu H, Wang FF, Peng XJ, Huang JH, Shen SH. (2019). Global phosphoproteomic analysis reveals the defense and response mechanisms of *Jatropha curcas* seedling under chilling stress. *Int J Mol Sci,* **20**: 208.

Liu S, Oshita S, Kawabata S, Makino Y, Yoshimoto T. (2016). Identification of ROS produced by nanobubbles and their positive and negative effects on vegetable seed germination. *Langmuir,* **32**: 11295-11302.

Liu Z, Jia Y, Ding Y, Shi Y, Li Z, Guo Y, Gong Z, Yang S. (2017). Plasma membrane CRPK1-mediated phosphorylation of 14-3-3 proteins induces their nuclear import to fine-tune cbf signaling during cold response. *Mol Cell,* **66**: 117-128 e115.

Liu Z, Wu Y, Yang F, Zhang Y, Chen S, Xie Q, Tian X, Zhou JM. (2013). BIK1 interacts with PEPRs to mediate ethylene-induced immunity. *Proc Natl Acad Sci U.S.A.,* **110**: 6205-6210.

Lobell DB, Field CB. (2007). Global scale climate–crop yield relationships and the impacts of recent warming. *Environ Res Lett,* **2**: 014002.

Lu YP, Li ZS, Rea PA. (1997). *AtMRP1* gene of *Arabidopsis* encodes a glutathione S-conjugate pump: isolation and functional definition of a plant ATP-binding cassette transporter gene. *Proc Natl Acad Sci U.S.A.,* **94**: 8243-8248.

Luan S. (2009). The CBL-CIPK network in plant calcium signaling. *Trends Plant Sci,* **14**: 37-42.

Lv DW, Li X, Zhang M, Gu AQ, Zhen SM, Wang C, Li XH, Yan YM. (2014). Large-scale phosphoproteome analysis in seedling leaves of *Brachypodium distachyon* L. *BMC Genomics,* **15**: 375.

Ma Y, Dai X, Xu Y, Luo W, Zheng X, Zeng D, Pan Y, Lin X, Liu H, Zhang D, Xiao J, Guo X, Xu S, Niu Y, Jin J, Zhang H, Xu X, Li L, Wang W, Qian Q, Ge S, Chong K. (2015). COLD1 confers chilling tolerance in rice. *Cell,* **160**: 1209-1221.

MacLean B, Tomazela DM, Shulman N, Chambers M, Finney GL, Frewen B, Kern R, Tabb DL, Liebler DC, MacCoss MJ. (2010). Skyline: an open source document editor for creating and analyzing targeted proteomics experiments. *Bioinformatics,* **26**: 966-968.

Mahmood Q, Ahmad R, Kwak S-S, Rashid A, Anjum NA. (2010)**.** Ascorbate and glutathione: protectors of plants in oxidative stress. In: Anjum NA, Chan M-T, Umar S, eds. *Ascorbate-Glutathione Pathway and Stress Tolerance in Plants*. Dordrecht: Springer Netherlands.

Mao J, Manik SM, Shi S, Chao J, Jin Y, Wang Q, Liu H. (2016). Mechanisms and physiological roles of the CBL-CIPK networking system in *Arabidopsis thaliana. Genes,* **7:** 62.

Maraghni M, Gorai M, Neffati M. (2010). Seed germination at different temperatures and water stress levels, and seedling emergence from different depths of *Ziziphus lotus. S Afr J Bot,* **76**: 453-459.

Marengo J, Cornejo A, Satyamurty P, Nobre C, Sea W. (1997). Cold surges in tropical and extratropical South America: the strong event in june 1994. *Mon Weather Rev,* **125**: 2759-2786.

Marshall A, Aalen RB, Audenaert D, Beeckman T, Broadley MR, Butenko MA, Cano-Delgado AI, de Vries S, Dresselhaus T, Felix G, Graham NS, Foulkes J, Granier C, Greb T, Grossniklaus U, Hammond JP, Heidstra R, Hodgman C, Hothorn M, Inze D, Ostergaard L, Russinova E, Simon R, Skirycz A, Stahl Y, Zipfel C, De Smet I. (2012). Tackling drought stress: receptor-like kinases present new approaches. *Plant Cell,* **24**: 2262-2278.

Marti MC, Stancombe MA, Webb AA. (2013). Cell- and stimulus type-specific intracellular free Ca^{2+} signals in *Arabidopsis*. *Plant Physiol,* **163**: 625-634.

Mastouri F, Bjorkman T, Harman GE. (2010). Seed treatment with *Trichoderma harzianum* alleviates biotic, abiotic, and physiological stresses in germinating seeds and seedlings. *Phytopathology,* **100**: 1213-1221.

Matros A, Peshev D, Peukert M, Mock HP, Van den Ende W. (2015). Sugars as hydroxyl radical scavengers: proof-of-concept by studying the fate of sucralose in *Arabidopsis*. *Plant J,* **82**: 822-839.

Mattei B, Spinelli F, Pontiggia D, De Lorenzo G. (2016). Comprehensive analysis of the membrane phosphoproteome regulated by oligogalacturonides in *Arabidopsis thaliana. Front Plant Sci,* **7**: 1107.

May MJ, Vernoux T, Leaver C, Montagu MV, Inze D. (1998). Glutathione homeostasis in plants: implications for environmental sensing and plant development. *J Exp Bot,* **49**: 649-667.

Medina J, Catala R, Salinas J. (2011). The CBFs: three *Arabidopsis* transcription factors to cold acclimate. *Plant Sci,* **180**: 3-11.

Meng X, Wang H, He Y, Liu Y, Walker JC, Torii KU, Zhang S. (2012). A MAPK cascade downstream of ERECTA receptor-like protein kinase regulates *Arabidopsis* inflorescence architecture by promoting localized cell proliferation. *Plant Cell,* **24**: 4948-4960.

Metsalu T, Vilo J. (2015). Clustvis: a web tool for visualizing clustering of multivariate data using principal component analysis and heatmap. *Nucleic Acids Res,* **43**: W566-570.

Mickky BM, Aldesuquy HS. (2019). Impact of osmotic stress on seedling growth observations, membrane characteristics and antioxidant defense system of different wheat genotypes. *Egypt J Basic Appl Sci,* **4**: 47-54.

Miki Y. (2015). Shotgun proteomics and phosphoproteomics analysis of cold acclimation and de-acclimation in *Arabidopsis thaliana*, Master thesis, Iwate University, Japan (In Japanese)

Miki Y, Takahashi D, Kawamura Y, Uemura M. (2019). Temporal proteomics of *Arabidopsis* plasma membrane during cold- and de-acclimation. *J Proteomics,* **197**: 71-81.

Miller G, Schlauch K, Tam R, Cortes D, Torres MA, Shulaev V, Dangl JL, Mittler R. (2009). The plant NADPH oxidase RBOHD mediates rapid systemic signaling in response to diverse stimuli. *Sci Signal,* **2**: ra45.

Minami A, Fujiwara M, Furuto A, Fukao Y, Yamashita T, Kamo M, Kawamura Y, Uemura M. (2009). Alterations in detergent-resistant plasma membrane microdomains in *Arabidopsis thaliana* during cold acclimation. *Plant Cell Physiol,* **50**: 341-359.

Mishkind M, Vermeer JE, Darwish E, Munnik T. (2009). Heat stress activates phospholipase D and triggers PIP accumulation at the plasma membrane and nucleus. *Plant J,* **60**: 10-21.

Mishra NS, Tuteja R, Tuteja N. (2006). Signaling through MAP kinase networks in plants. *Arch Biochem Biophys,* **452**: 55-68.

Mittler R. (2006). Abiotic stress, the field environment and stress combination. *Trends Plant Sci,* **11**: 15-19.

Mittler R. (2017). ROS are good. *Trends Plant Sci,* **22**: 11-19.

Mittler R, Blumwald E. (2015). The roles of ROS and ABA in systemic acquired acclimation. *Plant Cell,* **27**: 64-70.

Miura K, Furumoto T. (2013). Cold signaling and cold response in plants. *Int J Mol Sci,* **14**: 5312-5337.

Moreno-Romero J, Espunya MC, Platara M, Arino J, Martinez MC. (2008). A role for protein kinase CK2 in plant development: evidence obtained using a dominant-negative mutant. *Plant J,* **55**: 118-130.

Mosblech A, Konig S, Stenzel I, Grzeganek P, Feussner I, Heilmann I. (2008). Phosphoinositide and inositolpolyphosphate signalling in defense responses of *Arabidopsis thaliana* challenged by mechanical wounding. *Mol Plant,* **1**: 249-261.

Mulekar JJ, Bu Q, Chen F, Huq E. (2012). Casein kinase II alpha subunits affect multiple developmental and stress-responsive pathways in *Arabidopsis*. *Plant J,* **69**: 343-354.

Muller K, Carstens AC, Linkies A, Torres MA, Leubner-Metzger G. (2009a). The NADPH-oxidase AtrbohB plays a role in *Arabidopsis* seed after-ripening. *New Phytol,* **184**: 885-897.

Muller K, Linkies A, Vreeburg RA, Fry SC, Krieger-Liszkay A, Leubner-Metzger G. (2009b). In vivo cell wall loosening by hydroxyl radicals during cress seed germination and elongation growth. *Plant Physiol,* **150**: 1855-1865.

Munnik T. (2001). Phosphatidic acid: an emerging plant lipid second messenger. *Trends Plant Sci,* **6**: 227-233.

Nagasaki-Takeuchi N, Miyano M, Maeshima M. (2008). A plasma membrane-associated protein of *Arabidopsis thaliana* AtPCaP1 binds copper ions and changes its higher order structure. *J Biochem,* **144**: 487-497.

Nakagami H, Sugiyama N, Mochida K, Daudi A, Yoshida Y, Toyoda T, Tomita M, Ishihama Y, Shirasu K. (2010). Large-scale comparative phosphoproteomics identifies conserved phosphorylation sites in plants. *Plant Physiol,* **153**: 1161-1174.

Nick P. (2013). Microtubules, signalling and abiotic stress. *Plant J,* **75**: 309-323.

Nievola CC, Carvalho CP, Carvalho V, Rodrigues E. (2017). Rapid responses of plants to temperature changes. *Temperature,* **4**: 371-405.

Niittyla T, Fuglsang AT, Palmgren MG, Frommer WB, Schulze WX. (2007). Temporal analysis of sucrose-induced phosphorylation changes in plasma membrane proteins of *Arabidopsis*. *Mol Cell Proteomics,* **6**: 1711-1726.

Noctor G, Foyer CH. (1998). Ascorbate and glutathione: keeping active oxygen under control. *Annu Rev Plant Physiol Plant Mol Biol,* **49**: 249-279.

Novaković L, Guo T, Bacic A, Sampathkumar A, Johnson KL. (2018). Hitting the wall-sensing and signaling pathways involved in plant cell wall remodeling in response to abiotic stress. *Plants,* **7**: 89.

Nuhse TS, Stensballe A, Jensen ON, Peck SC. (2003). Large-scale analysis of in vivo phosphorylated membrane proteins by immobilized metal ion affinity chromatography and mass spectrometry. *Mol Cell Proteomics,* **2**: 1234-1243.

Oh MH, Wang X, Kota U, Goshe MB, Clouse SD, Huber SC. (2009). Tyrosine phosphorylation of the BRI1 receptor kinase emerges as a component of brassinosteroid signaling in *Arabidopsis*. *Proc Natl Acad Sci U.S.A.,* **106**: 658-663.

Olkowski AA, Laarveld B, Tanino KK. (2014)**.** Enhancement and control of seed germination with compositions comprising a transition metal catalyst and an oxidant (CA2949750A1). Canada: University of Saskatchewan.

Olsen JV, Ong SE, Mann M. (2004). Trypsin cleaves exclusively C-terminal to arginine and lysine residues. *Mol Cell Proteomics,* **3**: 608-614.

Olsson A, Svennelid F, Ek B, Sommarin M, Larsson C. (1998). A phosphothreonine residue at the C-terminal end of the plasma membrane H^+-ATPase is protected by fusicoccin-induced 14-3-3 binding. *Plant Physiol,* **118**: 551-555.

Orman-Ligeza B, Parizot B, de Rycke R, Fernandez A, Himschoot E, Van Breusegem F, Bennett MJ, Perilleux C, Beeckman T, Draye X. (2016). RBOH-mediated ROS production facilitates lateral root emergence in *Arabidopsis. Development,* **143**: 3328-3339.

Osakabe Y, Mizuno S, Tanaka H, Maruyama K, Osakabe K, Todaka D, Fujita Y, Kobayashi M, Shinozaki K, Yamaguchi-Shinozaki K. (2010). Overproduction of the membrane-bound receptor-like protein kinase 1, RPK1, enhances abiotic stress tolerance in *Arabidopsis. J Biol Chem,* **285**: 9190-9201.

Osakabe Y, Yamaguchi-Shinozaki K, Shinozaki K, Tran LS. (2013). Sensing the environment: key roles of membrane-localized kinases in plant perception and response to abiotic stress. *J Exp Bot,* **64**: 445-458.

Ou Y, Lu X, Zi Q, Xun Q, Zhang J, Wu Y, Shi H, Wei Z, Zhao B, Zhang X, He K, Gou X, Li C, Li J. (2016). RGF1 INSENSITIVE 1 to 5, a group of LRR receptor-like kinases, are essential for the perception of root meristem growth factor 1 in *Arabidopsis thaliana. Cell Res,* **26**: 686-698.

Pagamas P, Nawata E. (2007). Effect of high temperature during the seed development on quality and chemical composition of chili pepper seeds. *Jpn J Trop Agr,* **51**: 22-29.

Pandey P, Irulappan V, Bagavathiannan MV, Senthil-Kumar M. (2017). Impact of combined abiotic and biotic stresses on plant growth and avenues for crop improvement by exploiting physio-morphological traits. *Front Plant Sci,* **8**: 537.

Parra-Lobato MC, Gomez-Jimenez MC. (2011). Polyamine-induced modulation of genes involved in ethylene biosynthesis and signalling pathways and nitric oxide production during olive mature fruit abscission. *J Exp Bot,* **62**: 4447-4465.

Pawson T, Scott JD. (1997). Signaling through scaffold, anchoring, and adaptor proteins. *Science,* **278**: 2075-2080.

Perdomo JA, Conesa MA, Medrano H, Ribas-Carbo M, Galmes J. (2015). Effects of long-term individual and combined water and temperature stress on the growth of rice, wheat and maize: relationship with morphological and physiological acclimation. *Physiol Plant,* **155**: 149-165.

Peremyslov VV, Cole RA, Fowler JE, Dolja VV. (2015). Myosin-powered membrane compartment drives cytoplasmic streaming, cell expansion and plant development. *PLoS One,* **10**: e0139331.

Peremyslov VV, Morgun EA, Kurth EG, Makarova KS, Koonin EV, Dolja VV. (2013). Identification of myosin XI receptors in *Arabidopsis* defines a distinct class of transport vesicles. *Plant Cell,* **25**: 3022-3038.

Phadtare S, Alsina J, Inouye M. (1999). Cold-shock response and cold-shock proteins. *Curr Opin Microbiol,* **2**: 175-180.

Pi E, Zhu C, Fan W, Huang Y, Qu L, Li Y, Zhao Q, Ding F, Qiu L, Wang H, Poovaiah BW, Du L. (2018). Quantitative phosphoproteomic and metabolomic analyses reveal GmMYB173

optimizes flavonoid metabolism in soybean under salt stress. *Mol Cell Proteomics,* **17**: 1209-1224.

Pi Z, Zhao ML, Peng XJ, Shen SH. (2017). Phosphoproteomic analysis of paper mulberry reveals phosphorylation functions in chilling tolerance. *J Proteome Res,* **16**: 1944-1961.

Pickard WF. (2003). The role of cytoplasmic streaming in symplastic transport. *Plant Cell Environ,* **26**: 1-15.

Pospisil P. (2009). Production of reactive oxygen species by photosystem II. *Biochim Biophys Acta,* **1787**: 1151-1160.

Prado K, Boursiac Y, Tournaire-Roux C, Monneuse JM, Postaire O, Da Ines O, Schaffner AR, Hem S, Santoni V, Maurel C. (2013). Regulation of *Arabidopsis* leaf hydraulics involves light-dependent phosphorylation of aquaporins in veins. *Plant Cell,* **25**: 1029-1039.

Prak S, Hem S, Boudet J, Viennois G, Sommerer N, Rossignol M, Maurel C, Santoni V. (2008). Multiple phosphorylations in the C-terminal tail of plant plasma membrane aquaporins: role in subcellular trafficking of AtPIP2;1 in response to salt stress. *Mol Cell Proteomics,* **7**: 1019-1030.

Prasad PVV, Pisipati SR, Momčilović I, Ristic Z. (2011). Independent and combined effects of high temperature and drought stress during grain filling on plant yield and chloroplast EF-Tu expression in spring wheat. *J Agron Crop Sci,* **197**: 430-441.

Prasad SM, Dwivedi R, Zeeshan M. (2005). Growth, photosynthetic electron transport, and antioxidant responses of young soybean seedlings to simultaneous exposure of nickel and UV-B stress. *Photosynthetica,* **43**: 177-185.

Pratap V, Sharma YK. (2010). Impact of osmotic stress on seed germination and seedling growth in black gram (*Phaseolus mungo*). *J Environ Biol,* **31**: 721-726.

Queval G, Issakidis-Bourguet E, Hoeberichts FA, Vandorpe M, Gakiere B, Vanacker H, Miginiac-Maslow M, Van Breusegem F, Noctor G. (2007). Conditional oxidative stress responses in the *Arabidopsis* photorespiratory mutant *cat2* demonstrate that redox state is a key modulator of daylength-dependent gene expression, and define photoperiod as a crucial factor in the regulation of H_2O_2-induced cell death. *Plant J,* **52**: 640-657.

Rahman A, Kawamura Y, Maeshima M, Rahman A, Uemura M. (2020). Plasma membrane aquaporin members PIPs act in concert to regulate cold acclimation and freezing tolerance responses in *Arabidopsis thaliana*. *Plant Cell Physiol,* **61**: 787-802.

Raudvere U, Kolberg L, Kuzmin I, Arak T, Adler P, Peterson H, Vilo J. (2019). g:Profiler: a web server for functional enrichment analysis and conversions of gene lists (2019 update). *Nucleic Acids Res,* **47**: W191-W198.

Ray DK, Gerber JS, MacDonald GK, West PC. (2015). Climate variation explains a third of global crop yield variability. *Nat Commun,* **6**: 5989.

Renew S, Heyno E, Schopfer P, Liszkay A. (2005). Sensitive detection and localization of hydroxyl radical production in cucumber roots and *Arabidopsis* seedlings by spin trapping electron paramagnetic resonance spectroscopy. *Plant J,* **44**: 342-347.

Richards SL, Wilkins KA, Swarbreck SM, Anderson AA, Habib N, Smith AG, McAinsh M, Davies JM. (2015). The hydroxyl radical in plants: from seed to seed. *J Exp Bot,* **66**: 37-46.

Ruelland E, Cantrel C, Gawer M, Kader JC, Zachowski A. (2002). Activation of phospholipases C and D is an early response to a cold exposure in *Arabidopsis* suspension cells. *Plant Physiol,* **130**: 999-1007.

Ruzicka K, Strader LC, Bailly A, Yang H, Blakeslee J, Langowski L, Nejedla E, Fujita H, Itoh H, Syono K, Hejatko J, Gray WM, Martinoia E, Geisler M, Bartel B, Murphy AS, Friml J. (2010). *Arabidopsis PIS1* encodes the ABCG37 transporter of auxinic compounds including the auxin precursor indole-3-butyric acid. *Proc Natl Acad Sci U.S.A,* **107**: 10749-10753.

Saijo Y, Hata S, Kyozuka J, Shimamoto K, Izui K. (2000). Over-expression of a single Ca^{2+}-dependent protein kinase confers both cold and salt/drought tolerance on rice plants. *Plant J,* **23**: 319-327.

Savas JN, Stein BD, Wu CC, Yates JR, 3rd. (2011). Mass spectrometry accelerates membrane protein analysis. *Trends Biochem Sci,* **36**: 388-396.

Savitski MM, Lemeer S, Boesche M, Lang M, Mathieson T, Bantscheff M, Kuster B. (2011). Confident phosphorylation site localization using the Mascot Delta Score. *Mol Cell Proteomics,* **10**: M110 003830.

Savvides A, Ali S, Tester M, Fotopoulos V. (2016). Chemical priming of plants against multiple abiotic stresses: mission possible? *Trends Plant Sci,* **21**: 329-340.

Schopfer P. (2001). Hydroxyl radical-induced cell-wall loosening in vitro and in vivo: implications for the control of elongation growth. *Plant J,* **28**: 679-688.

Schopfer P, Liszkay A, Bechtold M, Frahry G, Wagner A. (2002). Evidence that hydroxyl radicals mediate auxin-induced extension growth. *Planta,* **214**: 821-828.

Schulze WX. (2010). Proteomics approaches to understand protein phosphorylation in pathway modulation. *Curr Opin Plant Biol,* **13**: 280-287.

Schulze WX, Schneider T, Starck S, Martinoia E, Trentmann O. (2012). Cold acclimation induces changes in *Arabidopsis* tonoplast protein abundance and activity and alters phosphorylation of tonoplast monosaccharide transporters. *Plant J,* **69**: 529-541.

Schwacke R, Ponce-Soto GY, Krause K, Bolger AM, Arsova B, Hallab A, Gruden K, Stitt M, Bolger ME, Usadel B. (2019). Mapman4: a refined protein classification and annotation framework applicable to multi-omics data analysis. *Mol Plant,* **12**: 879-892.

Schwartz D, Gygi SP. (2005). An iterative statistical approach to the identification of protein phosphorylation motifs from large-scale data sets. *Nat Biotechnol,* **23**: 1391-1398.

Schwarzlander M, Finkemeier I. (2013). Mitochondrial energy and redox signaling in plants. *Antioxid Redox Signal,* **18**: 2122-2144.

Shannon P, Markiel A, Ozier O, Baliga NS, Wang JT, Ramage D, Amin N, Schwikowski B, Ideker T. (2003). Cytoscape: a software environment for integrated models of biomolecular interaction networks. *Genome Res,* **13**: 2498-2504.

Shelden MC, Howitt SM, Kaiser BN, Tyerman SD. (2010). Identification and functional characterisation of aquaporins in the grapevine, *Vitis vinifera. Funct Plant Biol,* **36**: 1065-1078.

Shibasaki K, Uemura M, Tsurumi S, Rahman A. (2009). Auxin response in *Arabidopsis* under cold stress: underlying molecular mechanisms. *Plant Cell,* **21**: 3823-3838.

Silva-Correia J, Freitas S, Tavares RM, Lino-Neto T, Azevedo H. (2014). Phenotypic analysis of the *Arabidopsis* heat stress response during germination and early seedling development. *Plant Methods,* **10**: 7.

Silva EN, Vieira SA, Ribeiro RV, Ponte LFA, Ferreira-Silva SL, Silveira JAG. (2012). Contrasting physiological responses of *Jatropha curcas* plants to single and combined stresses of salinity and heat. *J Plant Growth Regul,* **32**: 159-169.

Singh RK, Gupta V, Prasad M. (2019). Plant molecular chaperones: structural organization and their roles in abiotic stress tolerance. In: Roychoudhury A, Tripathi D, eds. *Molecular Plant Abiotic Stress*: Willey.

Smertenko AP, Chang HY, Sonobe S, Fenyk SI, Weingartner M, Bogre L, Hussey PJ. (2006). Control of the AtMAP65-1 interaction with microtubules through the cell cycle. *J Cell Sci,* **119**: 3227-3237.

Soltani E, Ghaderi-Far F, Baskin CC, Baskin JM. (2015). Problems with using mean germination time to calculate rate of seed germination. *Aust J Bot,* **63**: 631-635.

Song W, Liu L, Wang J, Wu Z, Zhang H, Tang J, Lin G, Wang Y, Wen X, Li W, Han Z, Guo H, Chai J. (2016). Signature motif-guided identification of receptors for peptide hormones essential for root meristem growth. *Cell Res,* **26**: 674-685.

Sreeramulu S, Mostizky Y, Sunitha S, Shani E, Nahum H, Salomon D, Hayun LB, Gruetter C, Rauh D, Ori N, Sessa G. (2013). BSKs are partially redundant positive regulators of brassinosteroid signaling in *Arabidopsis. Plant J,* **74**: 905-919.

Stecker KE, Minkoff BB, Sussman MR. (2014). Phosphoproteomic analyses reveal early signaling events in the osmotic stress response. *Plant Physiol,* **165**: 1171-1187.

Steponkus PL. (1984). Role of the plasma membrane in freezing injury and cold acclimation. *Annu Rev Plant Physiol,* **35**: 543-584.

Stetson LC, Ostrom QT, Schlatzer D, Liao P, Devine K, Waite K, Couce ME, Harris PLR, Kerstetter-Fogle A, Berens ME, Sloan AE, Islam MM, Rajaratnam V, Mirza SP, Chance

MR, Barnholtz-Sloan JS. (2020). Proteins inform survival-based differences in patients with glioblastoma. *Neurooncol Adv,* **2**: vdaa039.

Sugiyama N, Masuda T, Shinoda K, Nakamura A, Tomita M, Ishihama Y. (2007). Phosphopeptide enrichment by aliphatic hydroxy acid-modified metal oxide chromatography for nano-LC-MS/MS in proteomics applications. *Mol Cell Proteomics,* **6**: 1103-1109.

Suh BC, Hille B. (2005). Regulation of ion channels by phosphatidylinositol 4,5-bisphosphate. *Curr Opin Neurobiol,* **15**: 370-378.

Sun H, King AJ, Diaz HB, Marshall MS. (2000). Regulation of the protein kinase Raf-1 by oncogenic Ras through phosphatidylinositol 3-kinase, Cdc42/Rac and Pak. *Curr Biol,* **10**: 281-284.

Supek F, Bosnjak M, Skunca N, Smuc T. (2011). REVIGO summarizes and visualizes long lists of gene ontology terms. *PLoS One,* **6**: e21800.

Suzuki N, Rivero RM, Shulaev V, Blumwald E, Mittler R. (2014). Abiotic and biotic stress combinations. *New Phytol,* **203**: 32-43.

Takahashi D, Gorka M, Erban A, Graf A, Kopka J, Zuther E, Hincha DK. (2019). Both cold and sub-zero acclimation induce cell wall modification and changes in the extracellular proteome in *Arabidopsis thaliana*. *Sci Rep,* **9**: 2289.

Takahashi D, Imai H, Kawamura Y, Uemura M. (2016a). Lipid profiles of detergent resistant fractions of the plasma membrane in oat and rye in association with cold acclimation and freezing tolerance. *Cryobiology,* **72**: 123-134.

Takahashi D, Kawamura Y, Uemura M. (2013a). Changes of detergent-resistant plasma membrane proteins in oat and rye during cold acclimation: association with differential freezing tolerance. *J Proteome Res,* **12**: 4998-5011.

Takahashi D, Kawamura Y, Uemura M. (2016b). Cold acclimation is accompanied by complex responses of glycosylphosphatidylinositol (GPI)-anchored proteins in *Arabidopsis*. *J Exp Bot,* **67**: 5203-5215.

Takahashi D, Li B, Nakayama T, Kawamura Y, Uemura M. (2013b). Plant plasma membrane proteomics for improving cold tolerance. *Front Plant Sci,* **4**: 90.

Takahashi F, Mizoguchi T, Yoshida R, Ichimura K, Shinozaki K. (2011). Calmodulin-dependent activation of MAP kinase for ROS homeostasis in *Arabidopsis*. *Mol Cell,* **41**: 649-660.

Tanou G, Molassiotis A, Diamantidis G. (2009). Hydrogen peroxide- and nitric oxide-induced systemic antioxidant prime-like activity under NaCl-stress and stress-free conditions in citrus plants. *J Plant Physiol,* **166**: 1904-1913.

Teige M, Scheikl E, Eulgem T, Doczi R, Ichimura K, Shinozaki K, Dangl JL, Hirt H. (2004). The MKK2 pathway mediates cold and salt stress signaling in *Arabidopsis*. *Mol Cell,* **15**: 141-152.

Tenhaken R. (2014). Cell wall remodeling under abiotic stress. *Front Plant Sci,* **5**: 771.

Thomas PD. (2017)**.** The gene ontology and the meaning of biological function. In: Dessimoz C, Škunca N, eds. *The Gene Ontology Handbook*. New York, NY: Springer New York.

Thomashow MF. (1999). Plant cold acclimation: freezing tolerance genes and regulatory mechanisms. *Annu Rev Plant Physiol Plant Mol Biol,* **50**: 571-599.

Tian T, Liu Y, Yan H, You Q, Yi X, Du Z, Xu W, Su Z. (2017). agriGO v2.0: a GO analysis toolkit for the agricultural community, 2017 update. *Nucleic Acids Res,* **45**: W122-W129.

Tichy A, Salovska B, Rehulka P, Klimentova J, Vavrova J, Stulik J, Hernychova L. (2011). Phosphoproteomics: searching for a needle in a haystack. *J Proteomics,* **74**: 2786-2797.

Tournaire-Roux C, Sutka M, Javot H, Gout E, Gerbeau P, Luu DT, Bligny R, Maurel C. (2003). Cytosolic pH regulates root water transport during anoxic stress through gating of aquaporins. *Nature,* **425**: 393-397.

Uchida A, Jagendorf AT, Hibino T, Takabe T, Takabe T. (2002). Effects of hydrogen peroxide and nitric oxide on both salt and heat stress tolerance in rice. *Plant Sci,* **163**: 515-523.

Uemura M, Joseph RA, Steponkus PL. (1995). Cold acclimation of *Arabidopsis thaliana* (effect on plasma membrane lipid composition and freeze-induced lesions). *Plant Physiol,* **109**: 15-30.

Uemura M, Steponkus PL. (1994). A contrast of the plasma membrane lipid composition of oat and rye leaves in relation to freezing tolerance. *Plant Physiol,* **104**: 479-496.

Uemura M, Yoshida S. (1984). Involvement of plasma membrane alterations in cold acclimation of winter rye seedlings (*Secale cereale* L. cv Puma). *Plant Physiol,* **75**: 818-826.

Umezawa T, Sugiyama N, Takahashi F, Anderson JC, Ishihama Y, Peck SC, Shinozaki K. (2013). Genetics and phosphoproteomics reveal a protein phosphorylation network in the abscisic acid signaling pathway in *Arabidopsis thaliana*. *Sci Signal,* **6**: rs8.

van Gisbergen PA, Li M, Wu SZ, Bezanilla M. (2012). Class II formin targeting to the cell cortex by binding PI(3,5)P(2) is essential for polarized growth. *J Cell Biol,* **198**: 235-250.

van Wijk KJ, Friso G, Walther D, Schulze WX. (2014). Meta-analysis of *Arabidopsis thaliana* phospho-proteomics data reveals compartmentalization of phosphorylation motifs. *Plant Cell,* **26**: 2367-2389.

Vile D, Pervent M, Belluau M, Vasseur F, Bresson J, Muller B, Granier C, Simonneau T. (2012). *Arabidopsis* growth under prolonged high temperature and water deficit: independent or interactive effects? *Plant Cell Environ,* **35**: 702-718.

Viotti C, Luoni L, Morandini P, De Michelis MI. (2005). Characterization of the interaction between the plasma membrane H^+-ATPase of *Arabidopsis thaliana* and a novel interactor (PPI1). *FEBS J,* **272**: 5864-5871.

Vreeburg RA, Airianah OB, Fry SC. (2014). Fingerprinting of hydroxyl radical-attacked polysaccharides by N-isopropyl-2-aminoacridone labelling. *Biochem J,* **463**: 225-237.

Wagih O, Sugiyama N, Ishihama Y, Beltrao P. (2016). Uncovering phosphorylation-based specificities through functional interaction networks. *Mol Cell Proteomics,* **15**: 236-245.

Wahid A, Perveen M, Gelani S, Basra SM. (2007). Pretreatment of seed with H_2O_2 improves salt tolerance of wheat seedlings by alleviation of oxidative damage and expression of stress proteins. *J Plant Physiol,* **164**: 283-294.

Wang C, Zhang LJ, Huang RD. (2011). Cytoskeleton and plant salt stress tolerance. *Plant Signal Behav,* **6**: 29-31.

Wang P, Hsu CC, Du Y, Zhu P, Zhao C, Fu X, Zhang C, Paez JS, Macho AP, Tao WA, Zhu JK. (2020). Mapping proteome-wide targets of protein kinases in plant stress responses. *Proc Natl Acad Sci U.S.A.,* **117**: 3270-3280.

Willems P, Horne A, Van Parys T, Goormachtig S, De Smet I, Botzki A, Van Breusegem F, Gevaert K. (2019). The Plant PTM Viewer, a central resource for exploring plant protein modifications. *Plant J,* **99**: 752-762.

Willick IR, Takahashi D, Fowler DB, Uemura M, Tanino KK. (2018). Tissue-specific changes in apoplastic proteins and cell wall structure during cold acclimation of winter wheat crowns. *J Exp Bot,* **69**: 1221-1234.

Wingenter K, Trentmann O, Winschuh I, Hormiller, II, Heyer AG, Reinders J, Schulz A, Geiger D, Hedrich R, Neuhaus HE. (2011). A member of the mitogen-activated protein 3-kinase family is involved in the regulation of plant vacuolar glucose uptake. *Plant J,* **68**: 890-900.

Wright E. (1931). The effect of high temperatures on seed germination. *J For,* **29**: 679-687.

Wu X, Sklodowski K, Encke B, Schulze WX. (2014). A kinase-phosphatase signaling module with BSK8 and BSL2 involved in regulation of sucrose-phosphate synthase. *J Proteome Res,* **13**: 3397-3409.

Wu XN, Xi L, Pertl-Obermeyer H, Li Z, Chu LC, Schulze WX. (2017). Highly efficient single-step enrichment of low abundance phosphopeptides from plant membrane preparations. *Front Plant Sci,* **8**: 1673.

Wu Y, Xun Q, Guo Y, Zhang J, Cheng K, Shi T, He K, Hou S, Gou X, Li J. (2016). Genome-wide expression pattern analyses of the *Arabidopsis* leucine-rich repeat receptor-like kinases. *Mol Plant,* **9**: 289-300.

Xiao Z, Ximing C. (2011). Climate change impacts on global agricultural land availability. *Environ Res Lett,* **6**: 014014.

Xin Z, Browse J. (2001). Cold comfort farm: the acclimation of plants to freezing temperatures. *Plant Cell Environ,* **23**: 893-902.

Xu T, Dai N, Chen J, Nagawa S, Cao M, Li H, Zhou Z, Chen X, De Rycke R, Rakusova H, Wang W, Jones AM, Friml J, Patterson SE, Bleecker AB, Yang Z. (2014). Cell surface ABP1-TMK auxin-sensing complex activates ROP GTPase signaling. *Science,* **343**: 1025-1028.

Xuan J, Song Y, Zhang H, Liu J, Guo Z, Hua Y. (2013). Comparative proteomic analysis of the stolon cold stress response between the C4 perennial grass species *Zoysia japonica* and *Zoysia metrella*. *PLoS One,* **8**: e75705.

Xue L, Wang P, Wang L, Renzi E, Radivojac P, Tang H, Arnold R, Zhu JK, Tao WA. (2013). Quantitative measurement of phosphoproteome response to osmotic stress in *Arabidopsis* based on Library-Assisted eXtracted Ion Chromatogram (LAXIC). *Mol Cell Proteomics,* **12**: 2354-2369.

Yamada K, Yamaguchi K, Shirakawa T, Nakagami H, Mine A, Ishikawa K, Fujiwara M, Narusaka M, Narusaka Y, Ichimura K, Kobayashi Y, Matsui H, Nomura Y, Nomoto M, Tada Y, Fukao Y, Fukamizo T, Tsuda K, Shirasu K, Shibuya N, Kawasaki T. (2016). The *Arabidopsis* CERK1-associated kinase PBL27 connects chitin perception to MAPK activation. *EMBO J,* **35**: 2468-2483.

Yamazaki T, Kawamura Y, Uemura M. (2009). Extracellular freezing-induced mechanical stress and surface area regulation on the plasma membrane in cold-acclimated plant cells. *Plant Signal Behav,* **4**: 231-233.

Yan SP, Zhang QY, Tang ZC, Su WA, Sun WN. (2006). Comparative proteomic analysis provides new insights into chilling stress responses in rice. *Mol Cell Proteomics,* **5**: 484-496.

Yang T, Chaudhuri S, Yang L, Du L, Poovaiah BW. (2010a). A calcium/calmodulin-regulated member of the receptor-like kinase family confers cold tolerance in plants. *J Biol Chem,* **285**: 7119-7126.

Yang T, Shad Ali G, Yang L, Du L, Reddy AS, Poovaiah BW. (2010b). Calcium/calmodulin-regulated receptor-like kinase CRLK1 interacts with MEKK1 in plants. *Plant Signal Behav,* **5**: 991-994.

Yao HY, Xue HW. (2011). Signals and mechanisms affecting vesicular trafficking during root growth. *Curr Opin Plant Biol,* **14**: 571-579.

Yoshida S, Uemura M. (1984). Protein and lipid compositions of isolated plasma membranes from orchard grass (*Dactylis glomerata* L.) and changes during cold acclimation. *Plant Physiol,* **75**: 31-37.

You J, Chan Z. (2015). Ros regulation during abiotic stress responses in crop plants. *Front Plant Sci,* **6**: 1092.

Yu G, Wang LG, Han Y, He QY. (2012). clusterProfiler: an R package for comparing biological themes among gene clusters. *OMICS,* **16**: 284-287.

Yuan F, Yang H, Xue Y, Kong D, Ye R, Li C, Zhang J, Theprungsirikul L, Shrift T, Krichilsky B, Johnson DM, Swift GB, He Y, Siedow JN, Pei ZM. (2014). OSCA1 mediates osmotic-stress-evoked Ca^{2+} increases vital for osmosensing in *Arabidopsis*. *Nature,* **514**: 367-371.

Yuan P, Yang T, Poovaiah BW. (2018). Calcium signaling-mediated plant response to cold stress. *Int J Mol Sci,* **19**: 3896.

Zabaleta E, Oropeza A, Assad N, Mandel A, Salerno G, Herrera-Estrella L. (1994). Antisense expression of *chaperonin 60β* in transgenic tobacco plants leads to abnormal phenotypes and altered distribution of photoassimilates. *Plant J,* **6**: 425-432.

Zeng H, Xu L, Singh A, Wang H, Du L, Poovaiah BW. (2015). Involvement of calmodulin and calmodulin-like proteins in plant responses to abiotic stresses. *Front Plant Sci,* **6**: 600.

Zhang JZ, Creelman RA, Zhu JK. (2004). From laboratory to field. Using information from *Arabidopsis* to engineer salt, cold, and drought tolerance in crops. *Plant Physiol,* **135**: 615-621.

Zhang L, Li Y, Lu W, Meng F, Wu CA, Guo X. (2012). Cotton GhMKK5 affects disease resistance, induces HR-like cell death, and reduces the tolerance to salt and drought stress in transgenic *Nicotiana benthamiana*. *J Exp Bot,* **63**: 3935-3951.

Zhang SH, Kobayashi R, Graves PR, Piwnica-Worms H, Tonks NK. (1997). Serine phosphorylation-dependent association of the band 4.1-related protein-tyrosine phosphatase PTPH1 with 14-3-3beta protein. *J Biol Chem,* **272**: 27281-27287.

Zhang WJ, Niu Y, Bu SH, Li M, Feng JY, Zhang J, Yang SX, Odinga MM, Wei SP, Liu XF, Zhang YM. (2014). Epistatic association mapping for alkaline and salinity tolerance traits in the soybean germination stage. *PLoS One,* **9**: e84750.

Zhao FY, Liu W, Zhang SY. (2009). Different responses of plant growth and antioxidant system to the combination of cadmium and heat stress in transgenic and non-transgenic rice. *J Integr Plant Biol,* **51**: 942-950.

Zhou J, Wang J, Shi K, Xia XJ, Zhou YH, Yu JQ. (2012). Hydrogen peroxide is involved in the cold acclimation-induced chilling tolerance of tomato plants. *Plant Physiol Biochem,* **60**: 141-149.

Zhu J, Dong CH, Zhu JK. (2007). Interplay between cold-responsive gene regulation, metabolism and RNA processing during plant cold acclimation. *Curr Opin Plant Biol,* **10**: 290-295.

Zhu JK. (2016). Abiotic stress signaling and responses in plants. *Cell,* **167**: 313-324.

Zulawski M, Braginets R, Schulze WX. (2013). PhosPhAt goes kinases--searchable protein kinase target information in the plant phosphorylation site database PhosPhAt. *Nucleic Acids Res,* **41**: D1176-1184.